

(2)

AEOSR-TR-91-0005

SDA11
LTR91-005

AD-A232 767

FINAL REPORT

ULTRA-DENSE OPTICAL MASS STORAGE

DTIC
SELECTED
S D
MAR 12 1991
D

Prepared for

USAF, AFSC
Air Force Office of Scientific Research
Building 410
Bolling Air Force Base, DC 20332-6448

Contract No. F49620-90-C-0056, Project No. FQ8671-9001527 1602/F1

"The views and conclusions contained in this document are those of the authors and should not be interpreted as necessarily representing the official policies or endorsements, either expressed or implied, of the Air Force Office of Scientific Research or the U.S. Government."

By

Steven A. Lis and Philip D. Henshaw

11 February 1991

INFORMATION STATEMENT A	
Approved for public release	
Distribution Unlimited	

SPARTA, Inc.
24 Hartwell Avenue
Lexington, MA 02173
(617) 863-1060

91 3 06 087

SDA11
LTR91-005

FINAL REPORT
ULTRA-DENSE OPTICAL MASS STORAGE

Prepared for

USAF, AFSC
Air Force Office of Scientific Research
Building 410
Bolling Air Force Base, DC 20332-6448

Contract No. F49620-90-C-0056, Project No. FQ8671-9001527 1602/F1

"The views and conclusions contained in this document are those of the authors and should not be interpreted as necessarily representing the official policies or endorsements, either expressed or implied, of the Air Force Office of Scientific Research or the U.S. Government."

By
Steven A. Lis

11 February 1991

SPARTA, Inc.
24 Hartwell Avenue
Lexington, MA 02173
(617) 863-1060



Accepted by:	J
File No.:	100-1000
Date:	10/10/91
Comments:	None
By:	C. A. Lis
Date:	10/10/91
Comments:	None
Dept:	100-1000
Comments:	None

A-1

UNCLASSIFIED

SECURITY CLASSIFICATION OF THIS PAGE

REPORT DOCUMENTATION PAGE

1a. REPORT SECURITY CLASSIFICATION Unclassified		1b. RESTRICTIVE MARKINGS										
2a. SECURITY CLASSIFICATION AUTHORITY		3. DISTRIBUTION/AVAILABILITY OF REPORT Approved for public release; distribution unlimited.										
2b. DECLASSIFICATION/DOWNGRADING SCHEDULE		5. MONITORING ORGANIZATION REPORT NUMBER(S)										
4. PERFORMING ORGANIZATION REPORT NUMBER(S) LTR91-005		7a. NAME OF MONITORING ORGANIZATION AFOSR/NE										
6a. NAME OF PERFORMING ORGANIZATION SPARTA, Inc.	6b. OFFICE SYMBOL (If applicable) NE	7b. ADDRESS (City, State, and ZIP Code) Bldg 410 Bolling AFB DC 20332										
8a. NAME OF FUNDING/SPONSORING ORGANIZATION AFOSR	8b. OFFICE SYMBOL (If applicable) NE	9. PROCUREMENT INSTRUMENT IDENTIFICATION NUMBER F49620-90-C-0056										
8c. ADDRESS (City, State, and ZIP Code) Bolling AFB, DC 20332-6448		10. SOURCE OF FUNDING NUMBERS <table border="1"> <tr> <td>PROGRAM ELEMENT NO. 63221C</td> <td>PROJECT NO. 1602/F1</td> <td>TASK NO.</td> <td>WORK UNIT ACCESSION NO.</td> </tr> </table>		PROGRAM ELEMENT NO. 63221C	PROJECT NO. 1602/F1	TASK NO.	WORK UNIT ACCESSION NO.					
PROGRAM ELEMENT NO. 63221C	PROJECT NO. 1602/F1	TASK NO.	WORK UNIT ACCESSION NO.									
11. TITLE (Include Security Classification) Ultra Dense Optical Mass Storage												
12. PERSONAL AUTHOR(S) Steven A. Lis												
13a. TYPE OF REPORT Final	13b. TIME COVERED FROM 1 Sep 90 TO 28 Feb 91	14. DATE OF REPORT (Year, Month, Day) 91/02/11	15. PAGE COUNT 93									
16. SUPPLEMENTARY NOTATION												
17. COSATI CODES <table border="1"> <tr> <th>FIELD</th> <th>GROUP</th> <th>SUB-GROUP</th> </tr> <tr> <td></td> <td></td> <td></td> </tr> <tr> <td></td> <td></td> <td></td> </tr> </table>		FIELD	GROUP	SUB-GROUP							18. SUBJECT TERMS (Continue on reverse if necessary and identify by block number) Optical Memory Spectral Hole Burning, Holographic	
FIELD	GROUP	SUB-GROUP										
19. ABSTRACT (Continue on reverse if necessary and identify by block number) This Final Report describes the results of a Phase I SBIR project to investigate the feasibility and practicality of utilizing Spectral Hole Burning (SHB) media as the basis of a high capacity optical memory system. Our concept has the potential for providing enormous storage capacities (on the order of 10^{12} bits and larger) in commercially viable systems. This report summarizes our analyses and shows that the necessary system components as well as material properties presently exist (or are under rapid development) which can make such a memory system a practical reality and not simply a theoretical possibility. The ultimate system design is expected to be a high capacity unit of modest physical size which has low power requirements, high data rate, and an access time suitable to be useful to a broadbased user community.												
20. DISTRIBUTION/AVAILABILITY OF ABSTRACT <input checked="" type="checkbox"/> UNCLASSIFIED/UNLIMITED <input type="checkbox"/> SAME AS RPT. <input type="checkbox"/> DTIC USERS		21. ABSTRACT SECURITY CLASSIFICATION Unclassified										
22a. NAME OF RESPONSIBLE INDIVIDUAL Steven A. Lis		22b. TELEPHONE (Include Area Code) 202-710-4931	22c. OFFICE SYMBOL NE									

UNCLASSIFIED

19. ABSTRACT (Continued)

The high capacity of our proposed system originates from the basic properties of the SHB medium. In most holographic recording media, storage capacity is limited by recorded image resolution and the number of angular positions which the reference beam is permitted. A combination of practical restrictions limits the capacity for most holographic media to 10^9 bits/cm³. SHB media provide far more storage capacity because independent holograms can be recorded at many laser frequencies (10^3 to 10^5 independent frequencies). When these media are considered as the basis for an optical memory, the capacity of the final system is raised to the range of 10^{12} to 10^{13} bits/cm³ in a practical system. In doing so the system has remained compact, and low cost, with performance specifications which make it attractive for a wide range of computer applications.

An important element in our proposed approach is the creation of "Frequency Channel" structures within the SHB medium which provide the ability to record phase holograms in a medium which is fundamentally absorptive in nature. Our analysis has shown that the utilization of these structures provides significant advantages in defining laser requirements and in enhancing the resistance to unintentional erasure.

Our system analysis has also examined the principal issue of erasure from the fundamental material point of view as well as the overall system viewpoint. The net conclusion is that several acceptable approaches are available which are simple to implement and transparent to the user and which will provide media erasability which makes this memory concept very acceptable to a wide user community.

Refrigeration is a significant practical point which can be key. Since all of the known SHB media require operation at cryogenic temperatures, a practical system must incorporate a compact and efficient cryogenic cooling system. Our examination of presently available systems as well as coolers which are presently under active development (and making rapid technical progress) indicates that compact systems of small size, modest cost and long life will be available. An interesting example is the microminiature refrigerator which is aimed at reaching 10 K in the very near future.

TABLE OF CONTENTS

1	Introduction	1
1.1	Organization of This Report	1
2	Concept	3
3	Economic and Performance Analysis	6
3.1	Applications	6
3.2	Current Mass Storage Device Characteristics	7
3.3	Cost Per Megabyte	8
3.4	The Effect of Access Time on Effective Data Rate	9
4	Data Requirements in a Holographic Memory	12
4.1	Introduction	12
4.2	Data Format	13
4.3	Bit Error Rate and SNR	15
4.4	SNR and the Selection of Detector	16
5	Erasure	18
5.1	Introduction and Requirements	18
5.2	Inactive System Data Decay	19
5.3	Reading Versus Erasure	19
5.4	Erasure and Data Rates	20
5.4.1	Burst Mode Operation	23
5.5	Intentional Erasure	23
5.5.1	Parallel Systems	24
5.5.2	Multiple Photochemical Species	24
5.5.3	π Phase Erasure	26
6	Using the Real Part of the Refractive Index	27
6.1	Background on Spectral Hole Burning	28
6.2	Modeling the Absorption Edge	28
6.3	Access to the Capacity of the Material	29
6.4	Detailed Modeling of Frequency Channels	29
6.4.1	Index Modulation Near an Absorption Band Edge	31
6.5	Creation of Frequency Channels in SHB Materials	32
6.5.1	Refractive Index Characteristics After Channel Formation	35
6.5.2	Computer Simulation and Results	36
6.6	Debye-Waller Factor	36
6.7	External Field Effects	41
6.7.1	Data Recording in Frequency Channels	42
6.8	Frequency Channel Storage Capacity	44
6.8.1	External Fields and Storage Capacity	45
6.8.2	Number of Holograms per Channel	45
6.9	Making Frequency Channels	46

6.10	Recording in Frequency Channels	47
6.11	Laser Linewidth Requirements	48
6.12	Summary of Frequency Channel Attributes	48
7	Absorption Hologram Storage	48
7.1	Absorption Hologram Limits	49
7.2	Cross-Talk Between Holograms	50
7.2.1	Cross-Talk Due to Angular Resolution	51
7.2.2	Cross-Talk Due to Frequency Spacing	51
7.3	External Field Effects	52
7.4	Absorption Hologram Storage Capacity	53
8	Materials for SHB-Based Optical Memory	54
8.1	High End System Specifications	54
8.1.1	Absorption Hologram Based Parameters	54
8.1.2	Phase Hologram Based Parameters (Frequency Channels)	55
8.2	Material Boundaries for Absorption Holograms	55
8.3	Material Boundaries for Phase Holograms	59
8.4	Analysis and Comparisons	60
9	Parallel Versus Serial Data Storage and Retrieval	62
9.1	Comparison of Components	62
9.2	The Impact on Materials Selection	63
9.3	Conclusion: Serial Versus Parallel	63
10	Supporting Components	65
10.1	Reference Beam Deflector	65
10.2	Detector Array	66
10.3	Spatial Light Modulator	66
10.4	Microcoolers and Cryostats for SHB Media	67
10.5	Electronic Interface	68
10.6	Laser Source for Writing and Reading	71
10.7	Component Development Summary	72
11	Experimental Plan for Phase II	74
11.1	Materials Selection for 4D Optical Memory Experiments	74
11.1.1	Selection of Host Material	74
11.1.2	Selection of Photochemical Species	76
11.2	Optical System Design for 4D Optical Memory Experiments	77
11.2.1	Cryostat, Detector and Erasure Optics	78
11.2.2	SLM and Reduction Optics	81
11.2.3	Beam Steering and Relay Optics	82
11.2.4	Laser and Beamsplitting Optics	82
11.2.5	Incrementally Assembling the Complete Design	84
11.2.6	Summary of the Experimental Design	84
11.3	Electronic Interface and Memory System Control	85

11.3.1	System Description	86
11.3.1.1	CCD Arrays	86
11.3.1.2	LCD Display and Controller	86
11.3.1.3	FAL and Controller	87
11.3.1.4	Electronic Shutter	87
11.3.1.5	Personal Computer	87
11.3.2	Summary of the Electronic Interface	87
12	Summary	88
A	A Bibliography of Papers on Spectral Hole Burning Materials	92

1 Introduction

This Final Report describes the results of a Phase I SBIR project to investigate the feasibility and practicality of utilizing Spectral Hole Burning (SHB) media as the basis of a high capacity optical memory system.

Our concept has the potential for providing enormous storage capacities (on the order of 10^{12} bits and larger) in commercially viable systems. This report summarizes our analyses and shows that the necessary system components as well as material properties presently exist (or are under rapid development) which can make such a memory system a practical reality and not simply a theoretical possibility. The ultimate system design is expected to be a high capacity unit of modest physical size which has low power requirements, high data rate, and an access time suitable to be useful to a broadbased user community.

The high capacity of our proposed system originates from the basic properties of the SHB medium. In most holographic recording media, storage capacity is limited by recorded image resolution and the number of angular positions which the reference beam is permitted. A combination of practical restrictions limits the capacity for most holographic media to 10^9 bits/cm³. SHB media provide far more storage capacity because independent holograms can be recorded at many laser frequencies (10^3 to 10^5 independent frequencies). When these media are considered as the basis for an optical memory, the capacity of the final system is raised to the range of 10^{12} to 10^{13} bits/cm³ in a practical system. In doing so the system has remained compact, and low cost, with performance specifications which make it attractive for a wide range of computer applications.

An important element in our proposed approach is the creation of "Frequency Channel" structures within the SHB medium which provide the ability to record phase holograms in a medium which is fundamentally absorptive in nature. Our analysis has shown that the utilization of these structures provides significant advantages in defining laser requirements and in enhancing the resistance to unintentional erasure.

Our system analysis has also examined the principal issue of erasure from the fundamental material point of view as well as the overall system viewpoint. The net conclusion is that several acceptable approaches are available which are simple to implement and transparent to the user and which will provide media erasability which makes this memory concept very acceptable to a wide user community.

Refrigeration is a significant practical point which can be key. Since all of the known SHB media require operation at cryogenic temperatures, a practical system must incorporate a compact and efficient cryogenic cooling system. Our examination of presently available systems as well as coolers which are presently under active development (and making rapid technical progress) indicates that compact systems of small size, modest cost and long life will be available. An interesting example is the microminiature refrigerator which is aimed at reaching 10 K in the very near future.

1.1 Organization of This Report

This report is organized in a manner which provides the sequential rationale for defining the proposed optical memory requirements and performance goals. This rationale begins with the economic and technical analysis which provides the driving force behind our optical memory system (Section 2). It continues with a brief examination of requirements for reliable data storage (Section 3) and then examines in detail the fundamental and systems issues of erasure (section 4).

Section 5 provides a detailed analysis of the "Frequency Channel" concept and the recording of phase holograms in SHB media. The recording of information as absorption holograms is examined in Section 6 and a direct comparison between phase hologram and absorption hologram recording in SHB media is presented in Section 7. Finally, an examination is made in Section 8 of the two competing data handling approaches (serial versus parallel) and how they define the selection of SHB media.

Section 9 discusses the present and anticipated technical progress of the necessary supporting system components (tunable laser, SLM, etc.). Finally, an experimental memory system is designed in Section 10 which indicates the optimal choices for SHB media as well as providing a detailed components list necessary for constructing a demonstration of a modest performance operational memory system which has all the principal attributes normally associated with a computer memory, including erasability.

Both the program goals and the specific tasks have all been appropriately completed during this Phase I effort. The program goals are stated below.

1. Examine further the frequency channel approach in terms of its quantitative relation to the known properties of existing candidate materials.
2. Carefully plan the critical experiments which are necessary to quantitatively confirm that this novel memory structure provides significant advantages for ultradense capacity optical memories.

In reference to the itemized Statement of Work for this program the specific tasks can be related to the sections of the report as given below.

1. Refine fundamental theory and optimal medium usage parameters; Section 5.
2. Define medium requirements for a holographic memory medium; Sections 4, 5, 6, and 7.
3. Define quantitative memory system requirements; Sections 2, 3, and 4.
4. Relate selected material candidates and system design factors to performance capabilities; sections 7, 8, and 9.
5. Define critical experiments and required performance goals to be achieved during a Phase II effort. Design experimental apparatus testing volume hologram storage capabilities; Section 10.
6. Prepare a Final Report describing the results of Phase I.

2 Concept

Our optical memory concept makes use of the unique properties of spectral hole burning materials to realize extremely dense data storage. Figure 1 illustrates the basic concept. Hologram recording and readout provides access to recording centers throughout a volume of material. Volume storage can make use of a very large number of recording centers. For example, a typical host medium can be doped to a level of 10^{19} recording centers per cm^3 . Achieving a fundamental signal to noise of 30 will require approximately 10^3 recording centers per bit. If we allow a factor of 10 for a "guard band", then the fundamental capacity of a 1 cm cube is about 10^{15} bits.

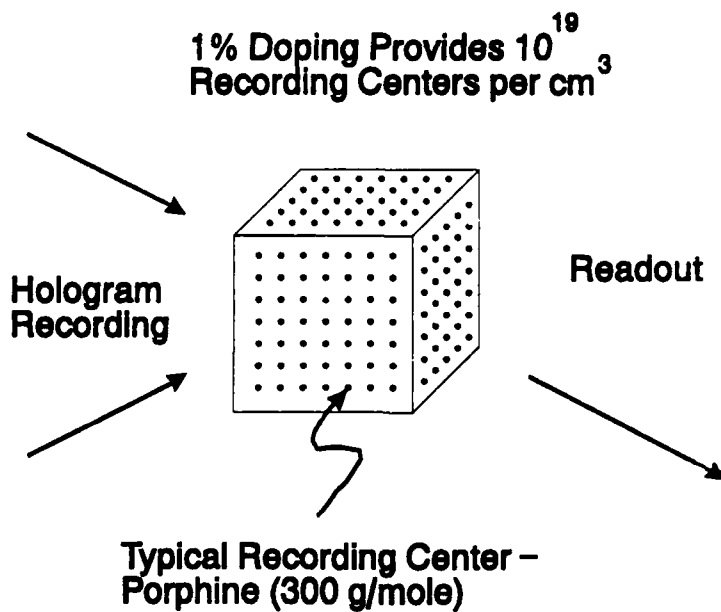


Figure 1. Fundamental information capacity of volume storage media.

Figure 2 shows the basic means by which SHB materials provide an additional dimension. The inhomogeneous absorption spectrum is made up of a large number of homogeneously broadened absorption lines. At low temperatures, the absorbing centers within a single homogeneously broadened linewidth can be addressed independently of any other population of recording centers. This allows data to be recorded at one wavelength which cannot be seen by any other wavelength. By selecting the laser wavelength, independent access to recording capacity is permitted. This laser frequency selectivity is effectively equivalent to a extra dimension, permitting greater access to the fundamental capacity of the recording medium.

One of the major factors which has kept conventional optical holographic memory from having commercial impact is the limited capacity. If a holographic memory device cannot provide more capacity than can be achieved with a board of semiconductor RAM chips, then the switch to this new type of memory will not be made. For 3D holographic memory, this capacity limit is imposed by the diffraction-limited resolution of the cone of rays used for the

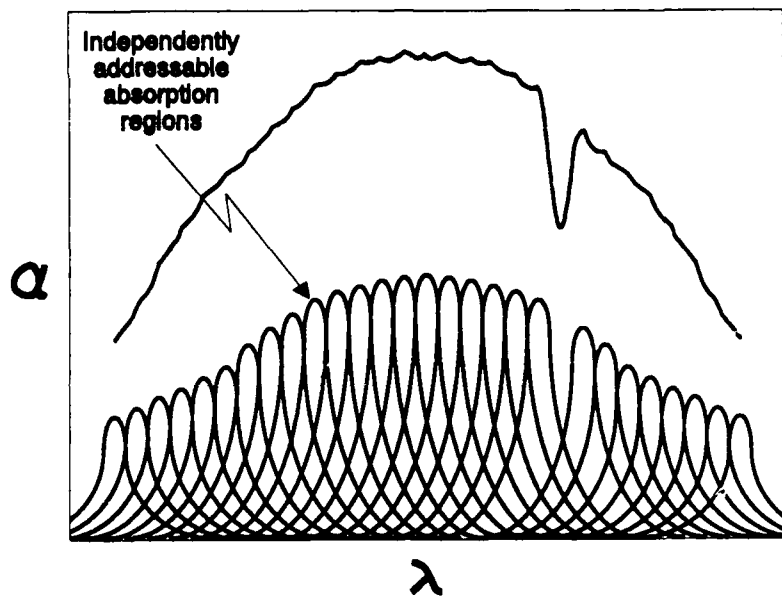


Figure 2. Spectral hole burning materials provide an additional dimension for holographic data storage which can be addressed using frequency agile lasers.

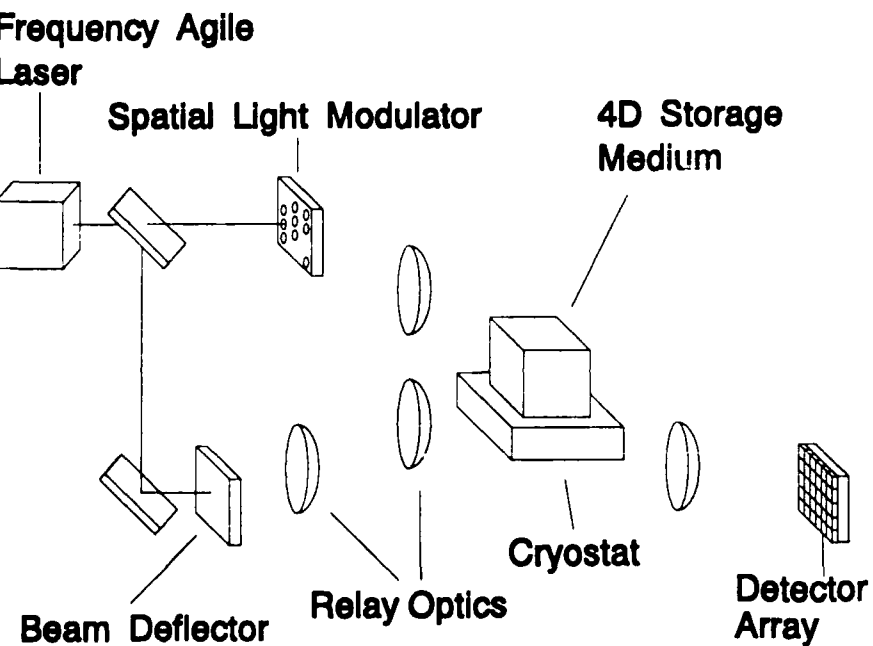


Figure 3. 4D holographic memory architecture.

reference and data beams. The net effect of this limited cone is to make only partial use of the spatial frequency response of the medium. The fringes recorded in the volume holographic medium will be approximately one wavelength in size in one spatial direction but will be many wavelengths on a side in other directions. This volume can contain many more recording centers than are actually needed in the case of heavily-doped material. These recording centers can be used more fully in the case of an SHB medium by addressing them by laser frequency. The ultimate limits on capacity may be imposed by the molecular density of the recording centers and fundamental noise considerations. Capacities of 10^{12} bits and greater appear possible in realistic and economical systems.

A 4D memory architecture designed to take advantage of the unique properties of SHB materials is shown in Figure 3. Table 1 shows the projected capabilities of this 4D holographic optical memory. This architecture includes a frequency agile laser, a beam deflector to provide conventional angle accessing, a spatial light modulator (SLM) to introduce the data, a volume recording medium, and a high-speed, low noise detector array. Except for the frequency agile laser, all of these components are common to both a 4D holographic memory and a 3D holographic memory. In an advanced version of the memory, electric field may provide an additional dimension by changing the frequency of absorption through the Stark effect.[1] This additional dimension can provide engineering room to access the full potential storage capacity of the memory medium.

Table 1. Projected capabilities of a realistic 4D memory system.

Parameter	Value
Capacity	10^{12} bits
Data Rate	10^9 bits/second
Access Time	1 msec

3 Economic and Performance Analysis

Mass storage devices are characterized by the capacity, the data transfer rate, and the access time. In this section, we will examine mass storage applications which require either high data rate or rapid access to determine reasonable goals for future mass storage devices.

A significant factor in the possible commercial success of any memory concept is the cost per on-line megabyte. Low cost memory allows large memory capacities to be purchased. In addition, low cost memories can be configured in parallel architectures which provide high data rates and the effect of rapid access. Because of the enormous capacity of the 4D optical memory concept, the expense of the optical components can be much lower than either existing electronic memory or mass storage devices, and much lower than projected 3D optical memory costs/megabyte.

As an example, we apply this criterion to mass storage technologies geared to rapid data access. A summary of mass storage requirements for several applications is presented in Table 2. Each of these applications requires a short access time, either directly, because of short timelines, or indirectly, because of the effect of access time on data rate. We have chosen access time as the vehicle for our discussion of mass storage goals for several reasons: it is a clear cut "market niche" which is currently unfilled, it clearly illustrates the importance of cost/megabyte, and it appears to be a problem which could be solved by developing new mass storage devices.

Table 2. Mass Storage Requirements for Several Applications

Applications Characteristics	Relational Database	Interactive Video	Telephone Services	Distributed (Teraops) Computing
Capacity (Mbytes)	≥ 1000	≥ 1000	7600 [2]	10^6 [3]
Data Rate (Mbytes/s)	0.1 - 12	6	1	1000
Access Time (ms)	<20	<5	1	?

3.1 Applications

Many significant military applications involve the implementation of software decision aids for wartime where large data bases must be searched for rules, associations, etc. based on rapidly changing inputs. This application may also require the added feature of removable media for classified data bases.

Rapid access to data on optical disks has the potential to play an important role in communication (telephone voice mail), interactive video, and relational database applications. In each case, the average access time is a key parameter which determines the limit of system performance.[4] The performance of relational database systems is currently limited by access time and effective data rate.[5]

Boston Technologies develops equipment for telephone company central offices which allows users within a local area to have personal mailboxes for voicemail and FAX, and call and FAX

forwarding from office to home, among other features.[2] The telephone company bills users \$3 per month for these services. A trial installation near Philadelphia resulted in a very high subscription rate. For a typical central office, 10 disk drives, with a total capacity of 7.8 GBytes, are used to store the menu messages and mailbox contents. Accessing a specific individual's mailbox to leave a message requires 27 disk accesses to the master system disk, and the total timeline should be kept under 3 seconds. In a typical central office system the presence of 120 to 150 simultaneous users results in noticeable delays, limited by disk access time. This load is equivalent to a disk access rate of 1000 accesses per second. Although this problem can be solved by arrays of Winchester magnetic disks, this solution has not been used because of reliability concerns. Currently this problem is solved by using large capacity semiconductor memory caches, however, this solution is expensive and complex, and limits the ultimate capacity of the system.

The Media Lab at MIT is examining how a convergence of information technologies will have a profound effect on our society, and interactive video is central to most of these applications.[6] Interactive video has many interesting applications: training aids, entertainment, editing of video sequences, and video newspapers, for example.

Reducing the total access time required to retrieve any piece of information from a large data base is a key to achieving interactive video. Interactive video is implemented by "coding" a video database – annotating the time, place, activities, and participants for any sequence of video frames, for example.[7] The code database is then used to determine which frames to retrieve based on interaction with a user. Very large data bases can be created very quickly in this environment. During operation, choosing which frame to retrieve from a database may involve a number of accesses to the code data base. For example, to retrieve frames showing fighting in a Middle East city, accesses to determine which frames contain war scenes, city scenes, and Middle East participants might have to be intersected to determine the number of possible frame sequences which apply. If the search finds more than one "hit," then the most recent sequence might be selected and shown if the application is a video newspaper. Ideally, all these accesses will take place and the frame sequence will begin in a time interval shorter than a single frame. In this example, five accesses in less than 30 msec leads to a required access time of less than about 5 msec.

3.2 Current Mass Storage Device Characteristics

Currently, when disk storage with high on-line capacity and a high data rate are desired, "disk farms", arrays of low-cost Winchester magnetic disks, can be configured to achieve these goals.[8] These configurations have been developed by companies such as Thinking Machines, Inc., and they are cost-effective because of the low cost of current Winchester drives as a result of their widespread use.[9] The limitation of disk farms, however, centers around concerns of reliability and the cost inefficiency associated with maintaining multiple copies of data to reduce access time. This use of disk arrays suggests that the cost/megabyte of on-line storage is a key issue for comparing our optical memory system to the competition.

SPARTA has examined the cost/megabyte and average access time for optical jukebox, optical and magnetic disk systems, and semiconductor RAM storage. These systems and projected capabilities for a rapid-access system are shown in Figure 4. We have assumed that an average access time greater than 5 msec is too slow for certain time-critical applications, and that a cost per megabyte greater than \$100 is too high. These lines are, of course, movable depending on

the specific applications, but they indicate the desirable region for rapid access mass storage devices. The line extending up to the right from the single-disk ovals indicates the performance that can be achieved with disk arrays. This line was derived by noting that a narrow band of tracks could be used to minimize seek time, and the data could be written multiple times around the disk to reduce the latency. Because the seek time and latency for current disk systems are similar, both problems must be attacked, leading to a reduced capacity (equivalent to an increased cost/megabyte) proportional to the square of the reduction in access time. This severe penalty has prevented the current use of low-cost disk arrays to solve the problem of slow access to data which currently limits important real-time applications such as decision aids and interactive video.

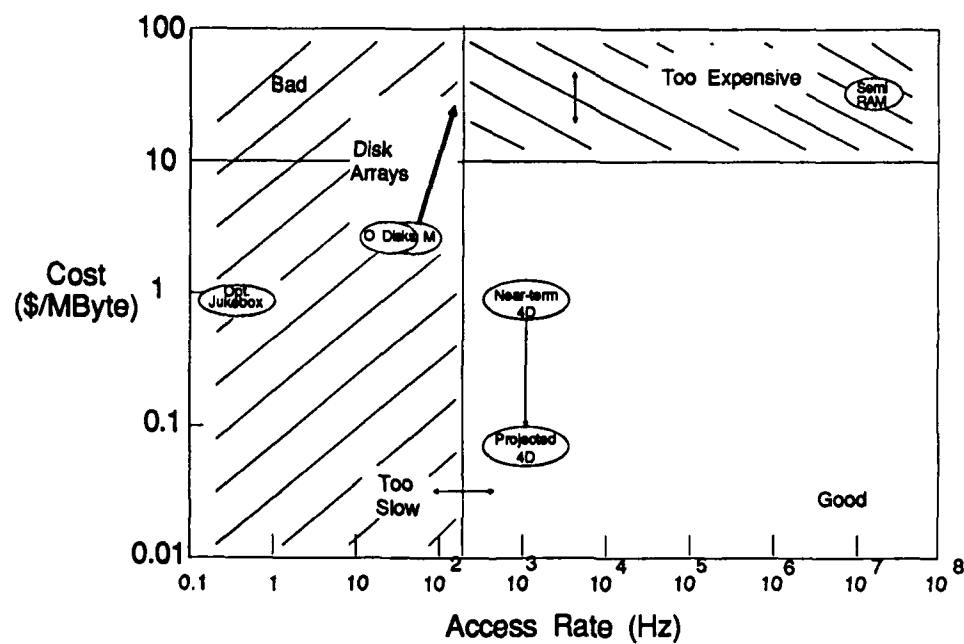


Figure 4. Cost/megabyte and access time for mass storage devices.

Short access time is not the only market niche which must deal with the cost/megabyte of competing technologies. For example, reliability can be traded for cost/megabyte by duplication of data, duplication of storage units, or encoding of data. In each case, increased reliability can be achieved with existing mass storage devices and an increased cost/megabyte. If the cost per megabyte of the existing technology is low enough, then R&D to develop a competing, high-technology solution will not provide a useful result. Similarly, increased data rate can be achieved by duplicating hardware to implement parallel transfer. Finally, capacity can be increased by simply buying more memory devices. The cost/megabyte will determine how much memory can be afforded for a given application. If form factor is not an issue, then the low-cost technology wins. (We have not analyzed whether form factor issues, such as compactness, ruggedness, and power consumption, can be addressed by using low-cost/megabyte hardware.)

3.3 Cost Per Megabyte

Table 3 shows estimated costs per on-line megabyte for two possible memory concepts, a 3D holographic memory and a 4D holographic memory. This chart makes the key point that the enormous capacity of the 4D memory lowers the cost per megabyte to a value which is much lower than 3D holographic memory concepts. The cost/megabyte for the 4D memory is also lower than other existing memory devices, such as magnetic or optical disk and semiconductor RAM chips.

Table 3. Estimated current and projected cost/megabyte for 3D and 4D holographic memory.

Component	3D Holographic Memory Component Costs		4D Holographic Memory Component Costs	
	Current	Projected	Current	Projected
Laser	\$50	\$10	\$30,000	\$3000
SLM	\$5000	\$100	\$5000	\$100
Deflector	\$1000	\$0	\$1000	\$100
Optics	\$1000	\$100	\$1000	\$100
Detector	\$1000	\$100	\$1000	\$100
Electronics	\$1000	\$100	\$1000	\$100
Cryostat	-	-	\$50,000	\$5000
Total Cost	\$9000	\$410	\$89,000	\$8500
Capacity	10^9 bits		10^{12} bits	
Cost/Mbyte	\$72	\$3.30	\$0.71	\$0.07

Several key assumptions went into determining the estimated subsystem costs shown in Table 3. First, we assumed that the spatial light modulator, the optics, the electronics, and the detector arrays required for the 3D and 4D holographic memories are identical. Second, we assumed that the cost of the laser for the 4D memory will be much higher in the near term, based on the requirement for rapid access to 1000 or more narrow lines. In the far term, we have assumed that the use of tunable laser diodes will lower the cost of this laser considerably. Finally, we assumed that the cost of the cryostat will be \$50K for a near term system, based on an estimate from Advanced Research Systems [10], but that this cost can be reduced considerably in a projected system based on the fact that the quoted system has a factor of approximately 100 excess cooling capacity. It is important to note that the cryostat cost, which is well-known in the near-term, dominates the cost of the other subsystems, and yet the cost/Mbyte of the 4D memory is still two orders of magnitude lower than the 3D memory.

3.4 The Effect of Access Time on Effective Data Rate

An approximate idea of some of the requirements for future computer memory systems can be estimated based on the stated goals of the Teraops program. These requirements include a data transfer rate of 1 Gbit/sec and a memory capacity of at least 10^{12} bytes. This section discusses how the effective data rate depends on the access time and the page size. The access time and page size requirements for computer memory are, however, very architecture-dependent.

A cache memory is a small, fast memory, used in most architectures as a place to store recently used data. The data are marked with the time of most recent use. Whenever there is a "fault" (the requested data cannot be found in cache) the "oldest" data in the cache is replaced by the just-requested data. Cache memories are characterized by a total capacity and a page size (the minimum amount of data transferred from cache at one time.)

A cache memory very close to the computer should probably have a small page size. For example, the SUN workstation architecture has an internal cache of 64 kbytes and a "page" size of 1 word. For virtual memory, the cache is further from the computer and has larger page sizes. For example, virtual memory page size is 512 or 1024 bytes in the SUN architecture. In large systems, a hierarchy of cache memories may be used. The delay time to access any device can be hidden by suitable choice of the architecture of the system.

Memory characteristics of current and projected memory devices are shown in Figure 5. The axes - page size and effective data rate - have been chosen to show the operating range of memory concepts considered for cache or main memory in a way independent of the choice of architecture. The page size P is the amount of data transferred during any given access to the memory. The effective data rate R_e is a function of the page size and combines the effects of the access time τ_a and the data transfer rate R . R_e in bits/second is given by

$$R_e = \frac{8P \times 10^3}{\tau_a + 8P/(R \times 10^3)} \quad (1)$$

where P is given in kilobytes, τ_a in seconds, and R in bits/second.

The two horizontal dotted lines in Figure 5 indicate the current data transfer rate of Ethernet, 10 megabits/second, and the projected requirements of teraops computers, 1 gigabit/second. The dotted lines sloping up to the right indicate the total amount of memory which can be read in the indicated times of 10 msec, 1 sec, and 100 seconds.

The solid lines indicate the operating curves of several different memory devices which have been used for mass storage or cache memory. The curve for a typical personal computer floppy disk with 40 msec access time, a data transfer rate of 40 kbytes/sec, and a total capacity of 720 Kbytes is shown near the lower left. The operating curve terminates at 720 Kbytes, since no page can be larger than the total diskette capacity. Clearly the design of this device to operate with a page size of 512 bytes was chosen to hide the effect of the slow device access. High-end devices shown here include the IBIS 2812 magnetic disk system[11] with an access time of 20 msec and a transfer rate of 100 Mbytes/sec and a single RCA optical disk [12], with an access time of 300 msec and a transfer rate of 100 Mbytes/sec. Both systems have a total capacity of 20 Gbytes. The RCA optical jukebox achieves a much greater total capacity of 2.5 Terabytes, at the same data transfer rate of 100 Mbytes/second but has a very slow average access time of 6 seconds.[13]

Each of these concepts leaves a gap in operating capability in the upper left corner of the chart, which obviously requires very large page sizes to hide the effect of access time. This gap limits these devices to use as a main memory or a cache memory some distance from the computer. The Storage Tek RAM is a semiconductor memory with an access time of 50 nanoseconds, a data transfer rate of 20 Mbytes/second, and a total capacity of 60 Mbytes[14]. This device fills in the region of high data rates and small page sizes not covered by the large capacity devices discussed above. A device such as the Storage Tek RAM cannot act as a cache

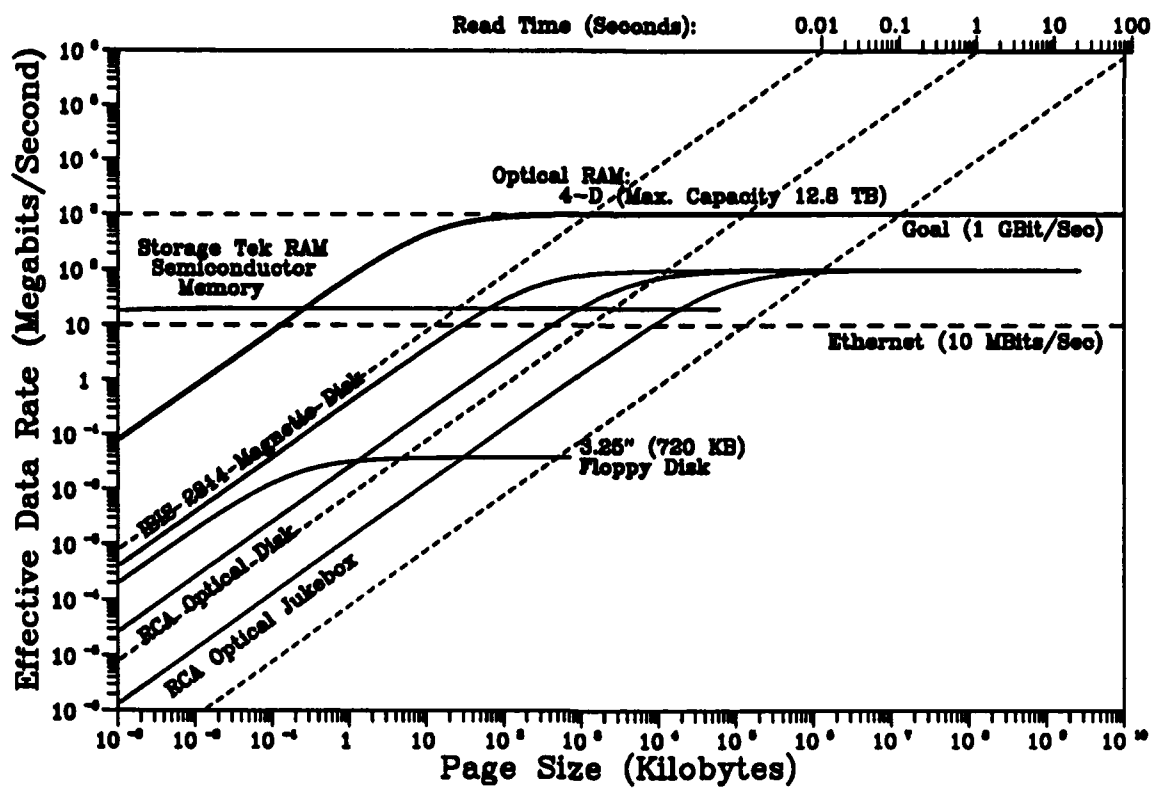


Figure 5. Operating characteristics of cache and main memory devices.

for a large capacity memory system, however, if the required page size to fill in the gap is much larger than the size of a typical data block to be transferred.

4 Data Requirements in a Holographic Memory

The holographic memory system which is under detailed consideration inherently contains the data in a page-oriented format. The data is presumed to be digital and is stored in its binary form. Data can be read in or out only in page-sized increments. The data rate available to the user is determined by the speed with which a single page page can be accessed and read, times the number of bits contained within that page. Because the reading and writing of information must be carried out rapidly and reliably, serious consideration must be given to the significant physical and practical limitations involved in the storage and retrieval of this information.

4.1 Introduction

The many boundary conditions imposed on the problem are both fundamental and practical. While the practical aspects are clearly subject to change due to the progress of technology, it is sensible to consider the significant practical aspects as they are presently apparent (or expected to be in the near future), as they can be used to approximate the operating environment of the proposed memory system.

One of these constraints is the page format dimensions. This is determined by several factors such as optical resolution, detector dimensions, holographic medium thickness and the dimensionality of the the Spatial Light Modulator (SLM). Let us first examine the SLM. We select an array 1024 pixels on a side, in a square format, which are independently addressable. A suitable contrast ratio would be of the order of 30 to 1 or greater. The desired frame rate woulud be selected based on the principal memory function for which the system was designed. In most cases this will probably be satisfied by an SLM frame rate of 30 to 1000 Hz. It should be noted that with a page format containing roughly 10^6 pixels, a frame rate of 1000 Hz corresponds to a data rate of 1 GHz. Even a frame rate of 30 Hz will yield a very respectable data rate of 30 MHz. These SLM characteristics are not unreasonable and are already being addressed through active SLM development programs.

Another constraint which we impose on the system is that the camera used for readout of the data be a relatively low noise detector operated in a mode which permits near photon counting capabilities. Clearly, the number of elements in the detector array must match the SLM, and a format of 1024 by 1024 elements would be optimal. The performance of realistic, and presently available detector arrays [15] is shown in Figure 6 and Table IV. The curves in Figure 6 can be readily calculated from a simple formula relating the SNR to the detector noise (N_n), photon collection efficiency (η_d) and the randomness of the photon counting statistics (number of photons = N_p).

$$SNR = \frac{\eta_d N_p}{\sqrt{\eta_d N_p + N_n^2}} \quad (2)$$

This SNR is not only fundamentally possible using modern CCD technology but is practically achievable so long as significant attention is given to the readout rate. By this, we mean that the detector array must be read out at a rate which permits low noise charge carrier collection. Most detector arrays presently read the pixels in a serial manner. The frame rate is then simply the single pixel reading rate divided by the number of pixels. To prevent serial readout from being a severe time restraint, one is simply required to read a number of the rows of pixels in parallel.

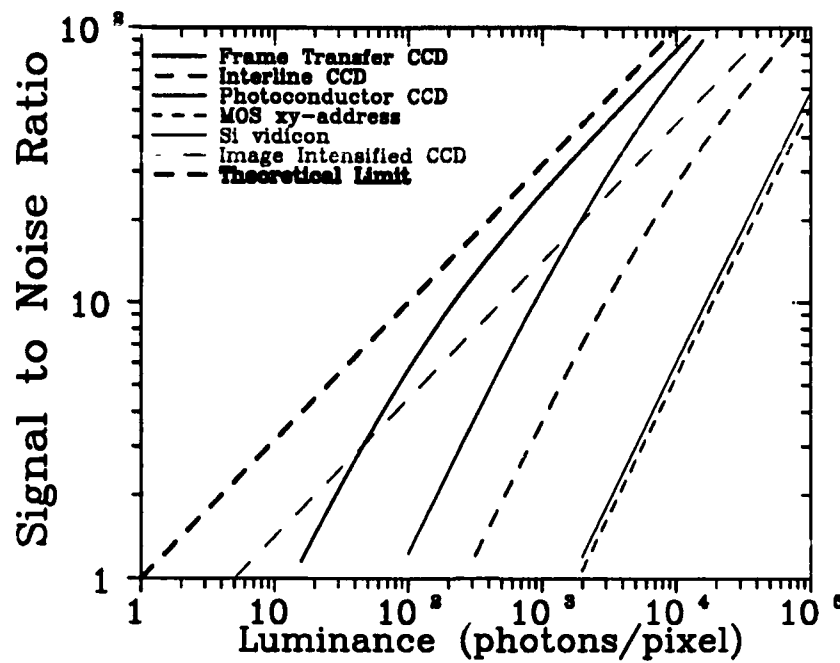


Figure 6. Photon-limited signal to noise ratio calculated from the data shown in Table 4 using equation (2). [15]

Parallel readout will keep the effective data rate high while the noise per pixel is kept low enough to permit photon counting to become practical. 32×32 pixel arrays with parallel readout are presently available and we have confidence in the potential for the commercial development of larger arrays by direct extension of present technology.

4.2 Data Format

The importance of the data format lies in the details of the permitted error rates and the known sources of systematic errors. At present, the principal sources of error in the system have been identified as the photon counting errors provided by the detectors and the cross talk errors which are possible when the storage medium nears its capacity limits. At present we shall assume that these cross talk errors can be described as somewhat statistical in nature if kept to small levels. This permits us to describe the error propagation characteristics in terms of Gaussian statistics.

The simplest data format would store each bit as an "on" or "off" in the recorded image. This data format would require each detector element to be either illuminated or dark upon readout and the reliability of the readout will be related to the signal to noise level involved in differentiating between the on and off states. The bits corresponding to a single byte might be stored on a single horizontal row, and a number of bytes could be stored on each row. At the end of each row (see Figure 7) is the customary checksum which records the number of "on" bits contained within a row. This checksum provides a commonly used error checking mechanism whereby the number of "on" bits is recorded at the end of the row in order to detect

Table 4. Characteristics of Modern Electronic Image Sensors.[15]

Sensor Type	Example	Application	Number of Pixels	Image Area (mm ²)	Sensor Noise (e/pixel)	Quantum Efficiency
Self-Scanned silicon sensors	Frame-Transfer CCD	Astronomy	2048×2048	55×55	9 (slow scan)	0.70 (thinned)
	Interline CCD	High-def TV	1280×980	12.7×9.5	36	0.14
	Photo-conductor over CCD	High def TV	1920×1036	14.0×7.8	52	0.65
Photo-conductive camera tubes	MOS xy-address	Color camcorder	649×491	8.6×6.5	745	0.40
	Saticon	High-def TV	1050000 (at 20 MHz)	12.7×9.5	1500	0.90
Image intensifiers	Si vidicon	Low light levels	210000 (at 4 MHz)			
	Image-intensified CCD Photon-Counting Imager	Scientific Astronomy	684×576 512×512 digital store	18mm (diagonal) Position-sensitive detector	High gain overrides noise	0.20 0.20

any erroneously read (or recorded) bits. In the event an error is detected, the page of data can be reread in order to determine the actual data correctly. To permit an efficient and rapid data flow, the required number of "rereads" should be kept to the 1 to 10 percent level, or even lower.

A reasonable permitted error rate which would invoke rereading might be 0.1 (10 percent). This error rate means that only one bit out of every 10^7 is permitted to be read incorrectly. The impact of this bit error rate (BER) can be estimated by examining the impact this might have on the "undetected bit error rate" (UBER). (The UBER would be the probability of reading a page of data and not knowing it is incorrect.) An undetected error can occur when both the checksum and the actual data within the same row contain errors which hide each other. The probability for this occurring when a single checksum is used is the probability of two errors occurring in the same row with one of the errors happening in the least significant bit of the checksum. The probability of this occurring is roughly 2×10^{-7} . Compared with typical digital data archival requirements, this is an unacceptably high error rate.

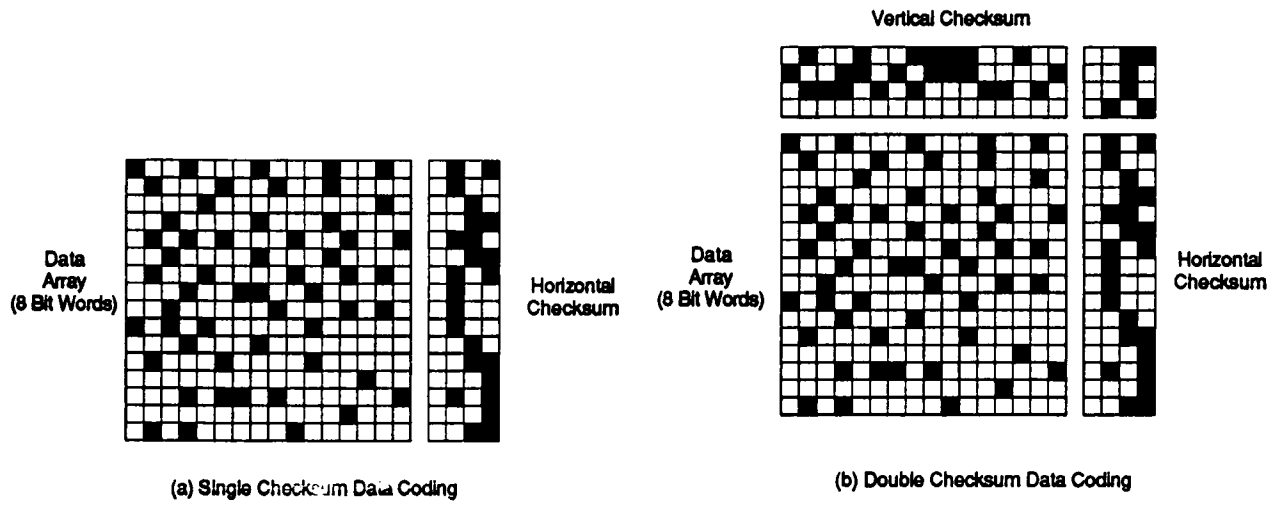


Figure 7. Schematic representation of a data coding scheme involving single (a) and double (b) checksums to provide a low BER and UBER. In an actual high capacity memory the dimensions of the array would be much larger (on the order of 1024 × 1024 bits) and the checksum segments would be proportionately much smaller.

Fortunately, this problem is relatively simple to overcome by the implementation of multiple checksum schemes. As simple example of such a scheme is seen in Figure 7(b) where an additional set of checksums are present for each column as well as each row of data. (We realize that a large number of potential schemes exist which are both efficient and simple, and this approach is given only as a simple example.) Under these conditions, any single error is actually detected by two separate checksums (one row and one column). This actually permits us to correct the data without rereading. Any two errors occurring simultaneously can now be detected. In fact, it now requires three separate errors, two of which must be located in the least significant bit of selected checksums, in order to prevent an error from being detected. Using this particular data storage scheme, the BER is now 10^{-8} while the UBER is 2×10^{-15} . This error rate would be very acceptable. At a data rate of 30 MHz, this would correspond to one error every 2 years, while at 1 GHz, this is one error every 23 days.

In order to implement this “double checksum” scheme we must dedicate a small amount of space at the end of each row and column for error correction. For rows containing 1024 pixels, the checksum must contain 10 bits. The total storage requirements then comprises only about 2 percent of the total memory capacity, and the reread rate is only about 1 percent. These modest requirements are quite acceptable.

4.3 Bit Error Rate and SNR

From the above analysis it is seen that a very acceptable BER is 10^{-7} . The probability that a particular single pixel will be in error can simply be related through Gaussian statistics as

$$BER = 2[1 - erf(SNR/2)]. \quad (3)$$

Equation (3) can be readily approximated by a series expansion.

$$BER = \frac{2e^{-x^2}}{\sqrt{\pi}x} \left(1 - \frac{1}{2x^2} + \frac{1 \times 3}{(2x^2)^2} - \frac{1 \times 3 \times 5}{(2x^2)^3} + \dots \right) \quad (4)$$

where $x = SNR/2$. This formula quickly converges for reasonable values of SNR and representative results are given in Table 5. The net conclusion which can be drawn from the results presented in this table are that a desirable SNR for the system would require a pixel level signal to noise of slightly less than 8. We can readily see that the reliability of the system is a strong function of the pixel level SNR, and that beyond a SNR of 10 it would seem that little is to be gained in realistic reliability. (We note that this estimate of acceptable errors assumes that the "false positive" errors are equal in probability to the "false negative" errors. The validity of this approximation is justified when considering the multiplicity of potential error sources such as detector noise and light scattering.)

Table 5. Pixel SNR Relation to System Probability of Error

SNR	P
5	1.24×10^{-2}
6	2.60×10^{-3}
7	1.55×10^{-6}
8	6.36×10^{-8}
9	7.27×10^{-10}
10	6.29×10^{-12}

This defines the required SNR for the entire system, which include "random" errors from all sources. If the error budget is composed of several factors, it may be reasonable to require that the contribution of any single error source must be a fraction of the total error. For this reason, we shall set a reasonable limit to the photon detection budget at a SNR of 11. This may overestimate the requirements but should provide a comfortable level of engineering latitude.

4.4 SNR and the Selection of Detector

From Figure 6 we can quickly determine that a SNR requirement of 11 would indicate a minimum of 121 photons at the detector plane per pixel for a perfect device. Because of advances in camera technology we can actually come quite close to this performance with either a frame transfer CCD (at 250 photons/pixel) or an image intensified CCD (at 605 photons/pixel). Both detector systems could provide excellent signal to noise at photon fluxes near the theoretical limits of reliable detectability. For the purpose of further analysis of memory system capacity we shall assume that the SNR required from other contributing sources be at least 11, and the photons per bit (PPB) requirement is fixed at 605 photons/bit.

Because the data are stored as simple binary bits, no A to D converter is required to interpret the data. A simple threshold arrangement will suffice. One might ask whether it would be of any advantage to store multiple bits within a single pixel by taking advantage of the potential for grey scale in the recorded image. The answer is no. The reason can be seen by realizing that an eight bit word is equivalent to 256 grey levels. The photon requirements per pixel go up

by a factor of 256, but the net gain in capacity per pixel is only 8. Because we shall see that the requirements of photons per bit is an important factor in determining system capacity, it is undesirable to increase capacity per frame at the expense of a greatly increased photon budget.

5 Erasure

The subject of data erasure is a significant one for most memory applications. On the one hand, one is required to be able to read the data without completely erasing it, either because erasure would mean that the data must be immediately rewritten, or because the potential that any information was read incorrectly will require that the same data set be read again. On the other hand, one would like to be able to erase (or at least write over) existing data so that the medium is effectively reusable. This ability to erase data at will can greatly extend the life of a usable memory, and greatly widen the range of interesting applications for even the largest possible storage capacity systems.

Similarly coupled with this issue is the longevity of the recorded information. The recorded information in an "inactive" system is simply a matter of determining if the recorded information spontaneously "decays" with time. This might be the case when the molecules used for storage are in an unstable state with a finite lifetime. The spontaneous decay of these molecules back to their original state could provide such a mechanism for data loss.

In an "active" system, the potential for data loss from spontaneous decay can be circumvented by periodically rewriting the data to prevent permanent loss. This approach to the decay of the data places a burden on the overhead maintenance of the memory by requiring that some fraction of the system operating time be devoted to simply "refreshing" the data. In many applications this may be an acceptable approach. As we shall see, the viability of this approach is principally determined by the data rate and amount of data actually stored in the system.

5.1 Introduction and Requirements

As was described earlier, the intended specifications of the envisioned memory system involve data rates which may range from 30 MHz to 1 GHz, and storage capacities of from 10^{12} to 10^{14} bits/cm³. The data is stored in binary form, and is recorded in a square page format 1024 pixels on a side (roughly 10^6 bits per page). If some active mechanism is required for refreshing the system, this activity should not impose more than a 10 percent overhead on the operation of the system, permitting the user rapid random access at all times.

There are several potential mechanisms for erasure which may be viable in a SHB-based holographic memory system.

1. Photoreversible chemical species. If the photochemical change induced by the laser is reversible by the action of light, one may be able to directly repopulate the bleached molecular set, thereby erasing the recorded data and permitting reuse of the same molecules for recording new data.
2. Thermally reversible chemical species. If the photochemical change can be reversed by warming the material to above the normal operating temperature, the stored information can be erased. This could be a viable approach when multiple memory units are used in parallel. The actual capacity of the system is the maximum capacity of all the units except one. The extra unit is used for the temporary storage of information. In this manner, while most of the units are under active use, the extra unit can be heated to a temperature high enough to completely erase the stored information and restore it to its initial level for recording new information.

Before we can address the issue of intentional erasure, however, we must face the problem

of unintentional erasure brought on by the laser light used to read the stored information.

5.2 Inactive System Data Decay

Only a modest amount of experimental data is available on this subject but it would appear that one can easily select SHB materials which provide data decay periods greater than years. [16] This is particularly true for organic photochemically bleachable species. The key element in the durability of the recorded information lies in maintaining the cryogenic temperatures required. This requirement may not seriously impact the usefulness of this approach because cryostat systems can be readily designed which will maintain their low temperatures without power for very extended periods (even months). This protects against the accidental loss of data and even may provide a means of providing substantial system life without the use of a refrigeration unit. (We shall discuss the issue of cryostats in a later section of this report.)

Some exceptions to the requirement of maintaining a low temperature have been found, however. A number of workers have shown that several organic materials can be raised to somewhat elevated temperatures (as high as 77 K) for extended periods with only a modest decay in the amplitude of the recorded image. Furthermore, one material (Sm^{2+} in BaClF [17]) has shown that the medium exhibits only modest loss of bleached amplitude when raised to room temperature. (Unfortunately this material is crystalline in nature and therefore does not have the large inhomogeneous linewidth desired for a large storage capacity medium.) It is possible that future materials research may permit an adequate solution to the problem of the durability of data at room temperature, but for now the engineering options in cryostat design can provide an adequate and, we expect, a cost effective solution to the problem through system design.

5.3 Reading Versus Erasure

The photon flux required to read a recorded hologram (Φ_r) is simply related to the number of photons per bit required at the detector plane(PPB), the number of bits in each page (N) and the efficiency with which the hologram was recorded (η) as

$$\Phi_r = \frac{PPB N}{\eta}. \quad (5)$$

The photon flux required to create the same hologram initially (Φ_w) is simply

$$\Phi_w = \frac{n_p N}{QE} \quad (6)$$

where n_p is the number of molecules used to record each bit reliably and QE is the quantum efficiency. At all times the flux required for reading the data must be less than that used to record it, otherwise the data can be assumed to be erased without successfully being read. (This is actually true only when the system is being used at near full capacity, which is a worst case assumption that we accept.) The number of reads permitted before the data must be refreshed (R_e) is then simply

$$R_e = \frac{\Phi_w}{\Phi_r} \quad (7)$$

or

$$R_e = \frac{n_p \eta}{PPB QE}. \quad (8)$$

5.4 Erasure and Data Rates

Equation (8) can take on a simple meaning when we examine the constraints provided by material heating during the recording of data. If we assume that the data is stored as absorption holograms, the maximum storage density is achieved by utilizing a material having an optical density of approximately 0.87. (This is because the maximum diffraction efficiency of an absorption hologram is obtained from a material having an optical density of 0.87. Under this circumstance, most of the light is absorbed in the medium, and becomes converted to heat. To maintain the SHB medium at a suitable temperature for achieving a narrow homogeneous linewidth the temperature must not be permitted to rise significantly. For example, if the normal operating temperature of the material is 4 K, the temperature should not be permitted to rise from this temperature by more than 1 degree.

The specific heat of a typical plastic material (such as polystyrene) at low temperature is about 4 mJ/g-K[18]. From typical organic material thermal conductivity values for materials such as polyethylene [19] we can estimate a value of about 1.3 mW/cm-K.

The quantitative problem of heat dissipation can be addressed by simply assuming conductive heat loss from the SHB host medium to the supporting cryostat. Under the circumstance where the conductivity of the host medium is the limiting factor the problem can be solved directly. Because organic polymers and inorganic glasses (which are the chief candidates as host materials) all have quite low thermal conductivities, we can safely identify the host medium as being the limiting factor.

The problem can be seen by reference to Figures 8(a) and 8(b). In the first case the SHB medium is in the form of a cube and is bounded on two surfaces by very conductive materials. We shall assume the simplest case of steady state heating conditions where the heat is supplied uniformly to the medium. (We realize that the heat will actually be imparted in a manner depending on the absorptive properties of the medium, but we believe this to be a relatively unimportant correction factor to the analysis at this time.) As stated above, our goal is to prevent any part of the SHB medium from increasing in temperature by more than 1 degree. This problem in heat flow can be solved exactly [20] and we find that

$$\Delta T = \frac{A_o(l/2)^2}{2 K} \quad (9)$$

where

A_o is the rate of heat generation in the material,

l is the length of one edge of the cube (1 cm), and

K is the thermal conductivity of the medium.

For the case shown in Figure 8(a) we can solve equation (9) for A_o and find that the maximum steady state heat load on the SHB medium is approximately 10 mW.

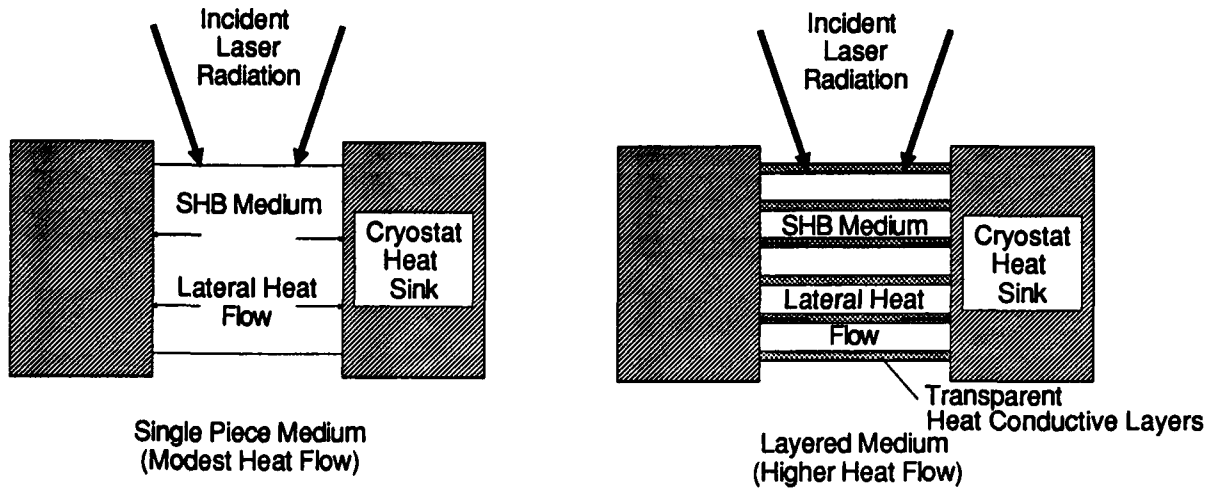


Figure 8. Schematic diagrams showing two potential structures for the SHB medium in the supporting cryostat. In case (a) the heat flow is somewhat limited by the low conductivity of the SHB medium. If highly heat conductive layers (b) are added (which are optically transparent) the heat load to the medium can be increased by a factor of 25 for a medium divided into as few as five layers.

Because the heat dissipation rate is related to the square of the thickness of the medium, a potential avenue for improvement lies in the approach of layering the medium and sandwiching the layers between pieces of much more conductive (but transparent) material. As shown in Figure 8(b), a small number of layers (5) might be used. The conductive material could be a crystalline salt such as KCl or NaCl which have conductivities as high as 10 W/cm-K [21] at cryogenic temperatures, yet are transparent and have refractive indexes very similar to that of organic polymers such as polyethylene. Under these conditions, the conductive medium need not occupy more than a modest fraction of the volume, yet can have a significant impact on determining the maximum heat load. Using equation (9) we now find that the maximum heat load can be increased to 250 mW with only a modest amount of complexity added to preparation of the SHB medium. Clearly, one could pursue this approach further by making even thinner layers, but then we might face new limits to the practical implementation. For example, a higher heat load capacity implies that the laser power is quite high, as well as the capacity of the cryostat being similarly high. These two factors are of relevance because laser powers or heat loads in the vicinity of 1 Watt or more can begin to make a significant impact on the power consumption of the complete memory system, or even on the technical feasibility of the entire approach in the near term.

The maximum permissible heat load (H_{max}) is equal to the maximum power allowed to write the holograms. The intensity (I_w) for writing (in photons/sec) is simply a function of the

data rate (DR) in bits per second, quantum efficiency, and number of molecules used to record each bit (n_p).

$$I_w = \frac{n_p DR}{QE}. \quad (10)$$

If we specify the wavelength of operation to be approximately 700 nm, then the minimum QE permitted (i.e. defined by the heat load limit) is

$$QE = \frac{hc n_p DR}{\lambda H_{max}}. \quad (11)$$

When combined with equation (8) we find

$$R_e = \frac{\lambda H_{max}}{PPB h c} \frac{\eta}{DR}. \quad (12)$$

In the above expression, the parameters corresponding to the wavelength, maximum heat load, and number of photons per bit are constrained. They are fixed by our general system design, and because of arguments presented earlier, they are determined by practical considerations. While the exact values of these quantities can be affected by technical progress, these factors are probably relatively fixed for the near term.

When we insert our present estimates for these parameters we get

$$R_e = 1.455 \times 10^{15} (\text{sec}^{-1}) \frac{\eta}{DR}. \quad (13)$$

The importance of the above expression lies in the fact that our read/erasure limit is intimately connected to our data rate and the hologram efficiency. As we shall see later, the hologram efficiency is a direct determinant of the storage capacity of the medium. The system capacity goes as the inverse of the square root of hologram efficiency, therefore **the data rate is inversely proportional to the square root of system capacity**. The net conclusion is that one can readily trade data rate for a reasonable cost in system capacity.

Earlier, we had indicated that the overhead required for refreshing data should not exceed 10 percent of the total system operating time budget. To accomplish this, it would then be reasonable to require that R_e should take on a value of approximately 20. We had earlier indicated that the interest for this memory system lay between two potential data rates, 30 MHz and 1 GHz. Using these as defining parameters we can then determine the limiting hologram efficiencies as being

$$\eta = 4.12 \times 10^{-7} \text{ for a 30 MHz data rate,}$$

$$\eta = 1.37 \times 10^{-5} \text{ for a 1 GHz data rate.}$$

These hologram efficiencies are defined by the practical limitations as mentioned so far. Clearly, one cannot utilize arbitrarily low hologram efficiencies because of the potential extraneous scattering which can effectively introduce an enhanced noise level and endanger our data reliability.

The anticipated scatter may be expected to be of the order of 0.1 percent even for a well designed system. If this scatter is isotropic, and we have an optical system with an N.A. of 0.15,

the fraction of the photon flux used in reading which will be directed towards the detector plane is about 2×10^{-6} . The scattered photons/pixel (S_p) is then given (from equation 5) by

$$S_p = \frac{2 \times 10^{-6} PPB}{\eta}. \quad (14)$$

It is probably justified to consider the scatter as being random and contributing to a somewhat uniform background for the readout of data. It would seem judicious to keep this background reasonably low, however, so that fluctuations in the scatter do not overwhelm the signal. This can be accomplished by requiring that S_p be less than half of the value of PPB. We may estimate this restriction to be satisfied when the hologram efficiency is maintained at 4×10^{-6} or greater. This hologram efficiency will be used later to define the system capacity limits. This hologram efficiency is not unreasonably low, as has already been demonstrated.^[15] In the first reported demonstration of hologram recording and readout in SHB materials, holographically recorded information was recorded with an efficiency of 10^{-6} and read out with a very acceptable signal to noise. This demonstration suggests that there are no apparent fundamental scattering issues in defining our limits with respect to scattering. In fact we are apparently being quite conservative in our estimates of performance.

5.4.1 Burst Mode Operation

The analysis above provided an argument describing the continuous operation data rate of the memory system and showed that the data rate was intimately related to the total system capacity. This analysis implies that one might need to trade access time for capacity. This need not be completely true for the transient reading of data at high rates, however. Because the heat capacity of the medium is 4 mW/cm^3 one has the option of supplying up to 4 mJ at a very high rate before being concerned about the overheating of the material and slowing down to a level compatible with the conductivity limitations of the material. This suggests that the SLM, beam steering, and detector components could be operated at maximum speed (whatever that may be) in order to minimize access times to modest sized data sets.

How large would one of these "modest sized" data sets be? The number of bits (N_{burst}) which can be read using 4 mJ of laser power is given by

$$N_{burst} = \frac{4 \text{ mJ } \eta \lambda}{h c PPB}. \quad (15)$$

Selecting the hologram efficiency to be the worst case situation of 4×10^{-6} we find that the data set size which can be read under burst mode operation is approximately 100 megabits. This burst mode capability may be of interest when data retrieval is not continuously required at a high rate, but initial access time must be short.

5.5 Intentional Erasure

The above discussion of reading versus erasure examined the systems issues surrounding the ability to store and retrieve information by considering the major components of the system and the properties of the host material for the photochemical species. We shall now examine the properties of the photochemical species of interest and how their selection impacts the ability to erase data at will in order to extend the useful life of the memory.

A number of potential schemes can be proposed which would permit molecular species to be photochemically altered reversibly, but we must not waste effort searching for fundamental properties which have not been observed, or which may be argued to be very unlikely from fundamental arguments. Based on this approach, we find that the interesting options are reduced to a selected few.

5.5.1 Parallel Systems

This would provide the simplest and most direct option to intentional erasure. In a parallel system architecture there is at least one system which is actively being written on. New data is recorded there, as well as old data being copied there from a previously filled system which has reached capacity. When all the data in the old system has been transcribed, the old system can be refreshed by heating the SHB medium to a temperature which restores the medium to its original state. When brought down to operating temperatures, it can again be used as an active system for recording. This refresh operation probably does not require much time when compared with expected system capacity and data rate, however it does require a duplicate set of electronic, optical, laser, beamsteering, SLM and detector components.

5.5.2 Multiple Photochemical Species

A similar approach can be utilized on the molecular level if the photochemical reaction can be reversed by illumination with light at a second wavelength. One has the option for refreshing the medium without raising its temperature. To take complete advantage of this approach, the principal wavelengths of absorption for the photoproduct should be well separated from that of the initial species. An excellent example of this is provided by the molecule chlorin shown in Figure 9. This molecule is simply a modified version of porphyrin in which one of the exterior double bonds has been converted to a single bond. This makes the two tautomers of this molecule nonequivalent due to this break in the symmetry. The energy states of these two tautomers are now separated enough to cause the absorbing transitions to differ by more than 50 nm.

The absorption spectrum for this material is shown in Figure 10 and indicates the clear separation between the initial and final states. For the case of chlorin, one could expect that the data could be recorded using laser wavelengths in the vicinity of 634 nm. When desired, the medium could be refreshed by illumination at 578 nm. Because the inhomogeneous broadening is seen to be of the order of 10 nm, one has the opportunity to use multiple photochemical species which have similar properties. For example, if a simple chlorin derivative had similar photochemical properties but an absorption spectrum which was shifted by 10 nm, one would find that the full range over which information can be recorded has been extended to 20 nm. This tactic can be repeated by using as many as 5 separate chemical species which would provide a total recording range of approximately 50 nm.

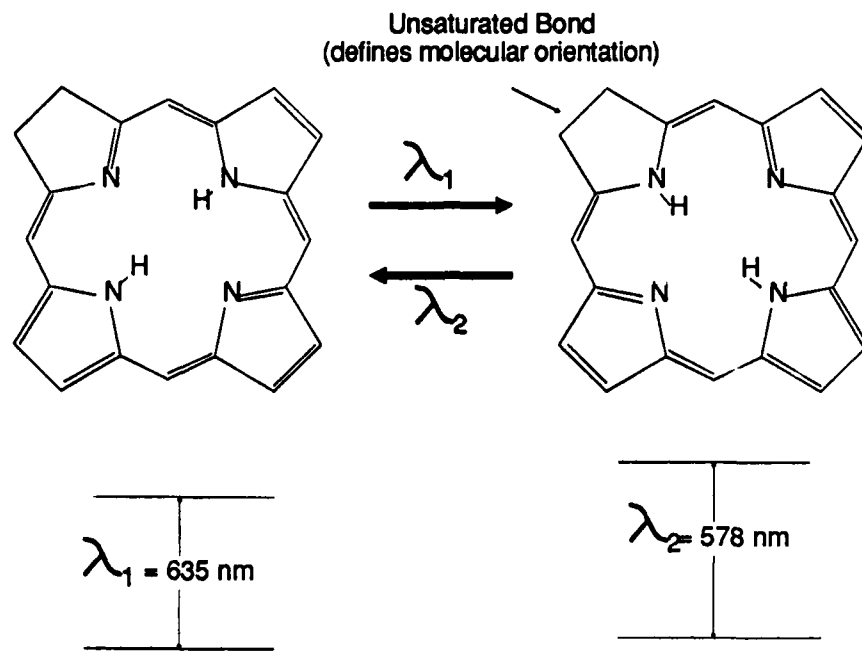


Figure 9. Schematic drawing of the chlorin molecule and the corresponding energy level diagram for the two tautomeric forms. Note that the saturation of one of the exterior carbon-carbon bonds lowers the symmetry of the molecule and causes the two tautomers to become well-separated in energy.[22]

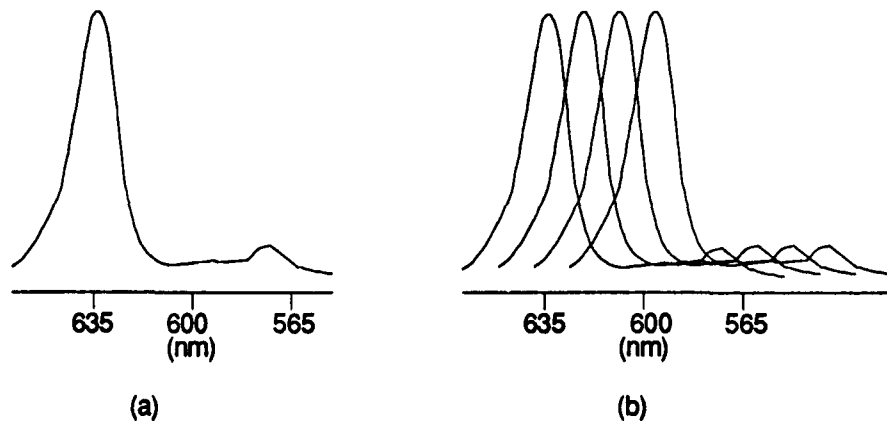


Figure 10. The absorption spectrum of the chlorin molecule and its photoproduct are shown in (a). Chemical modifications of this species could provide similar molecules with shifted absorption characteristics (b) which can extend the wavelength range of the medium as well as allow separate segments of the memory to be selectively refreshed during normal operation.[22]

Just as the recording range was extended by multiple species, so was the range over which the photoproduct absorbs. Because the different photoproducts absorb independently, one has the opportunity to erase one segment of the memory independent of the other segments simply

by selecting the proper wavelength in the photoproduct spectrum.

One can view the memory system as being subdivided into 5 segments. At any time, four segments are available for recording or transcribing data while the fifth segment is being refreshed photochemically. This accomplishes the same functionality as the use of parallel systems, but at a significant reduction in hardware cost by avoiding the duplication of hardware.

An attractive concept of photo-induced erasure would be to expect that because the wavelength of the bleached photochemical species is well-defined by the initial laser wavelength, one might expect a well-defined absorption "spike" in the photoproduct spectrum. Unfortunately, this is not the case, for the details of how the absorption spectrum is determined by the surrounding host molecules will depend on the details of the molecular bonding orbitals. Because this interaction is very complex, the absorption spectrum of the photoproduct will have a width which is comparable with that of the inhomogeneous spectral width. For this reason, we cannot be very selective in the erasure beyond that of refreshing large block segments.

We do have one advantage, however, in that the laser used to refresh a memory segment need not be tunable to a precise level, and it can even operate at the same time as the laser used for reading and recording. It will provide some heat load to the cryostat, but this can be handled by providing adequate cooling capacity. The refresh lasers need not even be tunable, as one would only require five independent light emitting diodes of coarsely selected wavelengths which would be of modest cost and performance.

5.5.3 π Phase Erasure

Another option for erasure which could be explored would involve selective erasure through the recording of holograms which are 180 degrees out of phase from the original data.[23] Erasure of selective sets of data can be accomplished by recording the same hologram on top of the original one but introducing a 180 degree phase shift in the reference beam. In this manner the initial data can be effectively erased by bleaching it away. Unfortunately, this operation uses some of the recording range of the medium and is therefore the equivalent of simply recording a new hologram of the opposite sign. The benefit of this approach only becomes significant when a small fraction of the data in a single page is to be altered or corrected. If a page consists of 10^6 bits, and only 100 bits need be erased, then the hologram which needs to be recorded only uses 1/10,000th of the number of molecules of a full page. We find that we use only a very small fraction of the recording range allotment in order to update a specific page of data.

We therefore see a means to extend the life of the recording medium by selectively erasing small segments of data from each page. This constitutes an erasure mechanism which may be of interest under special circumstances. The key factor in determining its usefulness lies in whether the type of data which is to be stored in the medium is of this type, and the cost of implementation of this approach. Because of the limited applicability of this approach for memory applications, designing this capability into the system may be of limited benefit except when special performance requirements indicate the need.

6 Using the Real Part of the Refractive Index

A problem with spectral hole burning as it has been studied so far is that it is largely absorption-oriented. In a bit-oriented memory scheme this is ideal because it provides a "black and white" demarcation of the bit which relates directly to the measured light signal. Bit-oriented optical memories, however, are limited generally to an optical thickness of the material related to the depth of focus (and, therefore, resolution) of the optical system used.[24] Therefore, the full volume of a thick material (0.5 to 1 cm) is difficult to address. This same absorptive attribute also limits the efficiency of the holograms that can be stored (and therefore their number). This limitation can be seen from consideration of Kogelnik's coupled wave analysis of mixed hologram efficiency. [25] The expression he derived is shown below and indicates that the modulation of either the real or imaginary components of the refractive index can contribute to the efficiency (η) of the hologram.

$$\eta = [\sinh^2(\alpha_1 d / 4 \cos \theta) + \sin^2(\pi n_1 d / \lambda \cos \theta)] e^{-\alpha_o d / \cos \theta}, \quad (16)$$

where

α_1 = the modulation of the absorbtivity,

α_o = the average absorbtivity of the material,

n_1 = the modulation of the real component of the refractive index,

θ = the the half angle between the incident and reference beam used to create the hologram, and

d = the thickness of the holographic medium.

If the holographic material has any average absorptive properties, then the overall efficiency of the hologram will be directly limited by simple absorption effects through the exponential term in equation (16). These inherent absorptive effects cause absorption holograms to be limited to 3.7 percent efficiencies, while phase holograms (stored in nonabsorbing materials) can reach efficiencies of 100 percent. In fact, if the dynamic range of the index modulation is large enough, multiple holograms, each of 100 percent efficiency, can be stored in the same material, at the same wavelength.

When one considers the storage of multiple holograms of modest efficiency (less than 1 percent) the quadratic terms in equation (16) simplify to being proportional to simple squares of the real and imaginary index modulations. Given this relationship we find that the hologram efficiency declines as $1/N_H^2$, where N_H is the number of holograms stored. This can be seen to limit the number of holograms which can be stored directly. If a hologram efficiency of 10^{-5} is required, equation (16) will permit the storage of only 60 holograms as absorption holograms. If the dynamic range of the real component of the refractive index permits the storage of a single 100 percent efficient hologram, then 316 holograms can be stored. Because the phase hologram approach has no fundamental limit (other than practical material property considerations), the number of phase holograms which can be stored is virtually unlimited. The key is to then explore material approaches which permit phase hologram storage and have the potential for large dynamic ranges.

Both bit-oriented and holographic memories based on absorption require large amounts of light to be absorbed during reading operations causing rapid erasure of the data. Refractive

index modulation (phase) holograms do not suffer from these problems. They have the ability to diffract the light without significant absorption. Using holograms permits data storage in depth, and using the real part of the refractive index permits reading of data without erasure; these are two critical factors in achieving a truly enormous data density in a useful system.

6.1 Background on Spectral Hole Burning

The concept of spectral hole burning (SHB) is best understood on the molecular level. A single molecule has a set of energy levels between which transitions are allowed. If the energy of the photon approximately matches one of the transition energies required, the photon can be absorbed by the molecule. If upon absorption, a chemical change to the molecule is induced, the absorption levels of the new molecule will not match the old ones. Therefore, the new molecule will not absorb light at the frequency of the first photon. In this way, the absorption capabilities of the molecule can be radically changed by exposure to light.

The width of the absorption peak is determined by the fundamental lifetime of the energy levels involved, and the vibrations of the molecule and the medium in which it is contained. The resultant spectral width is called the **homogeneous linewidth**. At low temperatures, the broadening because of thermal effects can be reduced to 10 to 30 MHz.[26-30] Because of the highly periodic structure of a crystalline lattice, a large number of molecules will absorb at the same frequency when immersed in a single crystal. If the molecules are contained in a glass with little or no short range order, however, each molecule sees a unique environment, providing separate absorption frequencies. This spread in frequency caused by the variation in molecular environment is known as the **inhomogeneous linewidth** and is generally quite large (10 THz or more[26]). (10 THz is about 12 nm wide at a wavelength of 600 nm.)

It is important to remember that the inhomogeneous absorption peak for a glass is composed of a large number of individual molecular populations which can be individually addressed by selecting frequency (see Figure 11). Exposure at a single frequency which causes a photochemical change can effectively make the medium more transparent ("burn a hole") in the medium over a narrow frequency range. The frequency width of the "hole" is simply the homogeneous linewidth of the medium.

This effect has been studied over the last 10 years in both organic and inorganic glasses and has been shown to be clearly observable with spectral widths ranging from 1 GHz at 77 K to 10 MHz at 1 K.[26] It has been previously shown by others that this approach could be used for storage of data via absorption holograms [31] and as bit-oriented spectral holes.[32] It has even been shown that multiple spectral holes can be made at the same frequency using different applied electric fields (i. e., Stark broadening).[1]

6.2 Modeling the Absorption Edge

The Kramers-Kronig relation[33] expresses the direct relationship between the real (refractive) and imaginary (absorptive) parts of the dielectric constants of a material (and therefore the real and imaginary parts of the refractive indices). For a single absorption line the relation is seen in Figure 12. Because of the spectral absorption at a single homogeneously broadened frequency the refraction is altered in the near vicinity of the absorption peak. The key point to be noted is that the absorption falls off more rapidly than the refractive effect. If the absorption could be modulated spatially, one could read a phase hologram when the reading frequency is off

resonance, and an absorption hologram when on resonance. If the modulation is large enough and the absorption at the reading frequency low enough, near 100 percent efficiency is possible with phase hologram storage.

If the absorption peak is made wider by using a multiplicity of populations centered over a range of frequencies, then the real part of the refractive index can be enhanced near the absorption edge. The effect is logarithmic with frequency width, but the effect can be large enough to make the peak of the real part of the refractive index modulation much larger than the peak of the imaginary part (see Figure 13). The location of the peaks of index and absorption modulation, in frequency space, are still shifted relative to each other, allowing reading in a low absorption region of the spectrum. This structure can be replicated many times in frequency space and each can be accessed independently simply by changing the illumination frequency.

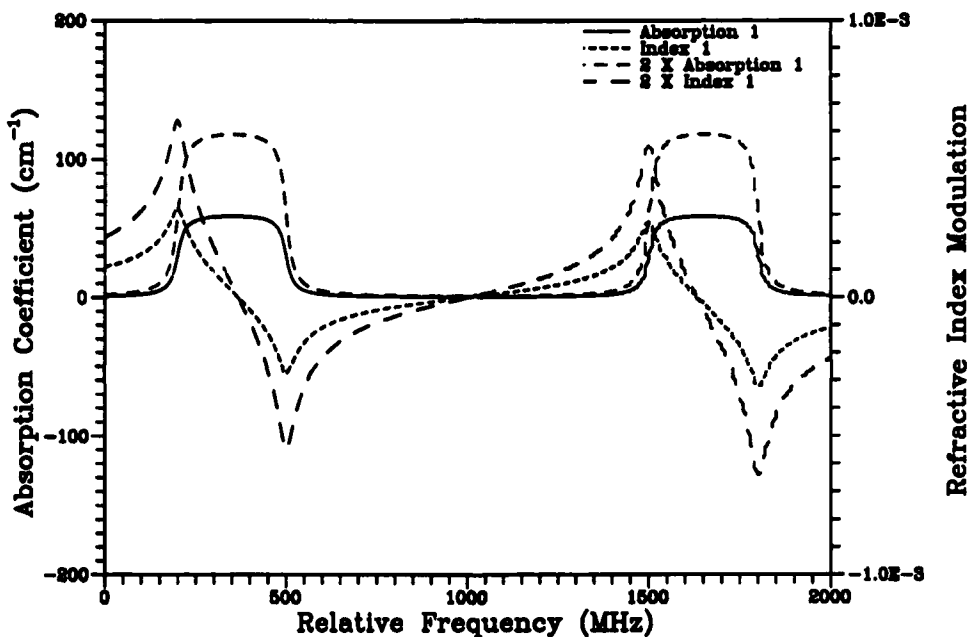


Figure 13. Schematic of two adjacent absorption structures showing the modulation of the resultant refractive index. Such a structure is possible with porphyrin in polyethylene at 4 K. The frequency coordinates of this structure will essentially scale as $T^{1.3}$.

6.3 Access to the Capacity of the Material

Increased access is allowed by adding more degrees of freedom (dimensionality). Storage as a function of frequency can provide such access. The frequency channel structures shown in Figure 13 are best viewed as access paths into and out of the material for reading and writing purposes. Without these channels, the material would be too opaque to permit reading or writing. Without the adjacent absorption structures, the material would permit inadequate access to realize the ultimate capacity of volume media. By structuring the material in frequency space, the material has been separated into sections permitting access and sections permitting storage.

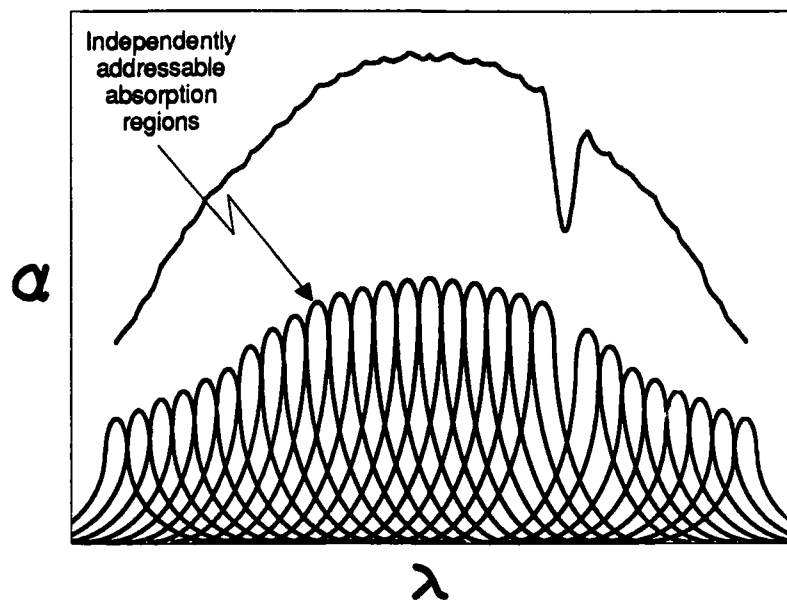


Figure 11. Schematic diagram representing the concept of individually selectable molecular populations within an inhomogeneously broadened spectral line.

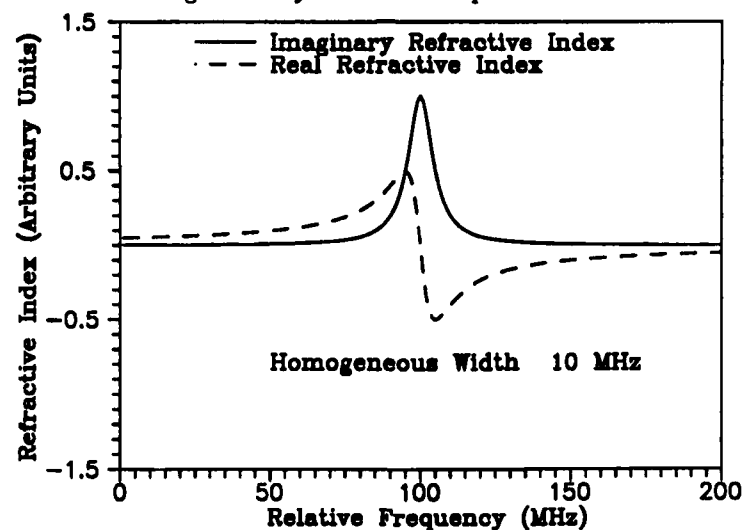


Figure 12. Real and imaginary components of the refractive index for a single damped oscillator. Note that the real part has a range that extends well beyond that of the imaginary component.

6.4 Detailed Modeling of Frequency Channels

To gain an understanding as to whether the frequency channel approach is of practical value, it is important to perform some detailed modeling of the key aspects of the approach. Two key issues are examined in detail in this section:

- 1) What is the magnitude of the refractive index modulation possible in a frequency channel structure of suitable dimensions?
- 2) Can such a structure be created in a manner which is practical, and yet provide the performance desired?

These two issues are addressed in the analyses shown below.

6.4.1 Index Modulation Near an Absorption Band Edge

If a single molecule is modeled as a harmonic oscillator with a small amount of damping, one can derive functions describing the real ($1 + n_1$) and imaginary (k) parts of the refractive index. (The imaginary part of the refractive index is related to the absorption coefficient (α) by the formula $\alpha = 4\pi k/\lambda$, where λ is the wavelength of light used.)

$$k(f, f_r) = \frac{K}{2f_r} \frac{\Delta f}{(\Delta f/2)^2 + (f - f_r)^2} \quad (17)$$

$$n_1(f, f_r) = \frac{K}{f_r} \frac{f - f_r}{(\Delta f/2)^2 + (f - f_r)^2} \quad (18)$$

where Δf is the homogeneous spectral width of the absorption, f_r is the resonance frequency of the oscillator, and f is the frequency of illumination. [33] The constant K is determined by the fundamental properties of the molecule. These functions are plotted in Figure 12 and show that the absorption falls off much more rapidly than the real part of the refractive index.

The formulae to be derived here represent a population of oscillators whose central frequencies are distributed over a finite range between f_1 and f_2 . A simple case will be used where the population density is a step function within the range and zero everywhere else. Upon integration we find that the formulae for the imaginary and real parts of the refractive index are simply

$$k(f) = K \left[\tan^{-1} \frac{2(f - f_2)}{\Delta f} - \tan^{-1} \frac{2(f - f_1)}{\Delta f} \right] \quad (19)$$

and

$$n_1(f) = -\frac{K}{2} \ln \frac{(f - f_2)^2 + (\Delta f/2)^2}{(f - f_1)^2 + (\Delta f/2)^2}. \quad (20)$$

It is equations (19) and (20) which are plotted in Figure 13. (k has been transformed into its equivalent absorption coefficient value in that figure.) This derivation represents a first order representation of a potential memory structure in frequency space.

The magnitude of the index modulation can then be directly translated into the phase hologram efficiency as is done in Figure 14. From the index modulations shown in Figure 13 we

can see that the efficiency of the phase hologram(s) which are stored can be quite substantial. An index modulation of 10^{-4} in the real component of the refractive index would seem readily obtainable in a frequency range where the absorption is acceptably low (less than 1 percent or lower absorption). When inserted in a material which is 1.0 cm thick, the dynamic range permits storage of 3 holograms of high efficiency (efficiency which is limited only by the modest absorption within the frequency channel). This will clearly permit a significant storage capacity.

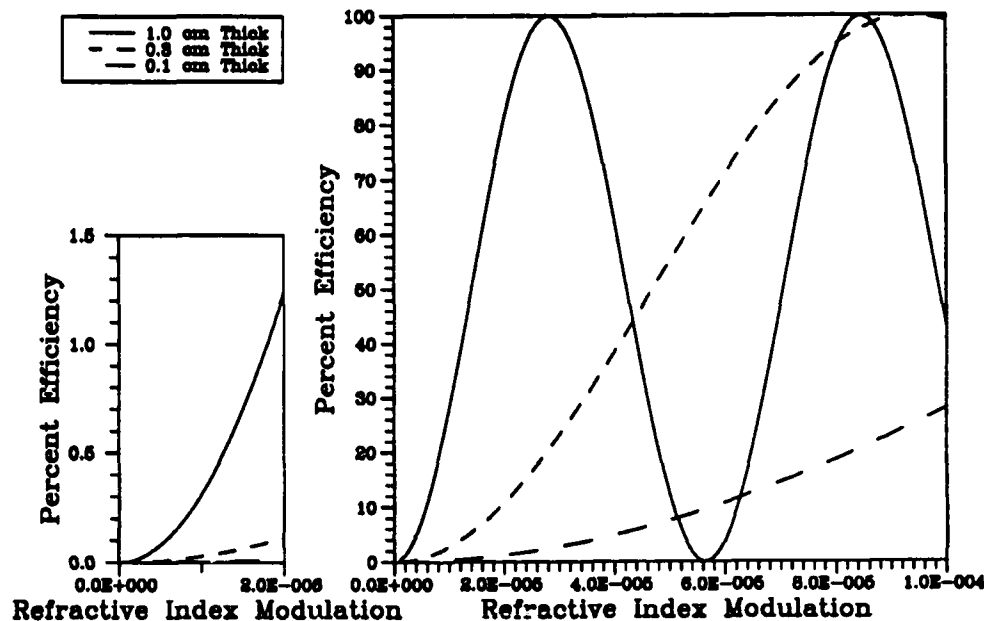


Figure 14. This diagram relates the magnitude of the modulation of the real component of the refractive index to the efficiency of the phase holograms which can be stored in the material. Several thicknesses of material are shown for comparison.

6.5 Creation of Frequency Channels in SHB Materials

In the above analysis, the means by which the frequency channels are created was largely ignored. It was simply assumed that the frequency channels could be completely bleached and had molecular distributions which could be represented by step functions. These theoretical simplifications are useful as a first approximation, and could represent adequate representations of the actual performance under certain circumstances. Such a circumstance would be one where the channels are created at a temperature lower than the operating temperature, with a very narrow linewidth laser, and with a large amount of time used in their creation. These circumstances may be impractical (or at least cumbersome), however. To model the effects of a more realistic channel creation process we have developed a model which takes into account the finite properties of the laser and homogeneous linewidths of the SHB material, as well as the limitations on the ability to bleach the material.

The bleaching process is characterized by the relationship

$$\frac{dN}{dt} = \frac{-N}{h} \int_{-\infty}^{\infty} \sigma(f, f_r) P(f, f_b) df \quad (21)$$

where

N is the instantaneous number density distribution of molecules,

t is time,

h is Planck's constant,

f_r is the molecular frequency,

f is the frequency of a photon,

$\sigma(f, f_r)$ is the molecular absorption cross section distribution function,

f_b is the instantaneous centerline frequency of the laser, and

$P(f, f_b)$ is the instantaneous power density distribution function of the laser.

The molecular absorption cross section is again assumed to be a Lorentzian function,

$$\sigma(f, f_r) = \frac{\sigma_o}{\pi} \frac{\Delta f_r/2}{(\Delta f_r/2)^2 + (f - f_r)^2} \quad (22)$$

where

σ_o is the total absorption cross section of the molecule and

Δf_r is the homogeneous linewidth of the molecule.

We shall assume that the process of creation of the frequency channels is one of simply sweeping the laser (as a function of frequency) across the frequency channel. The power density distribution of the laser spectrum will also be approximated by a Lorentzian function:

$$P(f, f_b) = \frac{P_o}{\pi} \frac{\Delta f_b/2}{(\Delta f_b/2)^2 + (f - f_b)^2} \quad (23)$$

where

P_o is the instantaneous irradiance of the laser beam and

Δf_b is the linewidth of the laser beam.

The population density after hole burning may be obtained by combining equations (21), (22), and (23); as *

* This formulation assumes that the laser operates at constant power from time t_o to time t_f . For cases in which this assumption is invalid, equation (24) is replaced by the equation

$$\frac{N}{N_o} = \exp \left(\frac{-\sigma_o}{h} \cdot \frac{1}{\pi} \int_{t_o}^{t_f} P_o \frac{\Delta f_b/2 + \Delta f_r/2}{(\Delta f_b/2 + \Delta f_r/2)^2 + (f_b - f_r)^2} dt \right)$$

and the subsequent analysis is somewhat more complicated. However, this can be directly integrated numerically.

$$\frac{N}{N_o} = \exp \left(\frac{-\sigma_o P_o}{h} \cdot \frac{1}{\pi} \int_{t_o}^{t_f} \frac{\Delta f_b/2 + \Delta f_r/2}{(\Delta f_b/2 + \Delta f_r/2)^2 + (f_b - f_r)^2} dt \right) \quad (24)$$

after evaluating the frequency integral in equation (16).

Phase hologram storage would be expected to be most effective when the edges of the channels are sharp relative to their width. In order to achieve the desired sharpness, both the linewidth of the burning laser and the homogeneous linewidth of the material must be small compared to the width of the channel. Assuming a constant slew rate during the creation of the channel leads to,

$$f_b = f_o + f'_b (t - t_o) \quad (25)$$

where

f_o is the initial frequency of the laser beam and

f'_b is the frequency slew rate.

Combining equations (24) and (25) and evaluating the integral,

$$\frac{N}{N_o} = \exp \left(\frac{-\sigma_o P_o}{h f'_b} \cdot \frac{1}{\pi} \left(\arctan \left(\frac{f_f - f_r}{\Delta f_b/2 + \Delta f_r/2} \right) + \arctan \left(\frac{f_r - f_o}{\Delta f_b/2 + \Delta f_r/2} \right) \right) \right) \quad (26)$$

where f_f is the final frequency of the laser beam.

In the above N/N_o is simply the depletion ratio (the fraction of molecules which remain after the channel burning process) at a particular frequency (see the lower section of Figure 15). The first factor in the exponential function, $\frac{-\sigma_o P_o}{h f'_b}$, effectively defines the asymptotic limit of the depletion ratio for infinitely wide channels. This term predicts, as expected, that a deeper channel can be created by increasing the power of the burning laser or by slewing more slowly.

Full exploitation of the frequency channel approach suggest that multiple frequency channels be burned into the material. The effect of burning several channels may be computed from the relationship:

$$\frac{N_m}{N_o} = \prod_{i=1}^m \frac{N_i}{N_{i-1}} \quad (27)$$

where

m is the number of channels,

i is the channel index, and

N_i is the molecular number density distribution after i channels have been burned.

If we assume that each channel is burned independently (i.e. there are no complicating physical phenomena which limit us) we can readily combine equations (26) and (27) as

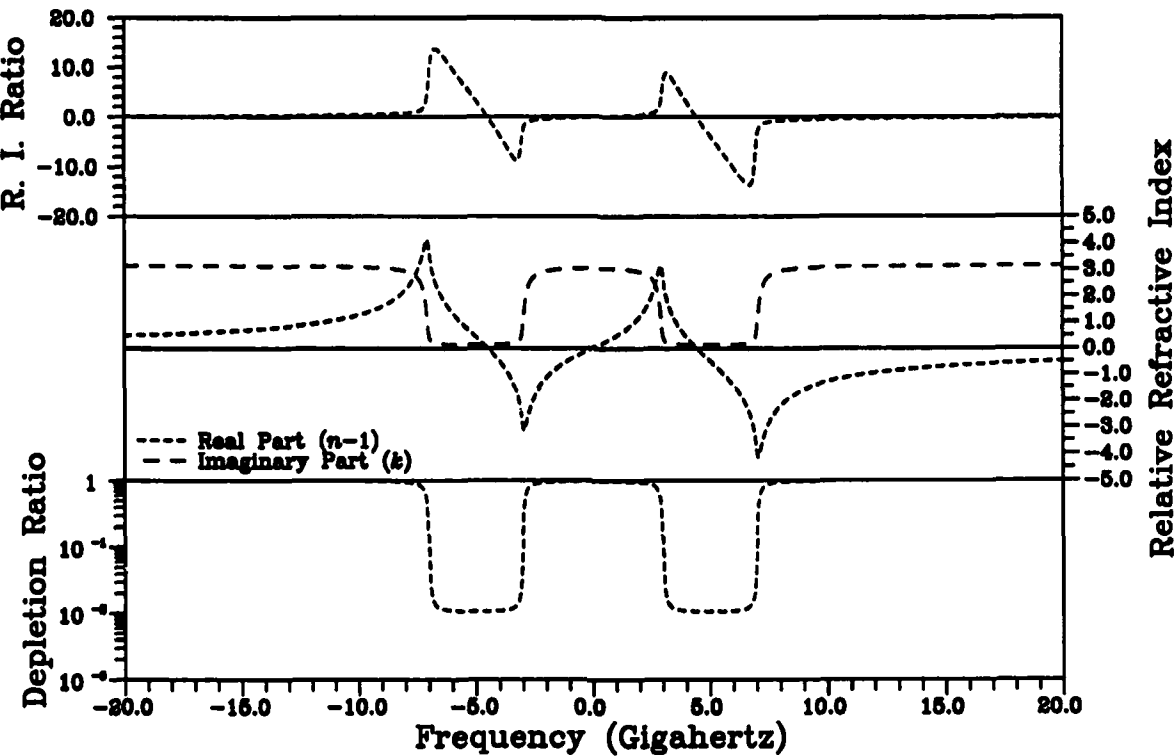


Figure 15. Calculated optical properties of a realistic model for a frequency channel structure. The laser linewidth and homogeneous linewidth are both 100 MHz.

$$\frac{N}{N_0} = \exp \left(\frac{-\sigma_0 P_0}{hf_b'} \cdot \frac{1}{\pi} \sum_{i=1}^m \left(\arctan \left(\frac{f_f^{(i)} - f_r}{\Delta f_b/2 + \Delta f_r/2} \right) + \arctan \left(\frac{f_r - f_o^{(i)}}{\Delta f_b/2 + \Delta f_r/2} \right) \right) \right) \quad (28)$$

where

$f_o^{(i)}$ is the initial frequency of the laser beam for the $(i)^{\text{th}}$ channel and

$f_f^{(i)}$ is the final frequency of the laser beam for the $(i)^{\text{th}}$ channel.

The characteristics of equation (28) are similar to equation (26), with the summation of arctangents always falling between 0 and π as long as the frequency channels are distinct.

6.5.1 Refractive Index Characteristics After Channel Formation

The magnitudes of the real and imaginary components of the refractive index can be directly calculated (using equations (17) and (18)) once the molecular distributions are provided by equation (28). Unfortunately the resulting expressions are not readily integrated through analytic techniques and therefore must be evaluated numerically. These results can be seen represented in the middle segment of Figure 15 and shows that the major qualitative and quantitative aspects of the refractive indices are retained when compared with Figure 13.

From an examination of equation (16) we can see that the key factor to be considered here is not the absolute value of the index modulation which is possible (we have already shown that the magnitude is quite substantial for thick materials) but the relative magnitudes of the real and imaginary components. By keeping the refractive index ratio (R.I. Ratio) of these components high it is possible to have significant phase modulation with acceptable absorption losses. From an examination of the upper segment of Figure 15 it can be seen that the ratio can easily attain magnitudes of over well over 10. This magnitude for the ratio is rather important. By reference to equation (16) and knowing that $\alpha = 4\pi k/\lambda$ we can immediately realize some reasonable performance capabilities. If α is defined so as to permit 50 percent transmission in a 1.0 cm thickness, then we find that the real component of the refractive index can take on a magnitude of about 3.3×10^{-5} . From Figure 14 this translates into a phase hologram efficiency of 100 percent which is then attenuated to 50 percent by simple absorption. In this way, the storage capacity of the material has been increased at a single frequency. Similarly, if the refractive index ratio is increased further, one can reduce absorptive losses almost proportionately, thereby increasing storage capacity, or reducing heat absorption by the SHB material. These tradeoffs can now be made to suit the specific operational needs of the 4-D memory system.

6.5.2 Computer Simulation and Results

SPARTA's computer simulation of the spectral hole burning process was designed so that additional effects, such as non-uniform initial molecular distributions and non-constant values of the constant K in the above analysis can readily be integrated and evaluated in conjunction with a follow-on effort. Figures 16, 17, and 18 show representative output from this simulation for the creation of multiple channels in a material having a homogeneous line width of 100 MHz using a laser with a line width of 100 MHz.

The most striking result of these modeling efforts is that the refractive index ratio (R.I. Ratio) peaks at a well defined frequency when a realistic absorptivity remains unbleached in the channel. This points to a clearly defined frequency at which optimal hologram readout should take place. (Such a clear choice of optimal frequency was not available from the simple analysis of a completely bleached channel.)

These figures also show that increasing the depth of the frequency channel (reducing the depletion ration by increased bleaching) seems to have modest influence over the R.I. Ratio. Adding extra channels does not change the fundamental features of the structure, and increasing the spacing between channels does not markedly increase the R.I. Ratio above 15. We do note that increasing the spacing between channels (see Figures 17 and 18) does have a noticeable effect upon the influence which adjacent structures have on each other. This influence between adjacent structures is effectively a measure of the level of cross talk between frequency channels. In a latter section of this document we shall determine that an acceptable level of cross talk is of the order of 1 part in 20. Since the magnitude of the cross-talk is proportional to the square root of the index modulation effects, we only require that the influence between structures be reduced to 1 part in 4.5. This translates into a spacing between these structures of the order of 3 GHz. If we arbitrarily increase the spacing to 10 GHz in order to keep the R.I. Ratio high, we will clearly have low cross-talk and high hologram storage capacity.

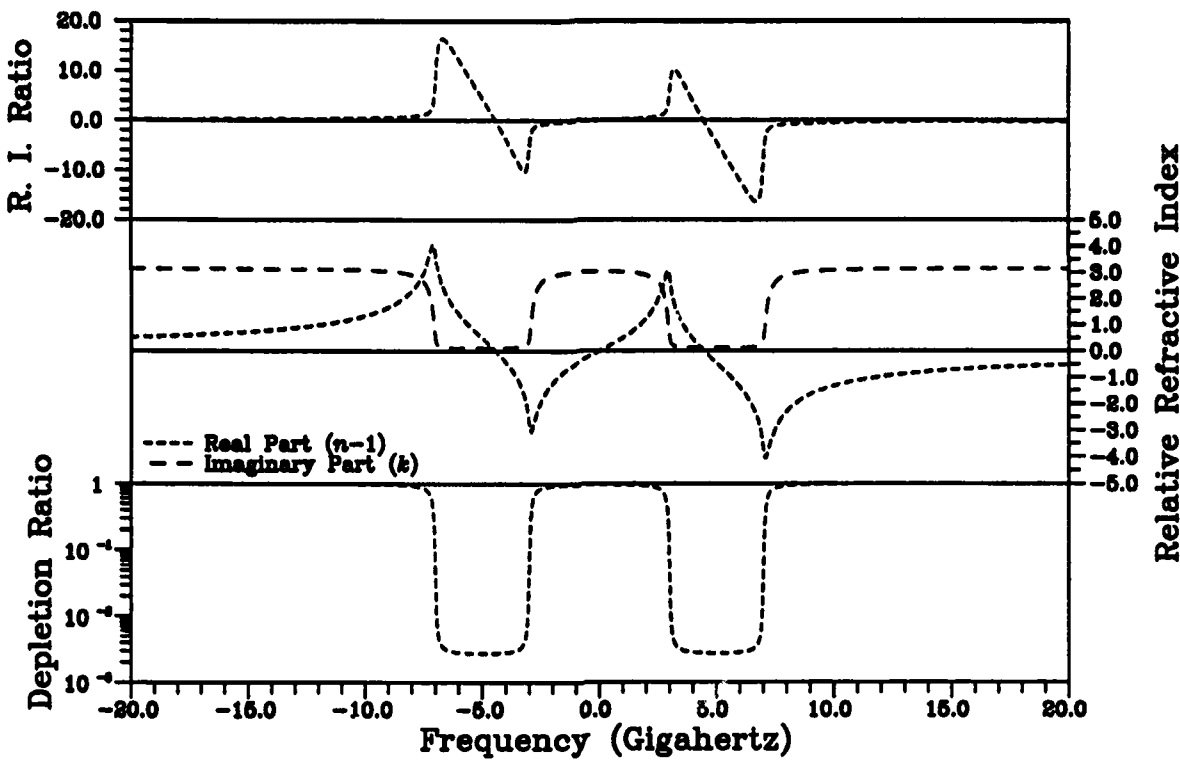


Figure 16. Calculated performance of the frequency channel structure assuming that the channel is bleached to a greater depth.

6.6 Debye-Waller Factor

The above analysis has been carried out in the complete absence of any concern about whether the materials exist which can provide the appropriate bleaching characteristics needed. In particular, the principal requirement is that the photochemical species be cleanly bleachable to a high degree, that is, to a level which is in the range of a few percent or less of the original absorptivity of the material. In an idealized SHB material this would pose no problem, but there is a complication which is introduced by the phonon sideband of the photochemical species when it is imbedded in a solid support matrix. The origin of the phonon sideband requires some discussion.

For an isolated photochemical molecule at low temperature the absorption spectrum is a single shape line with added satellite absorption lines at higher frequencies due to the contribution from vibrational excitations. (We shall assume that rotational excitation can be ignored because we shall assume the molecule to be static in space.) Upon introduction of the molecule into a supporting host material, the potential now exists that absorption of a photon can excite vibrations in the support medium. This potential for transferring some of the absorbed energy into vibrations of the medium provides a broad absorption band at energies which are higher than the sharp zero-phonon absorption line. One also has the potential for absorption at energies which are lower than the zero-phonon line because the vibrations of the support medium can also add energy to the photon and provide a broad but weak absorption in this manner.

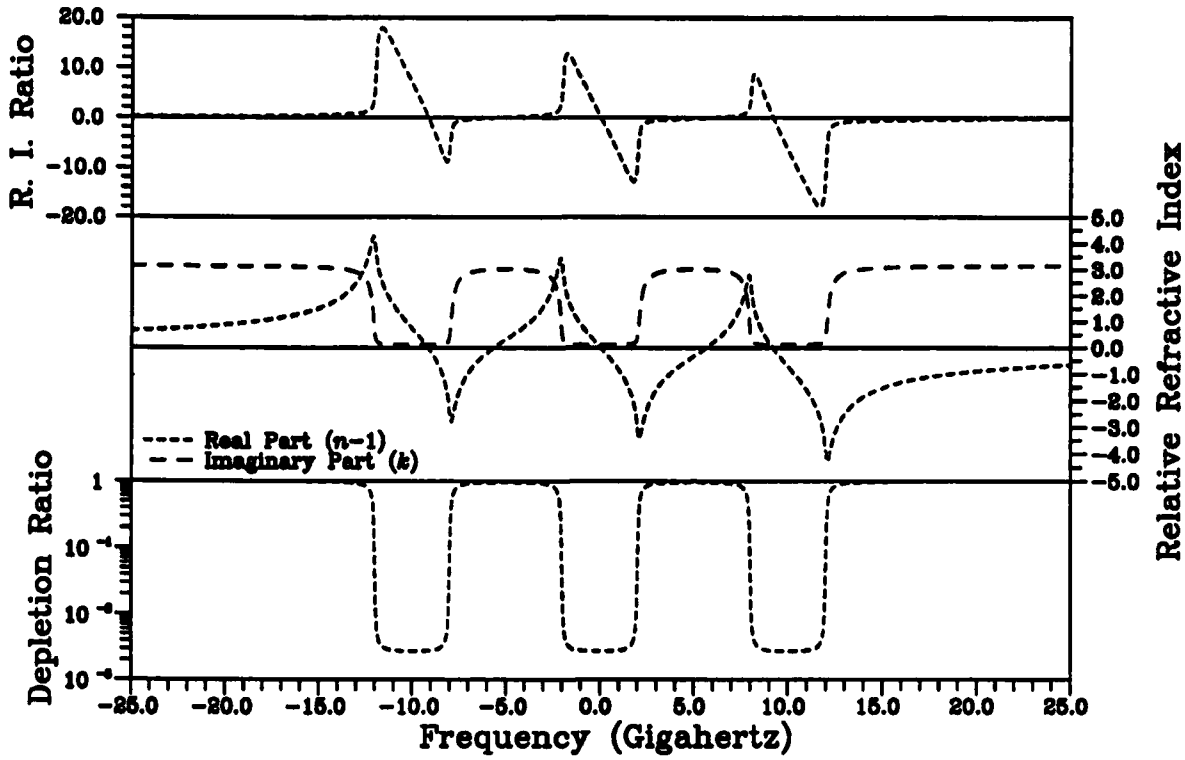


Figure 17. Calculated performance of the frequency channel structure showing how the increase in number of channels affects the index modulation.

The integrated amplitude of the zero-phonon line relative to the phonon sideband is determined by the Debye-Waller factor (α_{DW}). This quantity effectively measures the level of coupling which is present between the molecule and the host material and is defined as[34]

$$\alpha_{DW} = \frac{S_o}{S_o + S_p} \quad (29)$$

where

S_o is the integrated intensity of the zero phonon line, and

S_p is the integrated intensity of the phonon sideband.

The phonon sideband will be quite small as the Debye-Waller factor approaches 1. For our purposes, a Debye-Waller Factor of 1.0 would be ideal.

The fundamental coupling between the photochemical molecule and the host medium is driven by the Stokes shift of the lattice oscillators accompanying the electronic transition which dominates the absorption. This means that the details of how the excited state of the molecule interacts with the surrounding host medium are critical. For example, if the photochemical molecule has a dipole moment which changes upon absorption, and the host medium molecules also have permanent dipole moments, we can expect that there will be a strong interaction between the absorption process and the vibrations of the medium. This will cause the phonon side band to be large and the Debye-Waller factor to be small.

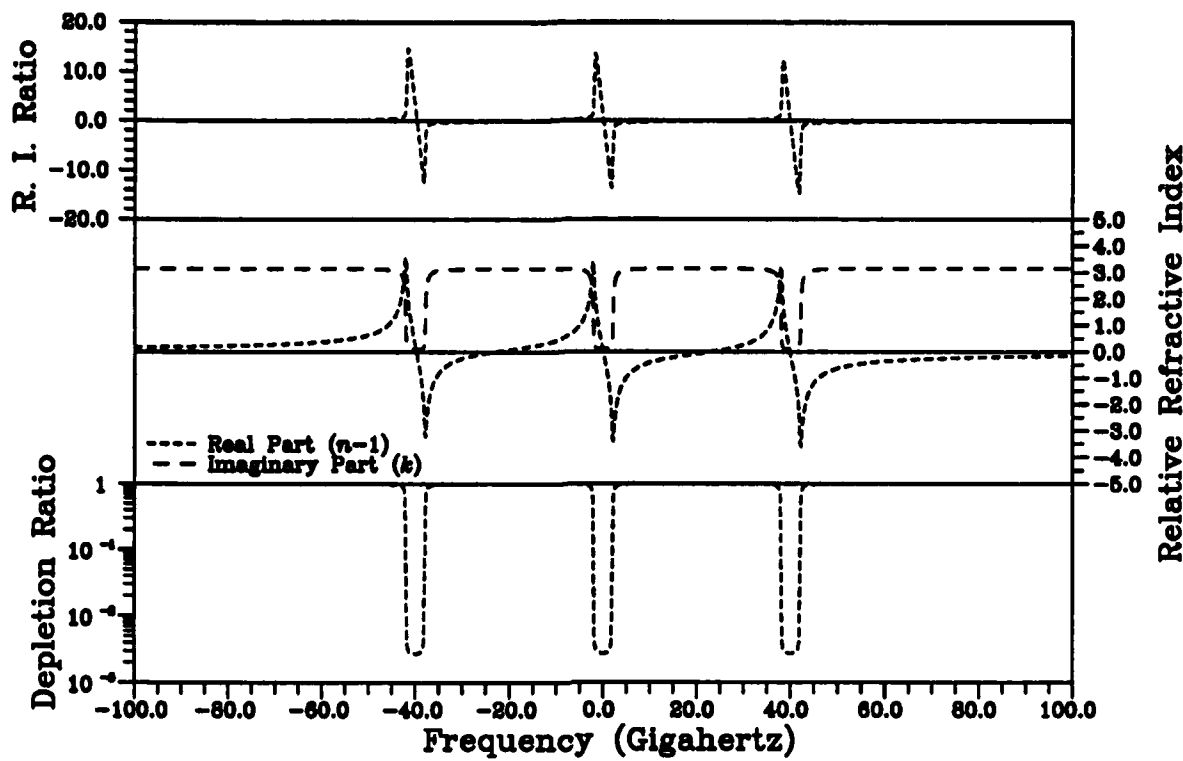


Figure 18. Calculated performance of the frequency channel structure showing how the increase in spacing between channels reduces modulation cross-talk effects.

Clearly this effect can be reduced by minimizing the interactions between the photochemical molecules and the host medium. This may not be a trivial task since the factor which provides the spectral diversity (inhomogeneous linewidth) in the first place is the interaction between the photochemical molecule and the host medium. However, in order to have a significant impact on the absorption spectrum, the phonon coupling to the electronic transition must occur by some rapidly operating mechanism such as dipole moment interactions.

It is unlikely that electron phonon coupling can ever be completely eliminated since even though the host medium may not have any permanent dipoles, it may be polarizable. Furthermore, the photochemical molecule may not have a net dipole moment, but it may possess a higher order moment of significance. The net result is that the Debye-Waller factor can be brought close to 1 by proper selection of the photochemical molecule and the host medium, but it can never be made to be exactly 1.

The reason the phonon sideband is of importance is seen in its effect on the absorption spectrum of an inhomogeneously broadened line (see Figure 19). If the Debye-Waller factor were to take on a nominal value of approximately 0.8, the fraction of the total absorption which is allocated to the phonon sideband is 20 percent. Since the phonon sideband is always associated with each zero phonon absorption line, the net effect is to have the broad absorption peak contain a baseline absorption which is 20 percent of the total absorption. This means that this virgin absorption medium cannot be bleached to a depth greater than 80 percent at a single wavelength without causing a broad band absorption to occur for a wide range of frequencies. This would

initially imply that our frequency channels in this material cannot be bleached to a depth greater than 80 percent instead of the 99 percent which would be desirable. There is a reasonable solution to this problem.

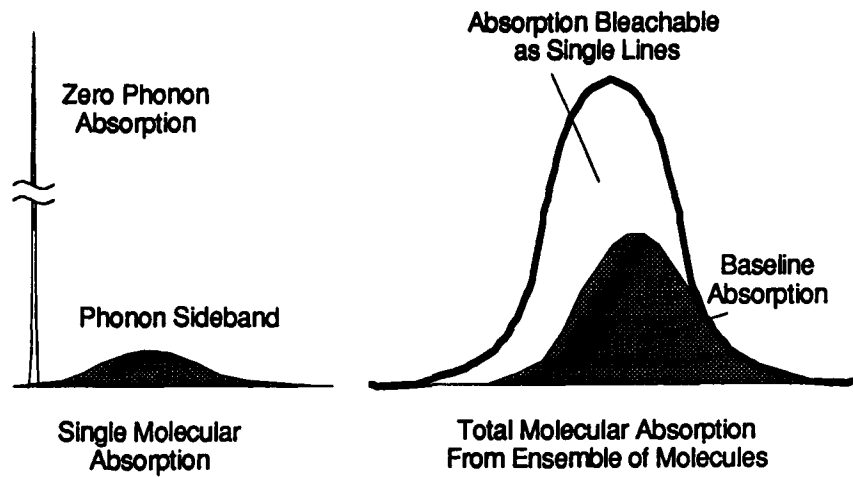


Figure 19. The effect of the Debye-Waller factor being less than 1 causes a baseline absorption which underlies the inhomogeneously broadened peak. It prevents a single spectral hole from being bleached below this baseline level but can be overcome by making the channels wider than the absorption structures.

The solution lies in the leveraging of the frequency channel structure itself. By bleaching away the molecules which are present in an entire series of frequency channels which span the inhomogeneous peak, we effectively eliminate the phonon sideband absorption which is also associated with these molecules. If the channels are wider than the remaining absorption structures, then the baseline absorption can be reduced by a factor which is the ratio of the channel width to the width of the absorption structure. For example, by making the channel width 10 times the width of the absorption structure, the channel depth can now be bleached to a level which leaves behind only 2 percent of the original absorption of the photochemical species.

We therefore find that two of the key factors in determining the depth (and therefore the quality) of the frequency channels are (1) the Debye-Waller factor which is influenced strongly by the selection of the photochemical molecule and the host and (2) the relative widths of the frequency channels and the absorption structure. The Debye-Waller factor can be measured directly by determining the depth of the bleached spectral hole. A typical reported depth is 80 percent[30] for an SHB medium. The relative widths of the channels and absorption structures will most likely run the range from 10 : 1 to 2 : 1. This range of variation will be determined by factors relating to system capacity, data rate, and other operational factors of importance.

The direct impact of material properties on system capacity can be directly seen through a comparison of the frequency channel structures seen in Figures 20, 21 and 22. In these examples we have arbitrarily chosen to reduce the channel depth and spacing between channels in order to estimate the index modulation which can be reliably obtained from these structures. As the baseline absorption (at the bottom of the bleached channel) is increased from 1 to 4 percent the

magnitude of the real component of the index modulation barely changes. As we shall see, the magnitude of the refractive index ratio (R.I. Ratio) is the principal determinant of the number of holograms which can be superimposed at a single wavelength. The number of superimposeable holograms goes roughly as the square of the refractive index ratio. From a close examination of Figures 20, 21 and 22 we can see that the R.I. Ratio seems to be proportional to the inverse of the square root of the baseline absorption. By increasing the baseline absorption by a factor of 4, the R.I. Ratio has been reduced by approximately 30 percent, which reduces the number of superimposeable holograms by a factor of approximately 2. As we can see, the frequency channel approach seems suitably tolerant of a significant baseline absorption due to materials issues related to the Debye-Waller factor. Furthermore, we shall see that we face a limit to the number of superimposable holograms due to systems related optics issues.

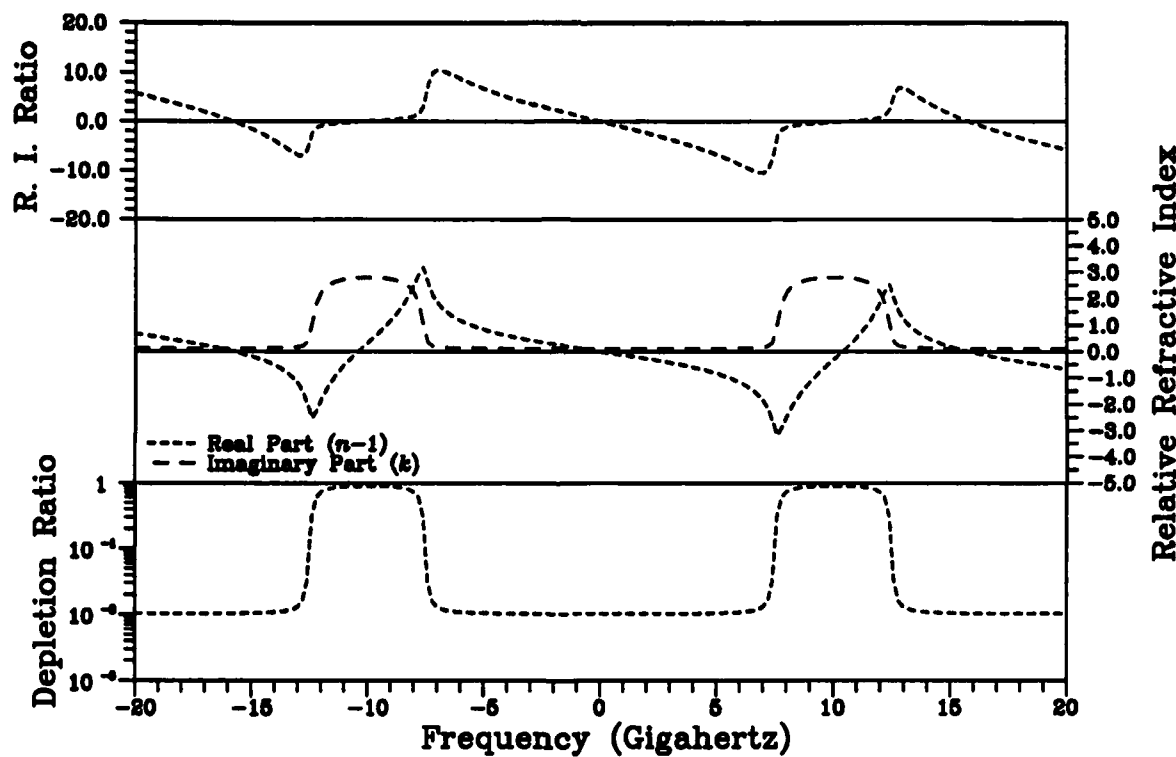


Figure 20. Calculated performance of the frequency channel structure assuming that the channel is bleached to a depth of 1 percent with a 20 GHz channel spacing.

6.7 External Field Effects

The application of an external field to an SHB material in which holes have been bleached can shift the energy levels which define the exact absorption frequencies corresponding to the bleached hole. Since the external field can interact with each molecule individually, the net effect can be to redistribute the molecules in a manner which spreads them in the frequency dimension. Two principal externally applied fields have been discussed in the literature, electric fields and stress fields.

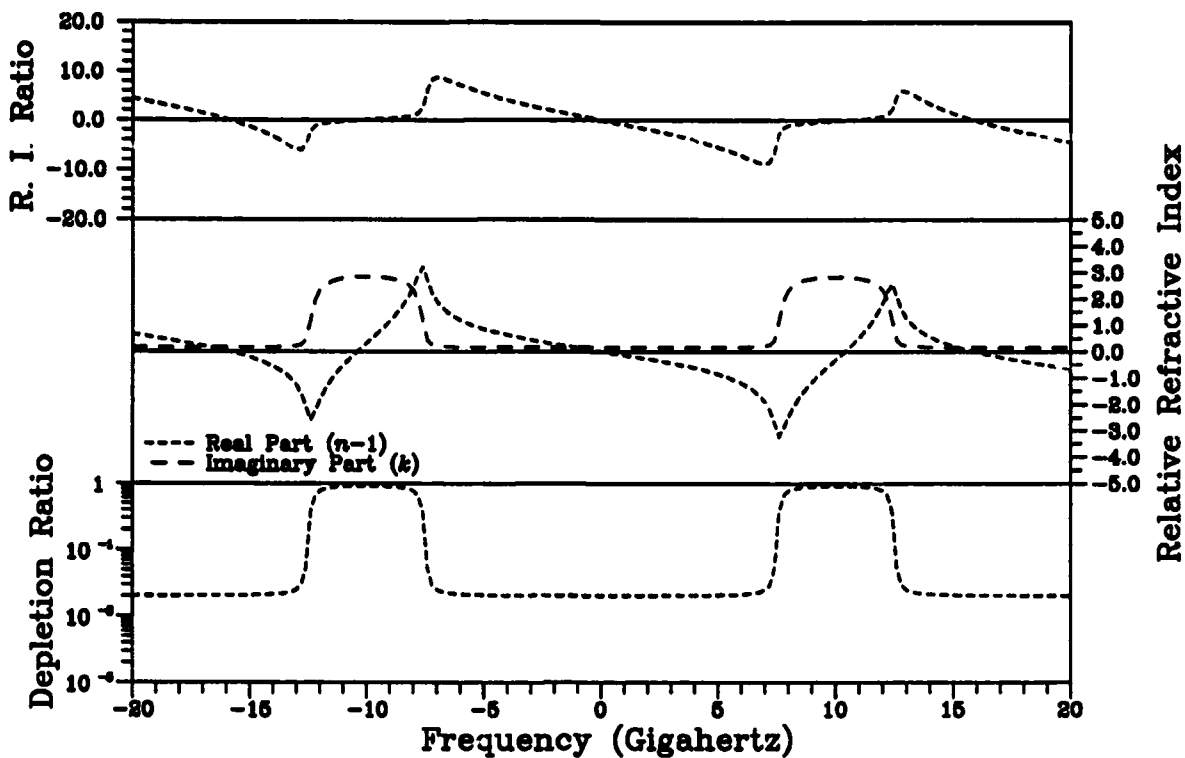


Figure 21. Calculated performance of the frequency channel structure assuming that the channel is bleached to a depth of 2 percent with a 20 GHz channel spacing.

An externally applied electric field has the opportunity to interact with the photochemical molecule through its dipole moment via the Stark effect.[1] In order to cause a shift in the absorption frequency, the transition from the ground to the excited state must involve a net change in the dipole moment. The combined Stark shift of the ground and excited states depends upon the angles of orientation of the dipole moments and provides the means by which a single molecule can alter its absorption frequency. The net change in the frequencies of an ensemble of molecules in an amorphous or glassy matrix is generally one where a narrow frequency distribution is broadened uniformly.

An externally applied stress field can alter the energy level of a molecule by slightly distorting the local environment surrounding the photochemical molecule. This generally causes a broadening of the absorption frequencies as well as a net shift of the absorption frequency.

These two external field effects have been suggested as means by which molecular ensembles can be rearranged in order to enhance the data storage capacity of the SHB medium. When considered in terms of the frequency channel structure, the application of an external field takes on a completely new significance. The reason for this relates to the way that the data must be recorded in the frequency channel concept.

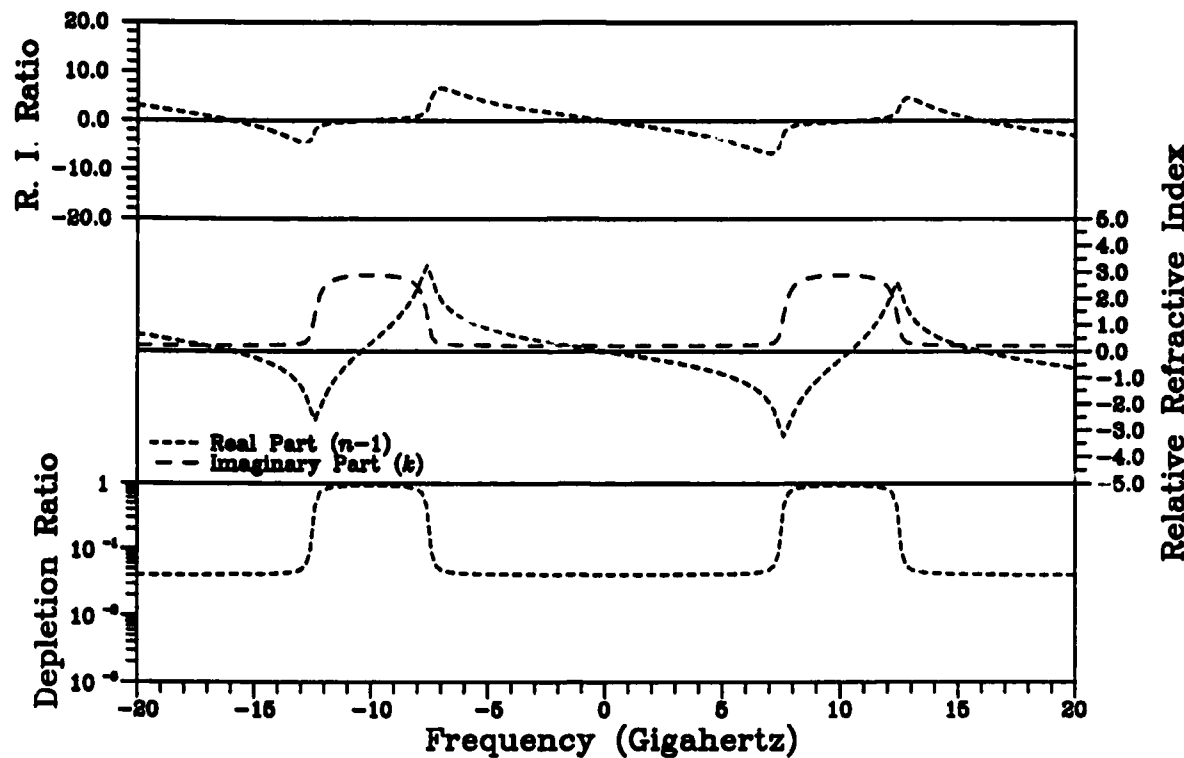


Figure 22. Calculated performance of the frequency channel structure assuming that the channel is bleached to a depth of 4 percent with a 20 GHz channel spacing.

6.7.1 Data Recording in Frequency Channels

A close examination of one of the absorption edges (see Figure 23) shows that the optimal location for reading phase holograms (the location where the refractive index ratio is a maximum) is actually offset from the absorption edge by a factor of 5 to 10 times the homogeneous linewidth. This means that the molecules which generated the index modulation that is being observed at these frequencies are located a significant distance away (in frequency space). Because of the long range (in frequency) effects of the real component of the refractive index, we might expect that the molecules which cause the index modulation are probably 10 to 30 homogeneous linewidths away (from the optimal reading frequency). The net impact this has on the reading operation is that these molecules are nearly impossible to bleach away using laser illumination at the optimal hologram reading frequency. The data almost cannot be unintentionally erased! This feature may play a significant role in the selection of the detector array and the overall system cost. The specifications on the detector array particularly come to mind because of how the SNR requirements and reading photon flux determine the noise requirements on the detector. If the photon flux can be comfortably increased then the detector requirements may be significantly reduced.

But then how can the data be recorded in the first place? One way to provide this capability is by the application of an external field. The application of an external field can redistribute the molecules which are situated within the absorption structure. This brings molecules from the center of the structure to the edge where they are then bleached by the writing laser beams.

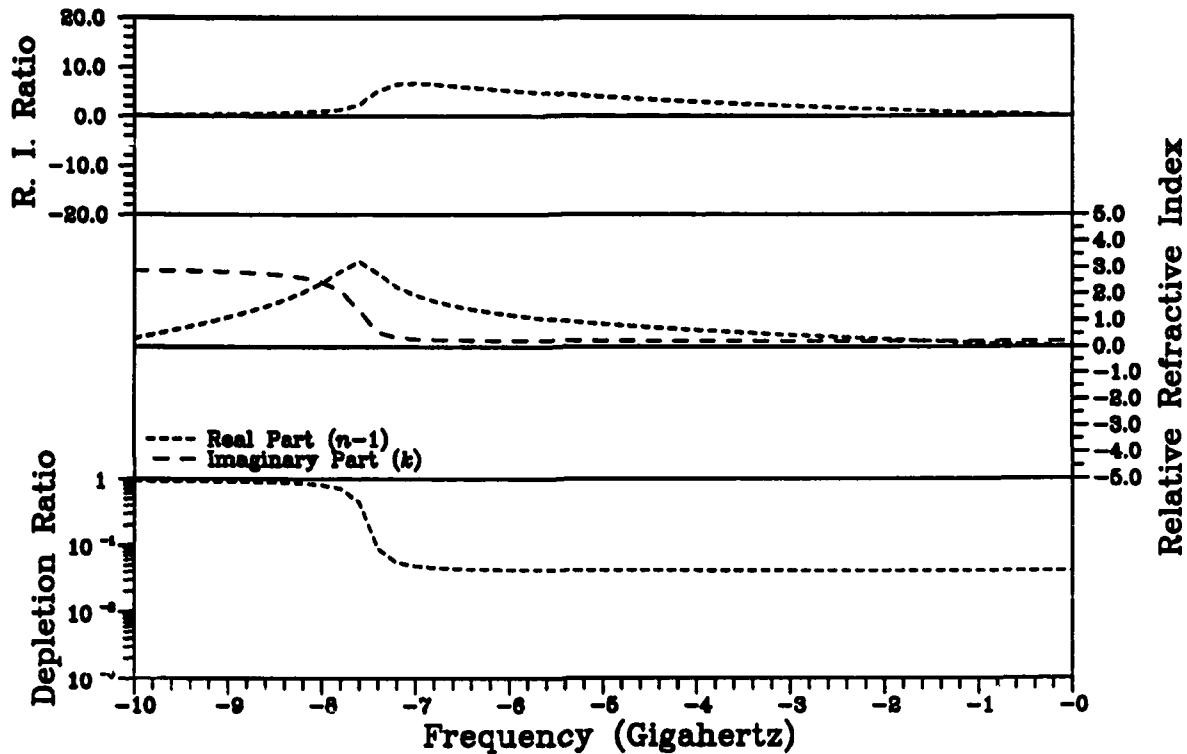


Figure 23. Closeup view of the calculated performance of the frequency channel structure assuming that the channel is bleached to a depth of 4 percent with a 20 GHz channel spacing. Note that the optimal point defined by the peak in the R.I. Ratio is significantly offset from the absorption edge.

After the external field is removed, the molecules redistribute over a wide range of frequencies which are confined to the absorption structure. We therefore find that the external field is a key element in the recording operation for the frequency channel structure.

Because most of the molecules are well separated in frequency from the reading frequency, the potential for absorption which will erase the recorded information has been reduced dramatically. The absorption due to a single molecule falls off as $(1/\Delta f)^2$ causing the absorption to be dramatically lowered as one is separated in frequency from the resonant frequency. When one is roughly 20 homogeneous linewidths away from the resonance frequency, the absorption will be down by about a factor of 1600. This can then permit one to either read a modest efficiency hologram with little danger of erasure, or read very low efficiency holograms more reliably. Because very low efficiency holograms may be difficult to read reliably due to optical scattering from various components in the system, it would seem more likely that the frequency channel structure represents an approach to providing a memory which is especially resistant to unintentional erasure. In fact, it would appear to almost completely decouple the sensitivity during reading and writing through operation of an external field.

6.8 Frequency Channel Storage Capacity

The issue of storage capacity for the frequency channel structure is somewhat more difficult to estimate than it is for the simple absorption hologram situation. Besides the issue relating to hologram efficiency and optical scatter, there is the problem of actually accessing all the storage capacity contained within the absorption structure. As was discussed above, access is provided by the application of external fields such as electric fields and stresses. We believe that with a judicious use of applied fields one might be able access nearly all the storage capacity represented by the refractive index modulation seen in Figures 15 to 22.

6.8.1 External Fields and Storage Capacity

The principal action of an external field is to change the resonant absorption frequency of a photochemical molecule. In terms of the frequency channel structure, this frequency shift can be used to separate the reading and writing operation. However one has the additional requirement that the recorded hologram not contain chromatic aberrations which can significantly reduce the image quality during readout. This translates into a limitation on how large the external field induced frequency shift is permitted to be before the reliability of the data is jeopardized.

This is most easily estimated by examining the optical characteristics of the proposed storage medium. From the Rayleigh criterion for permitted aberrations [35] we can estimate that the maximum permitted deviation of the hologram waveform that was initially recorded is $\lambda/4$. If we select the thickness and width of the SHB medium in our optical memory to be 1 cm, then the largest change in wavefront which is permitted from center to edge (0.5 cm) is limited to $\lambda/4$. This translates into a maximum permitted frequency shift of 15 GHz. To permit reasonably efficient use of the molecules contained within the absorption structure, it should be no wider than 30 GHz (this assumes that access to the holographically stored data can be achieved from both sides (in frequency space) of the holographic structure. In practice, we will probably find that the absorption structure will be roughly 5 to 10 GHz wide for optimal utilization.

The effect of an external field such as an electric field is to provide a symmetric spread to an ensemble of resonantly absorbing molecules contained within a homogeneous linewidth. When a field is applied to an absorption structure such as is seen in Figure 22, half of the molecules spread to one side, and half spread to the other. If we access (i.e. read and record data on) both sides of the structure then we find that much, but not all of the molecular population can be accessed. The population which was not accessed was the segment which only responded weakly, or not at all, to the applied field and therefore moved little in frequency space. This problem can be addressed by application of a second field (either an electric field with a different orientation, or a stress field) which then has an independent effect upon the ensemble of molecules. The net effect is to somewhat refresh the population available for recording so as to make better use of the molecules available. This occurs because a different ensemble of molecules is spread beyond the absorption edge in order to permit the recording of holograms.

The opportunity to reshuffle molecular populations in order to provide full access to all the molecules can be carried to nearly any level by using a number of externally applied fields, however, one probably reaches a reasonably efficient situation by using two independent fields.

6.8.2 Number of Holograms per Channel

The limitations on beamsteering devices coupled with the limitations of practical modest cost optics limits the number of independent holograms which can be stored at a single frequency to approximately 1000. The requirement must also be added that the next adjacent frequency for recording must be separated by a suitable distance in frequency space to prevent cross-talk. For the frequency channel structure this causes us to only permit 1000 holograms to be recorded in each structure. We have the option to record all the holograms on one side of the structure, or to have the number of holograms split to having half of the holograms stored on each side of the structure.

Because the refractive index effects of the frequency channel structure are so far reaching (in frequency) the two sides of the structure will probably not be independent enough to prevent cross-talk which could jeopardize the reliability of the data. While this could potentially be compromised somewhat under certain conditions relating to the type of data and channel dimensions, we shall take the conservative approach at the moment and limit our storage capacity to 1000 holograms per channel with the option that 500 holograms could be stored on each side of the absorption structure.

We have earlier argued that the Debye-Waller factor probably prevented us from achieving a bleached channel depth which was less than 1 to 2 percent of the original absorption, leading us to assume a maximum refractive index ratio of roughly 15 to 10 (respectively). Furthermore one should not allow the baseline absorption at the reading frequency to exceed 87 percent, which limits the absorption coefficient at the bottom of the channel to 2.0 (this is the optimal absorption for maximum efficiency). If we then limit ourselves to a refractive index ratio of 10, and require that the minimum hologram efficiency which we are permitted is 4×10^{-6} (from limitations of optical scattering), the maximum number of holograms which can be recorded on one side of the absorption structure is roughly 918. Utilizing both sides of the frequency channel permits us to reach a limit of 1836 holograms per absorption structure (at two wavelengths), well beyond our limit of 1000 holograms (imposed by our definitions of optics and beam deflection devices). We therefore see that some tradeoffs in spacing between channels may be permitted which lower our capacity per channel but raise the total capacity for the entire memory system.

A reasonable way to start is to reduce the refractive index ratio requirement to 5.5, which still permits us to store 1000 holograms in each channel (500 on each side). This refractive index ratio can readily be achieved with a spacing of roughly 20 GHz being allotted to each channel. It can be expected that a medium which contains several photochemical species may have a total storage range of up to 50 nm, which is roughly 50 THz in frequency units. This implies that as many as 2500 separate frequency channel structures may be available for recording. Assuming a capacity of 10^6 bits/hologram (bits/page) the system capacity can be estimated at roughly 2.5×10^{12} bits for a system based on 1 cm³ of SHB medium.

6.9 Making Frequency Channels

Since it has been established that the frequency channel structure can provide a significant capacity for storage one needs to address some of the practical issues surrounding their use. Before they are available for recording, the channels must be created by efficiently bleaching out the majority of the molecules present. For a single cube of SHB medium it is estimated that 10 mW power levels can be tolerated without substantial heating of the material. This would

permit sufficient heat to be dissipated for the creation of frequency channels in the materials under consideration. We have also established that a layered structure medium which has as few as 5 layers can easily tolerate up to 250 mW of laser heating without causing a temperature rise of more than 1 degree. Realizing that the creation of a 15 GHz wide channel may permit bleaching with a wider homogeneous linewidth than our ultimate 100 MHz requirement may permit us to raise the temperature even further during part of the channel creation process. It is probably reasonable to assume that local heating caused by the high absorption coefficient of the material would probably be easily tolerated by the medium.

To estimate the time required to bleach away the molecules contained in the channels one merely needs to estimate the number of molecules involved and the quantum efficiencies involved. The minimum number of molecules involved for reliable data storage is probably in the range of 400 molecules/bit. (This is a conservatively high estimate based on a fundamental SNR for storage of 20, which is much better than required in practice.) To create the frequency channels, we may bleach away 80 percent of the molecules, and use only 50 percent of the molecules remaining in the absorption structure to record data. This then argues that to record 2.5×10^{12} bits would require 10^{16} molecules. Estimating a quantum efficiency for bleaching of roughly 10^{-6} (which is conservatively low), one then requires 10^{22} photons to create the frequency channel structure. At a laser power of 250 mW, one can estimate the time required as roughly 3 hours; clearly an acceptable level of processing time.

The 3 hour processing time is sensitive to a number of factors, but whether it is 3 hours, 30 hours or 0.3 hours is not particularly important since it is an acceptable requirement under any circumstances for initial processing, and is even acceptable for the requirement of periodic refreshing of the memory in order to extend the long term usable life of the memory unit.

6.10 Recording in Frequency Channels

As was mentioned earlier, the recording mechanism effectively involves the application of an external field (electric field or stress field which redistributes the molecules contained within the absorption structure). To efficiently accomplish this task one must be able to shift the absorption frequencies of the molecules involved by approximately the width of the absorption structure (or more). Under the assumption that the absorption structure is 5 GHz wide, the necessary electric field would be approximately 40 kV/cm.[1] Since we expect to have a layered structure to the SHB medium containing 5 layers for heat dissipation concerns, the introduction of an electric field of 8 kV across each layer would seem acceptable.

For the case of stress, the application of roughly 1 MPa (10 atmospheres) is adequate to provide 5 GHz of line broadening. This level of stress can easily be applied uniaxially using piezoelectric devices.

One factor to consider is the fact that molecules which are located in the center of the absorption structure are typically 2.5 GHz from the optimal reading frequency. This means that molecules which are contributing to the index modulation are less effective in causing diffraction than if the diffraction were at the resonant absorption frequency. This "off resonant" diffraction will cause the net index modulation (real part) to be down by a factor of roughly 50 for a material having a homogeneous width of 100 MHz. What this simply means is that the initially recorded hologram would have a strength which is 2500 times stronger than that which is finally desired after the external field has been removed. For a final hologram efficiency of 4×10^{-6} the initial

hologram efficiency would need to be roughly 1 percent. This would also imply that, for the same molecular absorption properties, one is required to bleach 50 times as many molecules to store the same bit in the frequency channel structure as it would in a purely absorption hologram structure. This implies that it is generally desirable to utilize molecular species with rather high absorption cross sections when using the frequency channel structure in order to minimize the energy required to record the data as well as to create the channels initially. This will be discussed more fully in a later section.

6.11 Laser Linewidth Requirements

An interesting outcome from consideration of the frequency channel structure is that some of the requirements on the performance of the tunable laser are relaxed. To create the initial frequency channels the laser linewidth should be equal to or less than the homogeneous linewidth of the SHB material in order to provide efficient use of the available storage capacity. However, once the channels are created, neither the recording process nor the reading process requires the same narrow linewidth or tuning precision. These requirements can be relaxed by a factor of 5 to 10. This may be of importance in terms of the performance requirements of the laser in that it may permit very fast random access tuning for reading and writing without needing closed loop feedback except intermittently.

6.12 Summary of Frequency Channel Attributes

The principal benefits which we presently perceive for the frequency channel structure are:

1. More hologram storage capacity per recording frequency. - Reduced laser requirements.
2. Less sensitivity to laser tuning and linewidth performance. - Reduced laser requirements.
3. Greater resistance to unintentional erasure. - Potential for use of lower cost detector components, or greater durability of data with less overhead requirements for memory refreshing.
4. Wider range of material parameters are available for high end memory applications than are available for the absorption hologram storage situation.
5. Potential for recording high efficiency holograms. - Other new applications are possible where efficiency is required.

The principal drawbacks for this structure are:

1. The maximum storage capacity limits are actually lower (by approximately a factor of 4) below those possible with an absorption hologram based memory.
2. Increased preparation time is required to make the channels before they are useful for recording.

7 Absorption Hologram Storage

This section discusses some of the key aspects which define the limits of data storage permitted by "conventional" approaches to recording holograms in absorptive media. (By conventional approaches, we are excluding the frequency channel approach which is discussed in a separate section.) The principal points of interest lie in how many holograms can be superimposed at a single frequency, what capacity gains are permitted by the application of external fields, and what are the restrictions on capacity provided by SNR requirements?

7.1 Absorption Hologram Limits

The limit on hologram storage is strongly affected by the number of holograms which can be superimposed at the same wavelength. The independence of the recorded holograms is guaranteed by altering the angle of incidence of the reference beam. The classical limit on hologram storage in an absorptive medium is provided by reference to the expression for the diffraction efficiency (η) of absorption based thick transmission holograms,

$$\eta = [\sinh^2(\alpha_1 d / 4 \cos \theta)] e^{-\alpha_o d / \cos \theta}. \quad (30)$$

The above expression can be solved for the maximum hologram efficiency with the assumption that the index modulation (α_1) and average absorptivity (α_o) of the medium are the same. This identifies the maximum diffraction efficiency of a hologram recorded in the medium as being 3.7 percent. We also find that the average absorptivity of the medium required to generate this efficiency is 2.0. If we then define the minimum hologram efficiency which is required for the reliable reading of data (η_{min}) and realize that for small efficiencies the number of superimposable holograms goes as the square root of the hologram efficiency ratios we find that

$$N_{max} = \sqrt{\frac{\eta_{max}}{\eta_{min}}}. \quad (31)$$

For our purposes, we have two added complications.

1. The Debye-Waller factor prevents us from using the entire absorptive range in recording holograms. Due to electron-phonon interactions, we find that a sharp homogeneous spectral hole can probably only be bleached to a depth of 80 percent of the initial absorption.[30] Therefore, at least 20 percent of the absorption coefficient is unavailable for recording holograms.

When this is factored into equation (30) we find that the maximum diffraction efficiency is for a single hologram now of the order of 2.4 percent. If the minimum required diffraction efficiency of each hologram is 4×10^{-6} , the number of holograms which can be stored is approximately 77.

2. The above estimate of maximum efficiency is based on a fundamental absorption limit but ignores the process by which the holograms must be recorded. In our case, recording must be accomplished by the bleaching of a highly absorptive medium and successive holograms must be recorded sequentially. The light used to record sequential holograms will also partially bleach previously created holograms. This problem can be addressed by considering a recording schedule where the first holograms are recorded with greater

efficiency and the latter holograms are tapered in efficiency so that the final ensemble of holograms are all of equal efficiency.

An estimate of the impact of such a recording schedule can be made as follows.

x = fraction of absorption remaining after the creation of the first hologram.

$1 - x$ = absorption range used by the first hologram.

N_{max} = number of holograms which can theoretically be stored in the medium. (This number is proportional to the recording range of the medium.)

N = number of holograms actually recorded of equal final strength.

$1/N_{max}$ = fraction of the recording range required for the storage of a single hologram.

N/N_{max} = fraction of the recording range needed for the final state of the medium.

Two expressions defining the situation can be immediately written. The first is

$$(1 - x)\left(\frac{N}{N_{max}}\right) = \frac{1}{N_{max}}, \quad (32)$$

which states "that the recording range used by the first hologram times the fraction to which it is finally reduced by sequential recording operations is equal to the minimum recording range needed for reliable reading of the data (which includes a reserve for erasure resistance)". The second expression is

$$x^N = \frac{N}{N_{max}}, \quad (33)$$

which states that "the recording range remaining after N sequential writing operations must equal the summed recording range of the final holograms of equal strength".

These two expressions can be used to write an expression for N_{max} as

$$N_{max} = N \left(\frac{N}{N - 1}\right)^N. \quad (34)$$

When solved for N we than find that the number of holograms which can actually be recorded is about 27.

The above analysis ignores two factors which we believe roughly balance each other. The first is that as the holograms are recorded in the medium it becomes bleached. This lowers the overall absorption of the material and enhances the net efficiency of each hologram. The second effect is that the hologram is not uniformly recorded throughout the medium due to absorption and bleaching effects. The modulation at the back of the medium has received relatively little light so is only weakly bleached while the modulation at the front of the medium has been reduced by bleaching away of the initially recorded modulation. Based on these two opposing effects we believe that the net effect is roughly balanced and the above analysis gives us the approximate estimate of capacity we need.

7.2 Cross-Talk Between Holograms

If, in the process of reading holograms, the light is partially scattered by images which were stored and are being read out unintentionally, then they can contribute to false signals, which can effectively be considered as part of the SNR budget. Cross-talk can occur in two fundamental ways.

7.2.1 Cross-Talk Due to Angular Resolution

Two holograms which are stored at the same wavelength using reference beams which are closely spaced angularly can have an efficiency overlap. This comes directly out of the basic theory developed by Kogelnik [1]. From his analysis we can quickly see that the storage limits are determined largely by the thickness (T) of the material used. This militates towards using materials which are 0.5 to 1.0 cm thick. This would provide an angular selectivity at which cross talk can be reduced to less than 1 part in 20 for all holograms except very high efficiency (near 100 percent) phase holograms. These holograms are unlikely to be of significant concern for high performance requirements, so will not be considered seriously here. The angular selectivity (δ) for very low cross-talk can be estimated as

$$\delta = \frac{\lambda}{2n_0 T \sin \theta}. \quad (35)$$

If the angle of incidence (θ) is 10 degrees, and the wavelength is 0.7 microns, the angular selectivity for a 0.5 cm thick hologram would be 3×10^{-4} radians. For an optical system having a numerical aperture of about 0.15, this would allow one to cleanly resolve 1000 elements within the field of view. This also argues that one could tolerate as many as 1000 separate recording angles for the reference beam.

7.2.2 Cross-Talk Due to Frequency Spacing

The cross-talk between holograms which are at different wavelengths but the same angle (same row of input) also needs to be considered. Kogelnik's theory provides some wavelength selectivity, however this is quite inadequate. The greater selectivity is provided by the SHB material itself through consideration of the Kramers-Kronig relation. The principal point of interest is seen in Figure 24 where one notes that a modulation in the absorption as a function of wavelength (or frequency) is directly related to an accompanying change in the real part of the refractive index. Both parts of the complex refractive index can contribute to the strength of the hologram. The key element to be noted here is that the absorption modulation at ω_0 has an effective "range" in frequency space which can interfere with holograms which might be located nearby (in frequency). This effect will introduce cross-talk and will define a limit to the ability to "pack in" information in frequency space.

For simple modulations of the absorption, as seen in typical SHB structures, the effective strength of the hologram will fall off with frequency according to a simple formula [36] (for low efficiency holograms)

$$\eta(\omega) = C \frac{(\gamma/2)^2}{(\omega_0 - \omega)^2 + (\gamma/2)^2}. \quad (36)$$

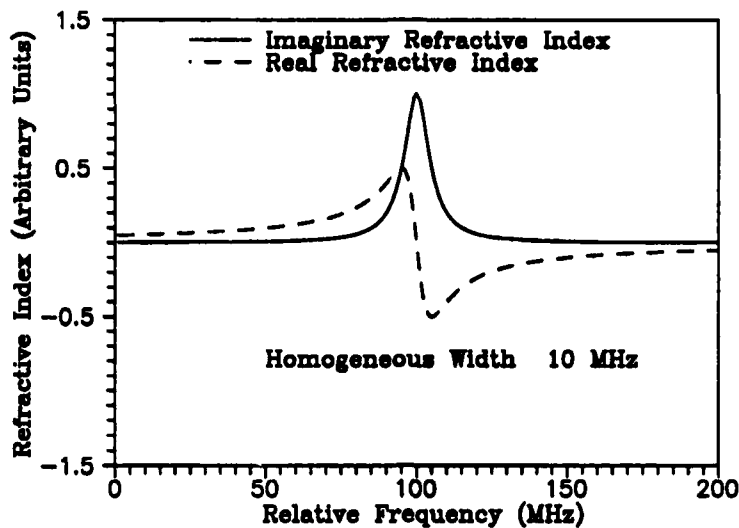


Figure 24. Real and imaginary components of the refractive index for a single damped oscillator. Note that the real part has an effective range that extends well beyond that of the imaginary component.

In the above, C is simply a constant which describes the background absorption, hole depth, and geometrical properties of the hologram, while γ is the spectral linewidth of the SHB material. (It is assumed here that the width of the absorption profile which was created was as narrow as was permitted by the material, and not limited by power broadening, linewidth of the laser, or other effects.) As discussed above, cross-talk between adjacent (in frequency) holograms should be considered a source of noise, and the SNR be kept above the required level of 11. Since noise can occur from holograms stored on either side (in frequency space) of the selected frequency, the actual SNR limit is doubled to 22. Since hologram storage is occurring in the 2 dimensional plane of frequency and reference beam angle one is required to enhance the spacing further by roughly $\sqrt{2}$ which then places the required SNR at 31. From equation (36) this would require that the holograms be spaced greater than 2.8γ apart.

The actual spacing between adjacent frequencies probably needs to be slightly greater due to effects relating to the finite laser linewidth, but this is only a modest increase. As we shall see, the details of the frequency spacing are not critical for determining system capacity since we overcome this limitation by the application of external fields.

7.3 External Field Effects

The application of an external electric field to a medium in which absorption holograms are written can scramble the absorption frequencies corresponding to the bleached hole. This can effectively provide a "clean slate" on which to record more holograms. The total absorptivity becomes averaged over frequency so that the bleached hole becomes filled in at the expense of reducing the peaks in the absorption left between spectral holes. This operation has two principal effects concerning storage capacity.

1. One can trade the number of recording frequencies for the number of discrete applied external fields. These fields can be electric fields, stress fields, or any combination of these which will provide an adequate separation between recorded holograms to a

level sufficient to prevent cross-talk. If we require a SNR of 31 between adjacent holograms in frequency space, the spectral holes must be spaced by at least a factor of 5.6 homogeneous linewidths in order to prevent cross talk. For a spectral hole 140 MHz wide, the frequency spread needs to be about 0.8 GHz. Several successive fields are required to permit a full range of recording capability. The number required is probably in the range of 10. Therefore, if only one external field is used, (such as an electric field) one needs to be able to induce frequency spreads of ± 4.5 GHz, which is roughly the magnitude required in the case of the frequency channel structure. To accomplish this spread for a typical SHB material would require an applied electric field of roughly ± 36 kV/cm, or ± 7 kV applied to a segmented medium divided into 5 sections.

2. The storage capacity of the medium is simply limited by the absorption of the medium (i.e. how many holograms can be superimposed at a single frequency) and the spectral hole width of the bleached material. This occurs because one eventually must run out of bleachable molecules after a number of recording operations. The maximum number of separate frequencies is simply the entire recording range (which is the inhomogeneous line width) divided by the spectral hole width (which is the combined width of the laser and SHB homogeneous linewidth).

7.4 Absorption Hologram Storage Capacity

We therefore see that the application of external fields extends the range of the medium for reliable recording up to a point. Once the fields are sufficient in magnitude, they do not provide greater advantage because the uppermost limit to the recording of information is provided by the number of molecules, laser linewidth and homogeneous linewidth. For a system having the following properties

10^6 = page size,
100 MHz = homogeneous linewidth,
100 MHz = laser linewidth,
140 MHz = resultant spectral hole width,
50 THz = total medium recording range,
the estimated capacity would then be (approximately)

$$\text{Capacity} = 10^6 \times 27 \times 5 \times 10^4 / 0.14 = 10^{13} \text{ bits.}$$

8 Materials for SHB-Based Optical Memory

Based on the considerations outlined in previous sections concerning recording, reading and erasing information from potential high capacity memory systems based on SHB materials we are now able to define the material properties boundaries for candidate materials. As we shall see, these boundaries permit us to use a number of the most commonly studied SHB materials and provide us the potential of realizing the proposed high capacity system envisioned.

In the previous sections we determined that there were some significant practical boundaries which could be defined for the reliable operation of the memory system. We also have selected some of the operating characteristics based on our estimates of the performance of system components which we expect to become available in the foreseeable future. In order to clearly define our starting assumptions, we shall list them below. It must be realized that the system capacity and performance are directly linked to the selected values of these parameters, and as such we have attempted to be suitably conservative in our performance estimates. Clearly, if the actual performance of any of these components can be exceeded, the system performance will benefit accordingly. In the discussion below we shall describe the performance of a system based upon 1 cm³ of SHB medium. While the consideration of multiple arrays of systems to provide extra capacity is possible, even probable because of their compact nature, we shall focus on a simple system unit and leave the extrapolation to larger system capacities to the reader.

8.1 High End System Specifications

In order to quantitatively address the viability of using existing SHB materials to create a high capacity memory system, we have adopted a set of system specifications as described below. These system specifications have been selected in a manner which is compatible with the material properties so that an acceptable level of performance is achieved. The performance achieved has been judged by us as being of interest to the computer community in general, and as we shall see, defines a set of material property boundaries in which we can find a number of commonly studied SHB materials.

These performance parameters are very important to the determination of the detailed location of the material boundaries, as well as determining whether the final system will be of use to the computer community as a whole. However, it must be noted that compromises can surely be made on the exact performance parameters as well as on the material boundaries. Therefore the diagrams which define the desirable material parameter space of interest should be viewed as defining approximate regions of interesting properties, rather than as spaces with sharply defined limits. In some cases we could be justified in expanding the materials parameter boundaries by as much as an order of magnitude if modest alterations in the performance requirements were made. With these caveats in mind we have proposed the following set of potential high capacity system specifications.

For both an absorption hologram based system as well as a phase hologram based system we have decided to examine systems having a capacity of 2.5×10^{12} bits with two potential data rates; 30 MHz and 1 GHz. We have also added the case of a 10^{13} bit capacity system for the absorption hologram situation to examine the maximum capacity situation.

8.1.1 Absorption Hologram Based Parameters

Accessible frequency range for hologram storage = 50 THz.

Laser linewidth = 100 MHz.

Homogeneous linewidth of the medium = 100 MHz.

Minimum hologram efficiency = 4×10^{-6} .

Maximum number of holograms stored per frequency = 27.

Maximum system capacity = 10^{13} bits, or 2.5×10^{12} bits.

System data rate = 30 MHz or 1 GHz.

Maximum laser power = 250 mW.

8.1.2 Phase Hologram Based Parameters (Frequency Channels)

Accessible frequency range for hologram storage = 50 THz.

Laser linewidth = 100 MHz.

Homogeneous linewidth of the medium = 100 MHz.

Minimum hologram efficiency = 4×10^{-6} .

Maximum number of holograms stored per frequency channel = 1000.

Maximum system capacity = 2.5×10^{12} bits.

System data rate = 30 MHz or 1 GHz.

Maximum laser power = 250 mW.

8.2 Material Boundaries for Absorption Holograms

In order to appropriately define the materials boundaries for each case we shall also describe the arguments behind each one.

1. *Photochemical Broadening.* There is a fundamental limit to the allowed quantum efficiency (QE) referred to as “photochemical broadening”. [24] This is brought on by the realization that a photochemical transformation which occurs too readily will most likely result in a shortened excited state lifetime which prevents us from achieving as narrow a homogeneous linewidth as we might like. An approximate limit for this is a QE of 0.1 and is shown in Figure 25.
2. *Spectral Diffusion.* A limit can be set in the number density of molecules in the SHB host medium. If this density is exceeded, the molecules are no longer assured of acting independently (which is a requirement for efficient recording). Following the arguments from the literature [24] this has been set at an arbitrary number density of 1 percent which defines the absorption cross section once the optical density and thickness of the medium are set.
3. *Thermal Broadening.* This boundary is defined by the power dissipated by the laser in writing the hologram. It is limited by the thermal conductivity of the SHB host medium and is directly related to the data rate for writing. (We have arbitrarily selected the data rates for reading and writing to be identical). In a previous section, the photon flux required for writing (Φ_w) was defined as

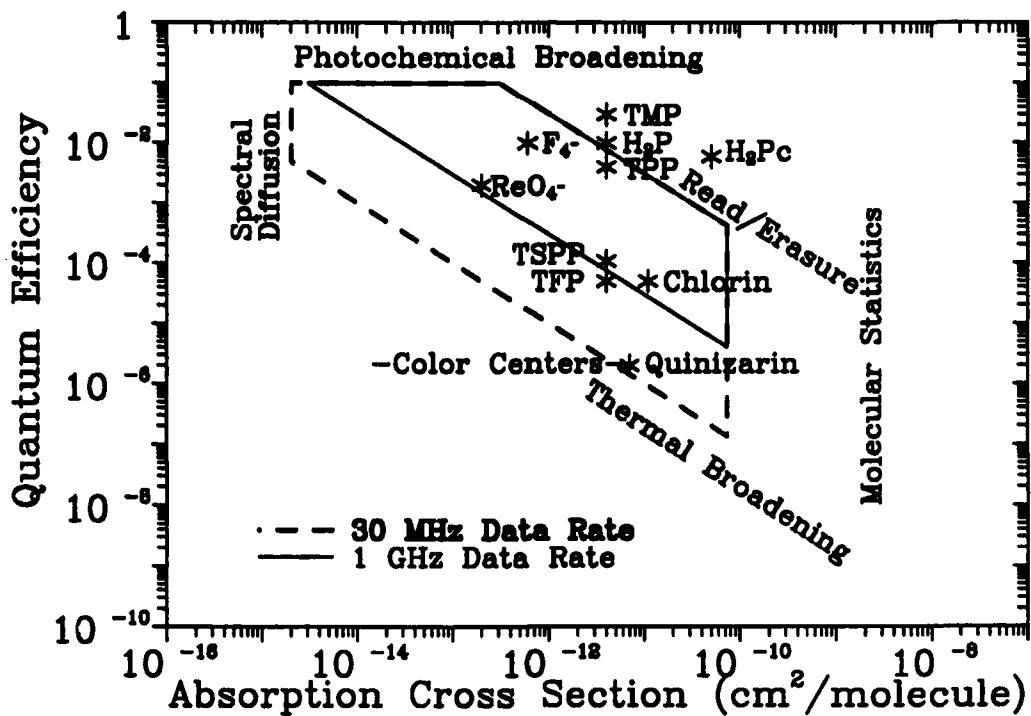


Figure 25. Material parameter boundaries defined for a memory system based on absorption holograms. The system capacity is 2.5×10^{12} bits/cm³.

TMP = tetrakis(4-methoxyphenyl)porphine[37].

H₂P = free base porphyrin[24].

TPP = tetraphenylporphine[37].

TSPP = tetrasodium 5,10,15,20-tetra(4-sulfonatophenyl)porphine[38].

TFP = tetrakis(pentafluorophenyl)porphine[37].

H₂Pc = phthalocyanine[24].

ReO₄- = perrhenate ion in alkalai halides[24].

Chlorin[1].

F₄- = color center in NaF:OH⁻[24].

Quinizarin[24].

$$\Phi_w = \frac{n_p DR}{QE} \quad (37)$$

where DR is the data rate and n_p is the number of molecules required to store a bit. Because (1) the absorption cross section is directly related to the absorption coefficient limit for efficient storage ($OD = 0.83$), (2) we have fixed the system capacity at 10^{13} bits/cm³, and (3) the number of molecules required to store each bit reliably is defined by counting statistics, we find that n_p is directly tied to the absorption cross section. When this is inserted into equation (37) we define the lower boundary in Figure 25. (Clearly, the exact location of this boundary is defined by the thermal conductivity of

the medium and the data rate as well as average duty cycle of the memory system.)

We find that this boundary location is directly proportional to the data rate of the system so that the 1 GHz boundary is higher by a factor of about 30.

4. *Molecular Statistics* On the far right of Figure 25 we find the boundary defined by molecular statistics. This is created by the limit imposed on the simple statistics of reliably recording a single bit. While it was earlier established that an SNR of 11 provided adequate reliability, we have decided that the SNR for molecular statistics should be about 20 (400 molecules) or greater for molecular counting statistics, in order to provide a suitable safety margin. Based on the number of bits to be stored in the entire system and the requirement of 400 molecules per bit, as well as the limitation in optical density of the medium, this boundary becomes uniquely defined.
5. *Read/Erasures*. In a previous section it was argued that the read/erasure ratio (R_e) could be directly related to some of the key parameters of the system as

$$R_e = \frac{\lambda H_{max}}{PPB \ h c} \frac{\eta}{DR} \quad (38)$$

or

$$R_e = 1.455 \times 10^{15} \frac{\eta}{DR}. \quad (39)$$

Because the data rate is directly tied to the quantum efficiency through equation (37), equation (39) defines a line parallel to the thermal broadening limit which is a simple multiple above it. That multiple is the read/erasure limit defined as being the case where the flux required to record as single hologram is the same as the flux required to read it.

The principal difference between the system having a capacity of 10^{13} bits and one having a capacity of 2.5×10^{12} bits is one of flexibility of engineering tradeoffs. As we can see from Figure 25, the read/erasure limit provides a significant limit to the selection of available materials and operational characteristics. If we select this aspect to be improved upon, we can expand the read/erasure limit by increasing the efficiency of each hologram at the expense of storage density. Decreasing the bit recording density by a factor of four permits us to reduce the flux used to read each hologram and increase the resistance to erasure by a factor of sixteen. The principal effect is to move the read/erasure boundary substantially upward, as is seen in Figure 26.

From Figures 25 and 26 we can define the maximum potential read/erasure limits:

10^{13} bits, 30 MHz, absorption hologram system = 200 reads/erasure.

10^{13} bits, 1 GHz, absorption hologram system = 6 reads/erasure.

2.5×10^{12} bits, 30 MHz, absorption hologram system = 3200 reads/erasure.

2.5×10^{12} bits, 1 GHz, absorption hologram system = 100 reads/erasure.

Another phenomenon has been noted which can limit the hologram writing rate. For phthalocyanine (H_2Pc) a "bottleneck" has been determined[30] which can fundamentally limit the writing speed for this material. The molecule is changed photochemically through a complex 4 level process (see Figure 27). Upon excitation, the molecule quickly decays from the initial excited state to a long lived ($350 \ \mu\text{sec}$) metastable state. From the metastable state, the decay

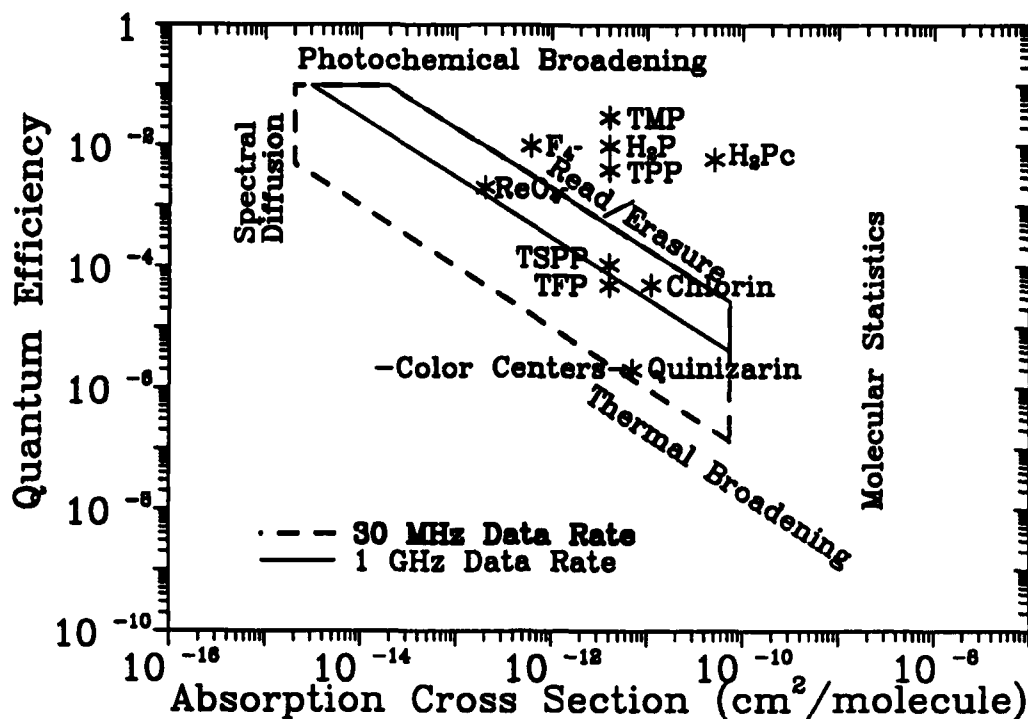


Figure 26. Material parameter boundaries defined for a memory system based on absorption holograms. The system capacity is 10^{13} bits/cm³.

branches to the chemically changed state (about 1 percent) or reverts back to the initial ground state. Under high photon flux conditions, all the molecules can be excited up to the metastable state, not permitting any further absorption until decay occurs. In general, this would suggest that the time to write the hologram factors into the problem through this potential kinetics bottleneck.

If this "bottleneck effect" were to be significant for all photochemical species of interest some concern must be given to the lowest quantum efficiency which is permitted. From a simple consideration of the lifetime of the intermediate state (τ) and the number of holograms to be recorded (N_H) within a given molecular population which is available to be bleached within a given exposure time (F) (i.e. the time per data page) we find that the lowest permitted quantum efficiency is

$$QE = \frac{\tau}{N_H F}. \quad (40)$$

For a material having a lifetime of $350 \mu\text{sec}$ we can therefore define a lower limit to the QE as being roughly 3×10^{-4} . As seen from equation (40) this limit scales directly with the data rate for writing and the intermediate state lifetime. This would not be expected to be a problem for all molecular species, and is certainly not a limit in defining the homogeneous linewidth. A homogeneous linewidth of 100 MHz would suggest a limiting lifetime of much less than $1 \mu\text{sec}$ in the absence of an intermediate state.

It is therefore concluded that if an SHB material possesses a long-lived intermediate state it should be avoided. If it cannot be avoided, its detrimental effects can certainly be mitigated

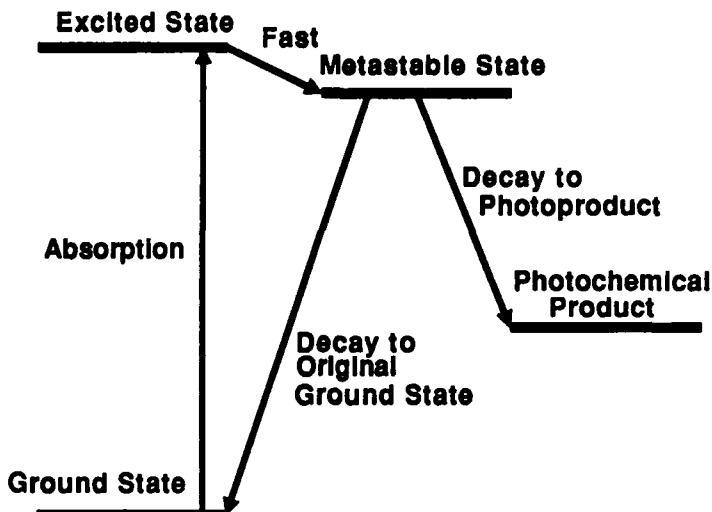


Figure 27. Diagram of the molecular energy levels for H_2Pc showing how the direct absorption leads to the population of a long lived ($350 \mu\text{sec}$) metastable state before decaying either back to the original ground state or toward the photochemical product state.

by increasing the frame time for writing (the reading time would not be as strongly affected). From the selection of materials available one would not expect this to be a serious problem.

8.3 Material Boundaries for Phase Holograms

While many aspects of the system would seem to be significantly altered by the change to the frequency channel approach, the impact these changes have upon materials selection is relatively straightforward. We can therefore estimate the materials boundaries from arguments which pertain to the absorption hologram storage but are modified by the details specific to the frequency channel structure.

1. *Photochemical Broadening.* This boundary is identical to the one specified for absorption holograms.
2. *Spectral Diffusion.* This boundary has been adjusted to the right in Figure 28 to account for the increased molecular absorption required for storage. We would expect that our system should have channels bleached to a depth of about 4 percent of the initial absorption. This causes us to start with a molecular absorption 25 times higher than for the absorption hologram case.
3. *Thermal Broadening.* This boundary is unchanged if the baseline unbleached absorption in each channel is set to an optical density of 0.83.
4. *Molecular Statistics.* This boundary moves to the right, for the same reasons as the Spectral Diffusion boundary.
5. *Read/Erasur*e. This boundary expands very significantly because of the mechanism by which writing and reading are separated from each other through the application of an external field. Because the molecular population can be expected to be shifted

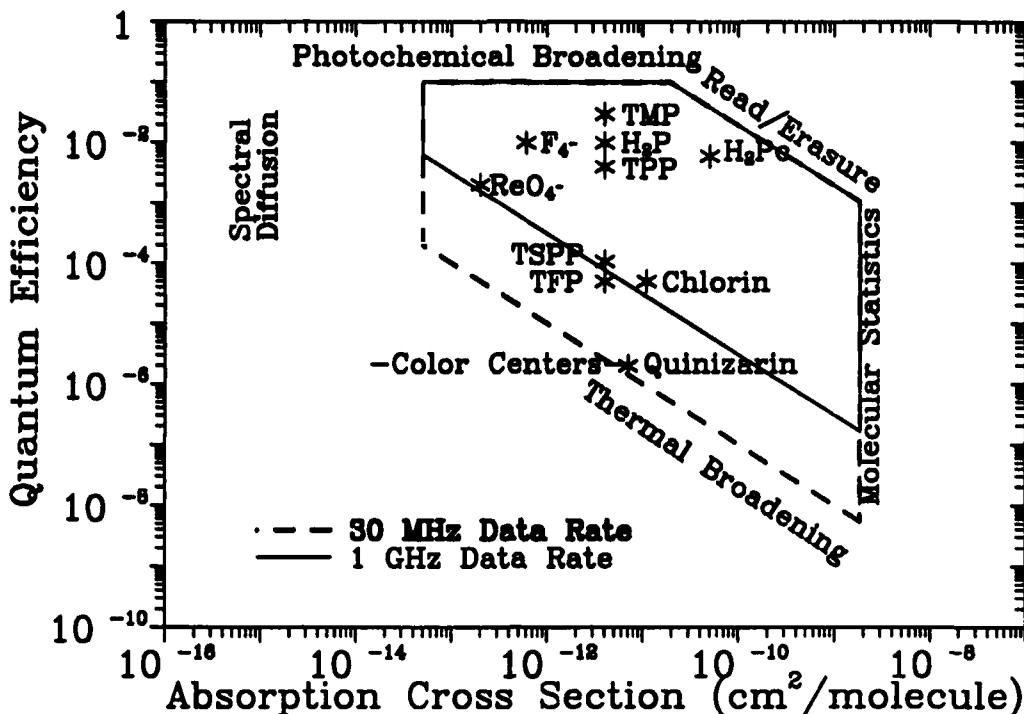


Figure 28. Material parameter boundaries defined for a memory system based on phase holograms and the frequency channel structure. The system capacity is 2.5×10^{12} bits/cm³.

by the external field roughly 20 homogeneous linewidths between reading and writing operations, the enhancement of the read/erasure limit can be a factor of 1600 or more. (This enhancement is over the read/erasure limit which was defined for the 10^{13} bit capacity system.)

From Figure 28 we can define the maximum potential read/erasure limits.

2.5×10^{12} bit, 30 MHz, absorption hologram system = 320,000 reads/erasure.

2.5×10^{12} bit, 1 GHz, absorption hologram system = 11,000 reads/erasure.

8.4 Analysis and Comparisons

The principal conclusion which can be drawn is that the holographic storage of information in a very high density format is consistent with the properties of the single photon SHB materials which have been studied by a number of groups over the past ten years. This conclusion is in direct contrast to the bit oriented mass storage requirements where serial readout at 16 MHz data rates are required [24] (see Figure 29). In the case of serial readout, one is forced to search for two photon SHB materials which have the desired properties. This gives us confidence in proposing that we should initiate the development of a mass storage device based on these materials.

The next conclusion is that the relaxation of capacity limits can have a very marked effect upon the system operation parameters such as acceptable data rate and resistance to unintentional erasure. This can be seen in the dramatic effect which a modest reduction in system capacity had upon the materials parameter space as indicated by Figures 25 and 26. These factors suggest

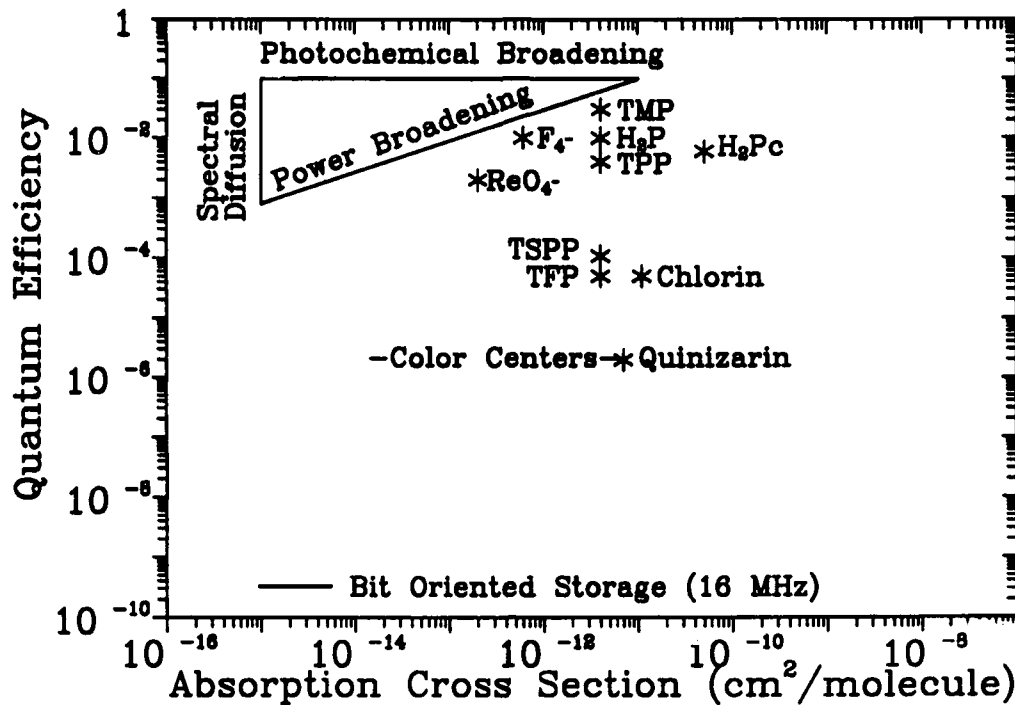


Figure 29. Material parameter boundaries defined for a bit oriented memory system based on serial data storage and readout.[24]

that a significant latitude can be expected at many levels in the detailed engineering design of the final system. This should not only permit the final system performance to have a high probability of being achieved, but it should also indicate that this performance may be obtainable at a very reasonable cost.

The third conclusion is that the frequency channel structure does provide a significant benefit in terms of an expansion of the materials parameter space and in terms of the read/erasure limits of the system. It is also seen that the frequency channel structure directly enhances both the final performance of the high capacity system and also makes the selection of optimal materials far easier.

Based on the above arguments we see the frequency channel approach as having significant benefit to the probability of success, as well as enhancing the system performance as perceived by the user.

9 Parallel Versus Serial Data Storage and Retrieval

There would appear to be at least two potentially competing approaches to the storage of digital data in SHB materials. The work of Moerner, et.al., [24] has principally explored the storage and retrieval of data in a serial manner. The approach addressed by our proposed system explicitly assumes a page formatted data structure which is recorded and retrieved in a parallel manner. In order to highlight some of the key attributes behind our approach, a critical comparison of these two data storage systems is warranted.

9.1 Comparison of Components

Our proposed parallel system has several major components.

1. SHB medium: Approximately a 1 cm cube of material, maintained in a cryostat.
2. SLM: Approximately 1 cm^2 , having 1024×1024 elements.
3. Detector array: Approximately 1 cm^2 , having 1024×1024 elements.
4. Frequency Agile Laser: Capable of addressing at least 1000 wavelengths with high precision and narrow linewidth.
5. Beamsteering Device: Capable of addressing roughly 1000 positions with a 1 msec access time.

Following the system details outlined by Moerner [24], the list of components for a serial readout system would be:

1. SHB medium: Approximately 0.2 mm thick layer, probably in a planar array format, maintained in a cryostat.
2. Detector(s): Multiple 8×8 arrays of high speed photodiodes.
3. Frequency Agile Laser: Capable of addressing at least 1000 wavelengths with high precision and narrow linewidth. Must be able to rapidly sweep the frequency domain in $30 \mu\text{sec}$. An added requirement for recording is that the laser must also be modulated at a rate comparable with the data rate of the system which is determined to be at least 16 MHz.
4. Multiple Beamsteering Devices: Capable of addressing all the data locations. (The number of locations required for a system having a 10^{12} bit capacity would seem to be on the order of 10^8 to 10^9 !)

From the above list of major components there would appear to be some significant differences in the components but these differences may in the long run be of only minor importance in the near future. One can argue the merits of requiring a high performance SLM in the parallel system versus the merits of the beamsteering device arrays required for the serial data system. Similarly, the use of a detector array which has a frame rate of 1 kHz (maximum) for the parallel system can be directly compared with the cost of large arrays of high speed photodiodes for the serial system.

Similarly, one could try to compare operating specifications such as capacity, data rates and access times, but one would again quickly reach a point where the cleverness in the design and the details of the approach are easily traded and again leave one without a clear advantage by one approach or the other.

This comparison could be lengthy and generally reduces to set of estimates concerning the anticipated cost and availability of components. Such a detailed, item by item examination would not seem suitable considering the rapidly progressing electrooptic industry as it stands today, but rather we may appropriately argue that the components required for both systems do not face any fundamental or significant cost limitations in the near future with the exception of the SHB material itself!

We have found that the decision to operate with a serial rather than a parallel data structure has serious implications for determining the material properties one finds desirable, and may directly determine whether one can ever implement any economically practical system based on SHB materials.

9.2 The Impact on Materials Selection

The heart of the memory system is the recording medium itself. There are specific requirements placed on it in order to provide storage capacities and data rates which are competitive with other technologies (such as electronic or magnetic memory devices). Each approach (serial and parallel) has been analyzed in terms of material property requirements.

Moerner's analysis [24] for the serial data structure requires that the data rate for each detector element be as high as 16 MHz which causes the photon flux required to read each bit to become quite high. Whether the data is stored as a contrast based image or holographically is of little or no importance since the signal to noise gain for holographic readout is not realized under the high photon flux, high data rate condition. This is a direct outcome of the Johnson noise of the detector at the bandwidth which it is required to operate at. Because of this high photon flux required for data retrieval, the photochemical molecules can be easily saturated or erased by the reading operation. To prevent this from happening one must restrict the required material parameters to a rather small segment of the molecular properties space when one is considering the use of a single-photon recording process. This small segment of space was identified by Moerner as containing no viable candidates. The net result was the focusing of efforts by Moerner and others on the use of two-photon recording materials which have the potential to overcome the reading/erasure problem for serial data recording and readout. Unfortunately, two-photon materials are more difficult to study and the selection of viable materials having appropriate properties has been quite limited.

Our analysis of the parallel data structure has two principal differences associated with it. (1) The data rate per detector element is only 1 kHz or less permitting near photon counting detectability. (2) Because the data is recorded as a page formatted image, the storage as a volume hologram is a natural approach to achieving low noise operation. (Holographic readout has an advantage because the diffracted output light is well separated spatially from the incident laser beam.) These two key factors permit us to read each recorded bit with a much lower photon flux and leads us to a significantly larger parameter space in which we now find acceptable materials which are based on single-photon processes. Moreover, the parameter space under consideration contains many of the most promising materials which have been studied by researchers over the past 10 years. Because the materials required already exist we have confidently proposed to go to the next step to begin development of an early experimental version of a parallel data structure memory system.

9.3 Conclusion: Serial Versus Parallel

The principal outcome of the serial versus parallel data structure analyses is that the selection of data structure has an explicit impact on the type of SHB material required. The **serial data structure requires the development of two-photon SHB materials.** The **parallel data structure permits the use of existing single-photon SHB materials.** It should be expected that during the course of the development of high performance optical memory systems some material optimization will be required, but at least an adequate number of material candidates can be presently identified which meet the fundamental needs in terms of molecular properties for the parallel data structure system that is proposed. Unfortunately, the serial data structure system would appear to require some significant research as well as development in order to provide the two photon materials which have all the properties explicitly required to make a high capacity system viable.

It is the SHB medium which provides the key fundamental properties which make the potential for an extremely dense memory system possible, and it seems to be a natural circumstance that these properties indicate a clear preference for the parallel data structure. In fact, it would appear that the proper argument is that the existing single photon materials prefer a parallel data format memory system over the serial data approach. From a materials point of view, we believe that the material properties should define the system architecture for obtaining optimal performance, not the other way around. This stance is appropriate when the other required system components are available (such as the SLM and detector array). With the present development efforts underway (by others) for providing these supporting components, we are confident that a high capacity parallel architecture system is viable in the near future.

10 Supporting Components

In this section, we discuss the components required to build an optical memory system based on SHB materials. These components are important for two key reasons. First, the performance of near-term demonstrations and prototype systems will be limited by the capabilities of the available components. Second, the cost per on-line megabyte of projected systems will be determined primarily by the cost of the components rather than the memory medium or the assembly time. As we have discussed elsewhere in this report, the cost per megabyte of a rapid access memory system will be a key factor in determining the eventual marketability of a memory system product.

The components of a 4D optical memory system are shown in Figure 30. These components include the frequency agile laser, SLM (spatial light modulator), reference beam deflector, relay optics, cryostat, detector array, and the electronic interface. In the examination presented below, we shall see that most of these principal components are either already available, or are presently under development to a level which gives us confidence that the final system components will become available for incorporation into a high capacity memory system. We expect that they will all be available within the next five years and will have manufacturing costs appropriate for a commercially viable memory system.

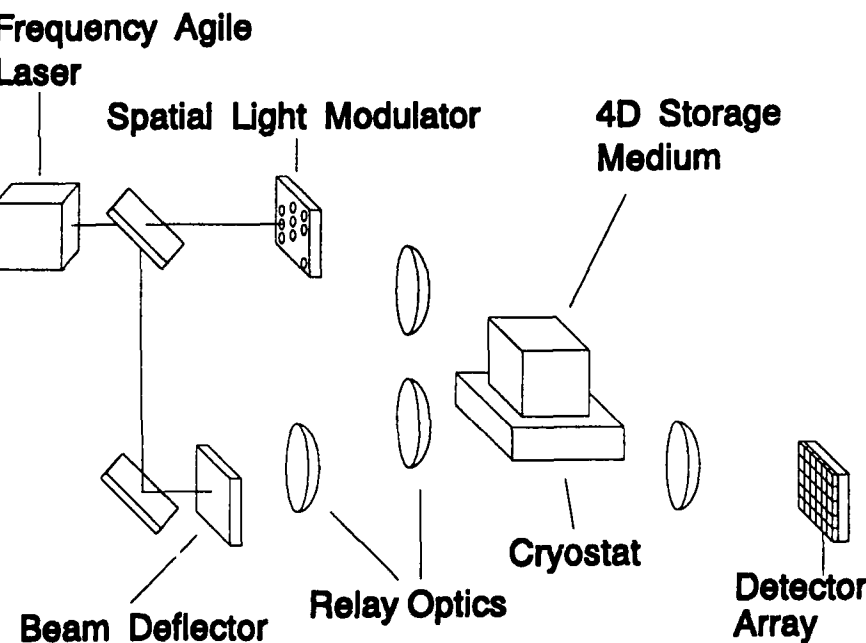


Figure 30. 4D optical memory system components.

10.1 Reference Beam Deflector

Our current approach to maximizing the data capacity of the 4D memory concept will require the recording of multiple holograms at each wavelength. In volume media, multiple holograms can be recorded and independently read out by recording each hologram with a reference beam having a unique angle of incidence. Bragg angle selectivity, which occurs in the plane defined by the reference and data beams, will determine the angular separation between reference beams to achieve readout of a single hologram of data. This angular separation is determined primarily by the thickness of the storage medium; for a 1 cm thick medium, the Bragg angle selectivity is approximately 0.3 mrad. The reference beam deflector must thus be capable of deflecting a 1 cm beam through an angle of approximately 20 degrees to achieve 1000 reference angles. (A near-term demonstration will require a much smaller number of holograms at each wavelength.)

The requirements for deflection of a 1 cm beam through 20 degrees are equivalent to a requirement for 5000 diffraction-limited beam positions. Current acousto-optic beam deflectors are unable to meet this requirement.[39,40] Galvanometer driven mirrors can easily meet both the beam size and angular deflection range requirements, while simultaneously achieving a deflection time of approximately a millisecond.[41,42]

Most galvanometers have both position sensing and feedback control to improve the accuracy of deflection. In addition, techniques have been developed to stabilize the position of a galvanometer within one half of the period of the lowest frequency mechanical resonance.[43] This technique uses a two-step driving waveform. The first step drives the mirror to the new position, and the second step stops it. The proper steps can be generated quite easily using a tapped delay line CCD circuit, for example. By adjusting the timing and amplitude of the two steps, mirror resonances can be cancelled. If more than one resonance contributes to mirror position errors, successive two-step circuits can be cascaded to eliminate both resonances. In this way both positioning accuracy and access time can be improved.

10.2 Detector Array

The number of bits which can be stored and retrieved per hologram will be determined by the number of pixels in the input and output devices. The readout rate of the detector array will determine the maximum data rate for reading. The lowest cost detector arrays with a large number of pixels are currently produced for low-light level television applications. By cooling the detector chip with a thermo-electric (TE) cooler, very low readout noise levels can be obtained. These currently available CCD arrays have approximately 600×600 pixels per frame.

Larger format detector arrays (1024×1024 and larger) are being developed for high-definition television (HDTV). These detector arrays have higher output data rates than current television camera chips to maintain a flicker-free frame rate. These arrays can also be operated at low readout noise levels using TE coolers.[44] Although the prices of HDTV equipment is currently high, as demand increases and production capability improves, these arrays will also be available at cost effective prices for optical memory readout.

Example TV and HDTV camera chips suitable for near-term and higher capability optical memory demonstration systems are shown in Table 6. We expect that future HDTV camera chip prices will approach those shown for current TV camera chips. Some HDTV chips are capable of even higher data rates than shown in this table.

Table 6. Camera Chips for Optical Memory Readout.

Camera Chip	Format	RMS Noise*	Chip Price
TV Philips 56471	604×588 50 Hz (CCIR) 5.8 MHz	6000 e ⁻	\$350 (no defects)
HDTV Thomson GHX31159	512×512 ≥60 Hz 10 MHz	200 e ⁻ (<10 e ⁻ at -40C)	\$3000
HDTV Thomson GHX31156	1024×1024 ≥60 Hz 40 MHz	200 e ⁻ (<10 e ⁻ at -40C)	\$15,000

*Room temperature performance

10.3 Spatial Light Modulator

The pixel format (and ideally the data rate) of the input spatial light modulator (SLM) must match those of the output data array. In the past, SLMs were the weak link in many types of optical processors, however, SLMs are currently being developed for a wide range of optical computing applications. The rapid progress in this area will continue independent of the needs of 4D optical memory systems.

The requirements for a near-term demonstration of 4D optical memory are a frame size of 64×64 pixels and a frame time of 200 msec. A second generation demonstration might require TV frame rates and a larger pixel format, up to 256×256 . The input requirements of optical memory systems have one major difference from those of other types of optical processors; the inputs need only be binary. This relaxation of the requirement for wide dynamic range allows different and potentially simpler technologies to be considered for SLM implementation.

A soon-to-be available SLM which can meet the near-term requirements is based on ferroelectric liquid crystal technology. (In principle the availability of this device could permit its utilization in our proof-of-concept demonstration.) This SLM has been developed by Display Tech.[45-47] This SLM will soon be available in 64×64 format, with 256×256 format projected. Frame rates of up to 10 KHz are achievable. The SLM is compact, with the form factor of a microprocessor chip, and it is functionally equivalent to a DRAM, simplifying the interface electronics. A sketch of this SLM is shown in Figure 31.

10.4 Microcoolers and Cryostats for SHB Media

Conventional cryocoolers have a cooling capacity far exceeding the requirements of our SHB memory medium. Projected heat loads are in the tens of milliwatts, caused primarily by the writing beam intensity. (This intensity is limited because of the heat conduction properties of the SHB polymer host.)

Microrefrigerators have been developed for rapid cooling of IR detectors to 77K.[48] These coolers make use of a Joule-Thompson cooling cycle implemented using microchannels etched in glass driven by a pressurized gas supply. Typical units can extract 250 mW of heat from

a cm-sized detector array at 85K and 100 mW of heat at 25K. These coolers have no moving parts and are thus vibration-free and reliable. These coolers have run continuously for more than 10,000 hours without failure; 85K, 250 mW coolers use 3 cubic feet of gas per hour. Closed cycle systems are available; a compressor to operate a multi-stage cooler could fit in an 8 inch cube. Figure 32 shows a typical configuration for a cooler of this type.

SDIO/IST is currently funding the development of two- and three-stage microcoolers which will operate down to 10K.[49] One application of these devices will be to cool Josephson junction devices for high-speed computing applications. The projected size, heat removal capacity, and cost are well-matched to our requirements. Potential problems include microparticles created by the freezing of impurities blocking the microchannels and expansion nozzles required for operation. Because of the need for cooling fluid purity (and thus expense) it may be necessary to operate these systems closed cycle. Information on the size and power consumption of closed cycle systems is not available at this time. These 10K systems are projected to be available in two to three years[50], well within the timeline for development of a prototype memory system.

More conventional commercial systems are presently available which are simple closed cycle refrigerators and of modest size (even in their present state of development).[51] For ground based applications, such cryostats could provide cooling capacity for as many as 10 of our proposed large scale optical memories. With some engineering development, these cryostats might also be reduced in size and power requirements to make them better matched to the requirements of our 4D optical memory system.

For space-based applications, the low heat dissipation and compact design again permits ready application of known technical approaches to permit operation for a year or more in space with only modest requirements put on weight and size, and virtually no impact on power requirements for operation. The use of solid-cryogen systems, which have been well tried and developed, should provide a very acceptable approach.[52]

10.5 Electronic Interface

The random access optical mass storage concept which we are proposing to develop can serve both supercomputer and workstation applications. Because of the much larger number of workstations and the blurring of the line between high end workstations and supercomputers, however, the high-end workstation market will be an important driver for commercial development of our memory concept. Many different bus architectures have been used and proposed for workstations. It will be desirable to choose a bus for our initial demonstrations which is common to a large user base and which has capability sufficient to support the high-end demonstrations of optical memory.

A table of the data and address widths and maximum data rates of a number of popular busses is shown in Table 7.[53,54] Most of the present bus systems have similar characteristics. A combination of two standard bus approaches appears to offer a near term approach with broad applicability. VMEbus is a commonly used system for image processing workstations, and drivers for many frame grabbers have been written to work with this bus. SCSI (not shown in the table) is more than just a bus system; it is actually an interface standard which can provide compatibility with a wide range of busses.

For future systems requiring high data rates and standard devices with the ability to interface with many computer architectures, a combination of SCSI-2 and/or Futurebus+ would seem to

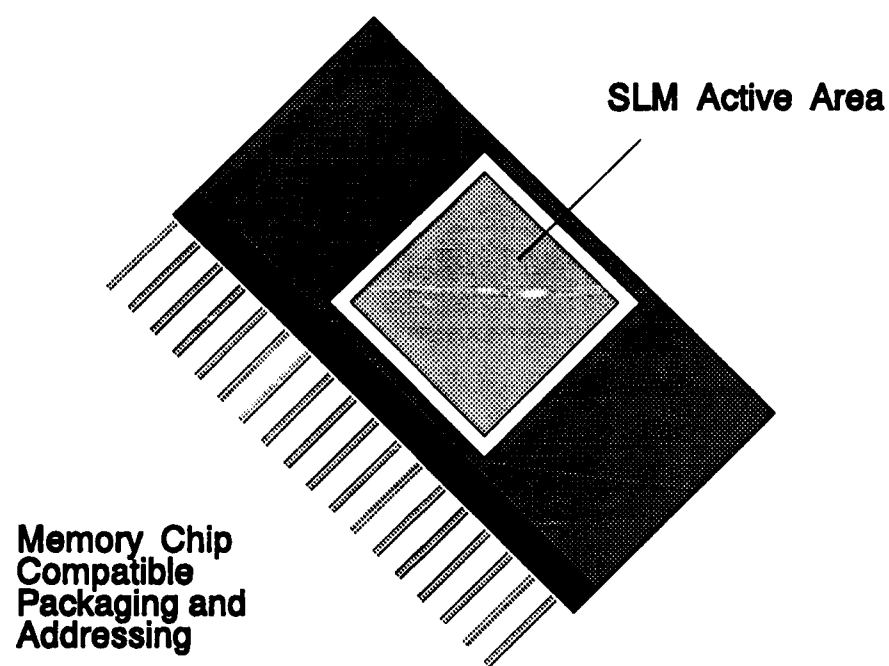


Figure 31. Display Tech Ferroelectric Liquid Crystal SLM.

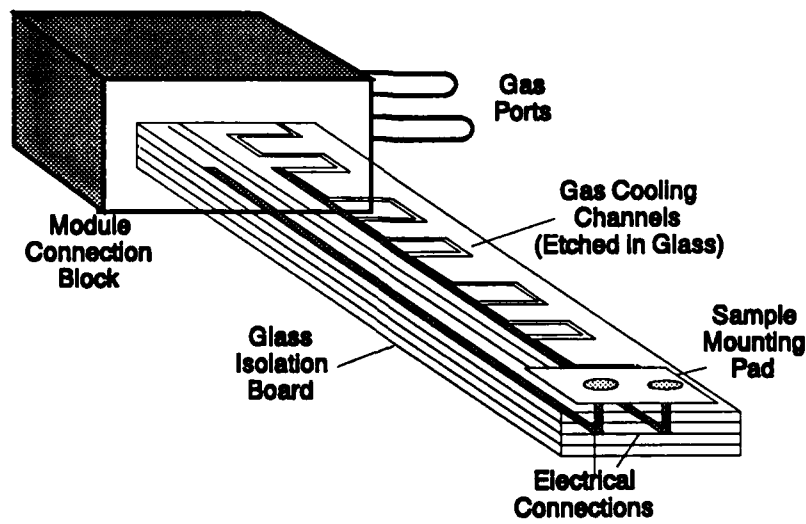


Figure 32. Typical microrefrigerator configuration.

be good choices with widespread acceptability and future expansion capability. It is clear that high data rate parallel readout detector and electronic architectures are being developed and will soon be commercially available.

Table 7. Characteristics of Common Bus Standards

Bus	Address Width	Data Width	Bandwidth (Mbytes/sec)
VMEbus	16,32	16,32	40
NuBus (Macintosh)	32	32	37.5
Multibus II	32	16,32	40
Microchannel (IBM PS 2)	16,24,32	8,16,32	17
EISA	16,24	8,16,32	33
S-bus (Sun)	32	16,32	57
Futurebus+	32,64	32,64 128,256	400 (32 bits) 3200

SCSI (Small Computer System Interface) is both a bus standard and a protocol. SCSI defines standard physical and electrical connections for devices. SCSI also incorporates communication protocols which treat peripherals as logical devices using a defined set of commands, eliminating hardware incompatibilities.[55,56] SCSI has been incorporated into the Micro Channel Architecture, and is expected to become the peripheral I/O interface for other architectures such as EISA. In SCSI-2, device command sets will include CD-ROM, optical drives, and jukebox storage systems.[57]

Futurebus+ is a scalable bus architecture.[58] Futurebus+ is basically a 64 bit data and address bus which can also accommodate 128 and 256 bit wide data. Data transfer on Futurebus+ is completely asynchronous, which means that the bus data transfer rate is not locked to a specific clock frequency. 32 bit systems will achieve an approximate data transfer rate of 100 Mbytes per second in 1991 and 256 bit systems will achieve a 3.2 Gbyte per second in 1995.

Another option which might provide both widespread acceptability and high I/O data rates is suggested by a recent Display Tech announcement. The Display Tech IC SLM eliminates special SLM controller electronics by using an addressing mode which is functionally equivalent to a DRAM chip. In this way, the SLM can be attached to any bus, since all busses are designed to handle cards of semiconductor memory. Although no product currently exists on the market, a similar approach could be used to obtain data directly from a detector chip. (In fact, memory chips are light sensitive and have been used as low quality detectors. A specially-designed detector chip could provide the advantages of a semiconductor RAM high data rate interface, low-noise readout by reading in parallel, and latching to produce reliable binary output.)

For efficient operation of the proposed high end optical memory the system will require a system control circuit (either a single chip or simple board) which will be dedicated to controlling

the laser wavelength and beam position for data storage and retrieval. The inputs and outputs required for operation of a holographic optical memory include FAL (frequency agile laser) control, beamsteering control, SLM input, and detector array output. FAL control for access to 1000 different wavelengths would include a power on, wavelength command (at least 16 bits), a wavemeter for closed loop wavelength control (16 bits), and a correction (16 bits). An acoustooptic beamsteering device, for example, would have similar inputs and precisions for closed loop access to 1000 beam positions. Temperature control and handshake bytes might also be of interest. These functions would reside on a simple driver card which would probably need to be microprocessor-controlled for closed loop wavemeter and beam deflector operation. SLM input and detector arrays outputs for writing and reading data might require a bit stream of up to 10^6 bits for each write or read operation.

10.6 Laser Source for Writing and Reading

The requirements for a tunable laser for optical memory access are shown in Table 8.

Table 8. Requirements for Demonstration and High-End Systems

Characteristic	Demonstration System	High-End System
Tuning range	10 nm	100 nm
Center wavelength	600 to 700 nm	600 to 700 nm
Linewidth	10 GHz	100 MHz
Tuning rate	30 msec	1 msec
Price	\$30,000	\$3000

SPARTA has developed an electrooptically tuned laser system[59] using a birefringent KDP tuner.[60] to tune a dye laser. The system uses a dye laser pumped by an argon-ion laser to produce over 300 W of tunable radiation in the middle of the visible spectrum. Rapid switching of voltages of ± 3000 V is required to tune the laser over 100 nm in the visible spectrum. The minimum cost of the tuner electronics is well over \$3K, and the total cost of the laser system approaches \$100K. Because of the need for dye flow and argon-ion pumping the system is not compact and is unlikely to be greatly reduced in cost.

The desired low cost laser for the high-end system implies that an external cavity diode laser and a low voltage tuner will be required. The external cavity diode laser can, in fact, do the entire job for even the high-end demonstrations of optical memory, however, completely integrated diode/tuner systems may ultimately be cheaper.

Many of the most promising SHB media, such as porphyrin, operate in the visible region of the spectrum, at shorter wavelengths than currently produced by standard laser diodes. The wavelength range of laser diodes is continuously being driven to shorter and shorter wavelengths by the desire to increase the density of data stored on optical disks. For example, NEC has recently reported laser diode operation at 671 nm, Philips Research Laboratories has reported room temperature operation at 626 nm, and Y. Kaneko of Sophia University (Japan) has reported

operation at 576 nm at 109K.[61] Laser diodes with broadband gain have been used in an external cavity configuration to achieve wideband tuning.[62] Achievement of continuous tuning, however, has been prevented to date by the tendency of the laser to lock to cavity modes of the semiconductor gain medium.[63]

Laser diode amplifiers which require coatings with less than 0.1% reflectivity per facet, have been developed for use at 1300 and 1500 nm.[64] The same techniques could be used to eliminate the Fabry-Perot resonances due to facet reflection for shorter wavelength amplifiers. These AR-coated amplifiers could be used in an external cavity laser configuration with an intracavity tuning mechanism.

MIT/Lincoln Laboratory has recently reported remarkable success stabilizing and tuning semiconductor lasers using external cavity techniques.[65,66] A company has been formed to exploit the commercial possibilities of this technology.[67] The MicralaseTM laser, with a stability of better than 1 MHz and an output power of >25 mW, in a package of size $2 \times 2 \times 8$ inches, is a typical laser system which could be used for 4D optical memory applications.

Three-section distributed feedback (DFB) lasers are a long-term alternative laser source; these lasers have been demonstrated in the $1.6 \mu\text{m}$ region of the spectrum.[68] These lasers, which are used for optical fiber communications, have linewidths of less than 100 MHz[69], which is sufficiently narrow for operation with organic dyes in organic host materials. The lasers have three sections, an active section, a passive, section, and a grating section. The active section provides gain. The passive section can be used to adjust the cavity length by modulating the index of refraction through control of the free carrier concentration. The grating section provides feedback at a narrow range of wavelengths within the gain bandwidth of the active gain section. The peak wavelength of the feedback can be adjusted by modulating the carrier concentration in much the same way as for the passive section. Continuous tuning is achieved by varying the current in the passive and grating sections in a coordinated manner. Wavelength stability can be maintained by placing the diode in a temperature-stabilized package.

10.7 Component Development Summary

Table 9 presents a summary of the status and expected future development of the components necessary for a 4D optical memory system. Many of the components are available, others are under development for other applications, several will be developed by SPARTA in the course of developing an optical memory system, and one, the frequency agile laser, will probably require a dedicated development program. As discussed above, however, there are no fundamental reasons why a frequency agile laser cannot be developed.

The key conclusion from this section is that all the components necessary for a 4D memory system will become available in the near future. These components will have a form factor, a cost, and power consumption consistent with the goals of a 4D memory system development program.

Table 9. Summary of Optical Memory System Component Development

Component	Development Plans
Optics	Standard, low-cost elements
Beam deflection	Available
Detector arrays	Available (astronomy) High-definition TV
Spatial light modulator	In progress, Many applications
Microrefrigerator (10K)	In progress, SDIO funded
Electronic interface	SPARTA
Memory manager system	SPARTA
Frequency channel medium	SPARTA
Frequency agile laser	Unique requirements, Engineering required

11 Experimental Plan for Phase II

This section discusses the results of Task 5 of our Phase I Statement of Work, Development of an Experimental Plan to investigate the storage and retrieval of volume hologram storage capabilities in SHB materials with particular emphasis on the frequency channel structure. In this section, we will describe in detail our plan for an experimental demonstration of our 4D memory concept.

The major issue to be addressed during our Phase II work is the experimental confirmation of the analysis and simulation performed by SPARTA prior to and during our Phase I contract. Our experimental configuration has been defined in such a way that an electronic interface is readily implemented. The resulting system will provide an adequate demonstration of the potential of these SHB materials in providing a capability for information storage compatible with modern computer needs. The demonstration will be a low-end realization of an entire optical memory architecture.

11.1 Materials Selection for 4D Optical Memory Experiments

A survey of the literature concerning candidate SHB materials has been made. A bibliography of the references consulted during this survey is presented in Appendix A. It is concluded that the optimal choice (at this time) for a host material would be copolymers of ethylene and methyl methacrylate, however, for our initial work planned for the Phase II effort, host materials such as PMMA and PVA are also suitable candidates.

The preferred photochemical species have been reduced to a group of five candidates. It is believed that the selection of one or two of these species for experimental use in Phase II of our program should provide a suitable vehicle to demonstrate the short term and long term capabilities of a 4D optical memory based on these materials.

From our Phase I work, it is clear that many of the SHB materials which have been widely studied by previous workers are prime candidates for consideration in holographic storage applications. Therefore the materials selection task is not a significantly difficult one, but it does require some thought and care so as to provide results which can properly represent the true capabilities of these materials when addressing the optical storage application.

The primary requirements for a high end application device permitting 2.5×10^{12} bit storage capacity within a 1 cm^3 volume are represented in Figures 25 and 28. This diagram bounds the parametric space related to photochemical quantum efficiency and absorption cross section. A secondary requirement is that the homogeneous linewidth should be less than or equal to 100 MHz. This homogeneous linewidth requirement has some assumptions behind it concerning the inhomogeneous linewidth. In particular, it was assumed that the useful inhomogeneous linewidth was approximately 50 THz wide. It is known that the selection of the host and of the photochemical species can influence both the inhomogeneous as well as the homogeneous linewidths. Furthermore, it is easy to envision using several photochemical species in the same host material to effectively enhance the frequency range of operation. This would argue that if a single photochemical species cannot provide the full 50 THz recording range, multiple species can be used in the same host material. This approach seems quite feasible because several of the favorite host materials (such as polyethylene (PE) and polymethylmethacrylate (PMMA)) have been used by a number of researchers for a reasonably wide range of photochemical species.

11.1.1 Selection of Host Material

There are six principal requirements for the host material:

1. The photochemical species must be soluble in the host to a level which is determined by the absorption cross section. For the proposed 4D memory system, the material thickness required is of the order of 0.5 to 1.0 cm, and the optical density required is approximately 1 for absorption holograms and 25 for phase holograms. The boundary on doping density corresponding to 1 percent also represents the boundary of spectral diffusion. Therefore, all of the photochemical species shown in Figure 25 and 28 have only modest solubility requirements of the order of 0.01 percent or less for absorption hologram applications. For phase holograms (where higher molecular densities are desired) in organic species (H_2P and chlorin) the solubility requirements are again not severe, but the inorganic species (F_4^- and ReO_4^-) may be reaching solubility limitations. Because organic species generally require organic hosts, we shall focus our attention on organic hosts.
2. The host must be optically clear. This is mostly a matter of material preparation, and previous workers have described simple techniques which have been used to achieve the quality necessary.
3. The host must be either a glass (random structure) or a partially crystalline structure. This provides a widely varying molecular environment around each SHB molecule.
4. The host must be capable of absorbing and conducting away significant amounts of heat while at very low temperatures. The selection of a host should not be completely governed by this requirement, but if high data rates are desired and thermal broadening is to be avoided, as well as having a high read to erasure ratio, then a more thermally conductive host may be desirable. This desire, however, may be in conflict with the basic need for a glassy material, as thermal conductivity is much better in crystalline materials.
5. The host should be relatively easy to handle and cast into samples of the order of 1 cm thick. This is a practical requirement, not a fundamental one, but it can be a significant requirement for the early experiments if the host is not well chosen.
6. The host should be chemically inert with respect to the photochemical species and it should also have fundamental properties which allow for long storage life of the spectral holes.

These requirements are generally well met by the common organic polymers polystyrene (PS), polymethylmethacrylate (PMMA), polyvinyl alcohol (PVA), and copolymers of ethylene and methyl methacrylate. In fact, these four hosts have been used in a substantial fraction of all the SHB research studies and have been used with most of the favored photochemical species. The reasons for the favored use of these three host materials relates strongly to their ease of handling and preparation. Both thin film[70] and thick cast samples[71,72] can be readily prepared containing a wide range of organic photochemical species. The use of these host materials by a number of researchers points to the reasonably high solubility of the photochemical species in these materials. Their optical properties are excellent, providing samples of suitable optical clarity and uniformity when appropriate care is taken. The thermal properties of these materials are typical of materials having a randomized structure, so they are quite representative. The preparation of these materials is quite simple, with little or no chemical synthesis required because they are readily available as "off-the-shelf" items in high purity and at modest cost.

Being commonly used base materials in electronics and for household items, they are of course quite stable chemically. They have also been shown to provide spectral holes which have a measured long term persistence.[71]

Based on these attributes, we can readily narrow the field to these four host materials as the primary media into which to introduce the selected photochemical species.

11.1.2 Selection of Photochemical Species

It is of course assumed that the photochemical species selected must have cross sections and quantum efficiencies which fall within the parametric regions defined in Figures 25 and 28. The only significant requirements to permit experimental investigations of the selected species are largely practical ones related to spectral hole width, solubility in the host materials, and potential hazardous effects of the photochemical species selected. Luckily, much of the information related to hole widths and solubilities are already determined adequately and the toxicity of these material is not significant. Once introduced into the host matrix and solidified these photochemical species become chemically inert so as to make handling of no significant concern.

Within the constraint of being contained in the three selected host media, a number of interesting candidate photochemical species can be selected and have already been characterized adequately to prove useful in our planned experiments. The candidate materials are shown in Table 10. This list of candidate materials and their properties are well defined by the literature for some of the cases. A recent publication [73] has shown that a relatively simple relationship exists between the homogeneous linewidth of a species in a given host and how it can be expected to behave in a wide variety of host media. This permits us to extrapolate performance of these materials to a wide range of hosts as needed so that performance may be anticipated. Furthermore, of the photochemical species listed, we find them to be closely related chemically, which permits us to expect that the homogeneous linewidth of all these species should be very similar.

An additional factor which has been considered in selecting this list of photochemical species is their potential for photoreversibility which can permit erasure of the stored information. We consider this to be a key property which can influence the long term acceptability of these materials for general information storage applications. In the case of chlorin, the photoproduct is separated from the initial species by roughly 50 nm, while the other species can be returned to their initial states by illumination with light at a wavelength of 600 nm or less.

An interesting concept to explore experimentally is to have multiple photochemical species present in the same host. This concept would allow one to extend the effective frequency range for storage of information. Such a combination might be TFP and TPP in PMMA. The center wavelengths are close enough that they would be accessible when using the same laser. While the absorption peaks are not close enough to permit overlap, it may be expected that suitable materials may be available in the future if this concept of multiple photochemical species can be shown to be compatible with the needs of a high end system.

The issues associated with quantum efficiency can be addressed directly in the future by some selective "engineering" of the photochemical species. This has been shown to be feasible[76] with a capability to alter the quantum efficiency of selected molecular structures by changing chemical side groups. Such a series is seen in Figures 25 and 28 and represented by the points

Table 10. Properties of Selected SHB Materials. Items in parentheses are estimated from literature values extrapolated to the host materials indicated. All values indicated correspond to 4.2 K.

Material	Host	Center Wavelength	Inhomogeneous Linewidth	Spectral Hole Width
H ₂ P	PE PMMA	611 nm	4.5 THz 4.5 THz	40 MHz 1 GHz
Chlorin	PE PMMA	635 nm	(12 THz) 12 THz	(100 MHz) 1 GHz
TMP	PE PMMA	653 nm	(10 THz) (10 THz)	(100 MHz) (1 GHz)
TPP	PE PMMA	646 nm	(10 THz) (10 THz)	(100 MHz) (1 GHz)
TSPP	PE PMMA	640 nm	(10 THz) 10 THz	(100 MHz) (1 GHz)
TFP	PE PMMA	659 nm	(10 THz) (10 THz)	(100 MHz) (1 GHz)

PE polyethylene.
 PMMA polymethylmethacrylate.
 TMP tetrakis(4-methoxyphenyl)porphine.[74]
 H₂P free base porphyrin.[24]
 TPP tetraphenylporphine.[74]
 TSPP tetrasodium 5,10,15,20-tetra(4-sulfonatophenyl)porphine.[75]
 TFP tetrakis(pentafluorophenyl)porphine.[74]
 Chlorin.[1]

labeled TMP, H₂P, TPP, TSPP, and TFP. This approach leaves the main properties of the photochemical species intact (homogeneous and inhomogeneous width) while altering a major factor which can directly affect system performance. It can be expected that similar chemical modifications to the critical components of the SHB materials (host as well as photochemical species) will be carried out in the future in order to optimize performance.

11.2 Optical System Design for 4D Optical Memory Experiments

An optical system design is presented in this section which incorporates all the necessary attributes of the 4D memory architecture. The details are presented to a level which would allow costing and purchase of the specific optical elements. The optical design satisfies all the requirements for the initial grating experiments as well as for a significant demonstration. The design presented would allow for direct data input from a 64 by 64 element plane, or roughly 4,000 bits per image.

The fundamental architecture of the proposed 4D optical memory system has been shown in

Figure 33. The major components are the SHB material itself, an input plane SLM, an output plane detector array, a beamsteering device and a frequency agile laser. A reference laser beam is deflected by a galvanometer and uniformly illuminates the SHB medium during recording and readout. This beamsteering device provides the capability to record multiple holograms at the same wavelength. The illumination is provided by a tunable laser, which has the capability of providing the frequency diversity required for storage of holograms at multiple frequencies. Upon readout of the holograms, the light is detected by a CCD array and digitized for direct usage by standard electronic computers.

To properly implement this architecture with efficiency in light usage and to provide high contrast holograms requires the careful implementation of some relatively standard optical principles and a detailed optical design. One also has the ancillary requirement that the components used for this first experimental demonstration of a 4D optical memory system be commercially available and be implemented with a minimum of complexity and cost. These compromises require that the experimental system proposed here be larger than a working system might be and actually have more components than the working system. With these compromises in mind, the general layout of the experimental optical system is presented in Figure 34. The primary segments of the system will each be examined in sufficient detail to understand and implement each of the necessary functional properties.

The general layout of the system is in two parallel optical trains which are spaced 8 cm apart. These two trains are of approximately equal length and are located in close proximity to minimize the effects of air turbulence upon the stability of the laser beams. The total length is approximately 0.6 meters, and the total width and height is less than 12 cm, allowing the system to be covered to minimize turbulence and eliminate stray light, as well as to be designed into a brassboard configuration. All components will be antireflection coated (when possible) to reduce scattering and enhance system performance.

The complete system is divided into four sections which can be treated as largely independent of each other. This independence will not only aid in the following discussions but also in their implementation during the program. These sections are:

1. Cryostat, Detector, and Erasure Optics,
2. SLM and Reduction Optics,
3. Beam Steering and Relay Optics, and
4. Laser and Beam Splitting Optics.

The electronic interface is not shown and will be discussed in a later section.

11.2.1 Cryostat, Detector and Erasure Optics

This segment of the system contains the central input and output optics of the optical memory and is shown in detail in Figure 35. It is largely symmetric with each of the four separate legs of the system having nearly identical optical properties. The input image is brought to a focus at the left side of the figure and the pupils of these simple lenses are located inside the SHB material. The two beam paths have an angle of 15 degrees with respect to each other and are simply combined and later split by the reflective prisms. The lower input image actually corresponds to the focal point of the relay optics used in the beamsteering device. After passing through the SHB material, the beams are again separated, with one being reimaged onto a CCD detector

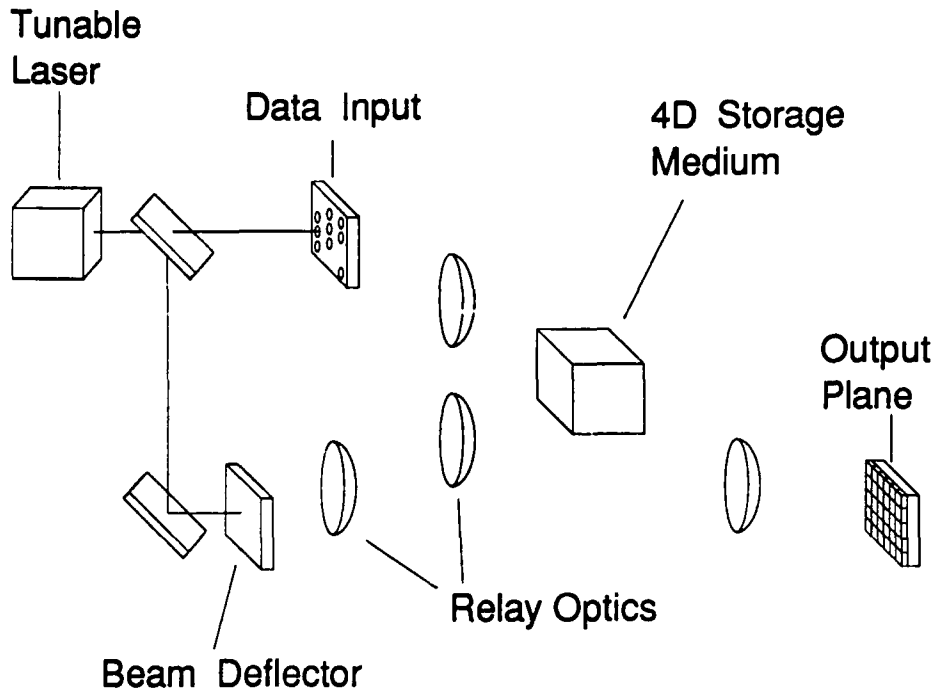


Figure 33. Schematic optical layout for the experimental version of the proposed 4D optical memory computer.

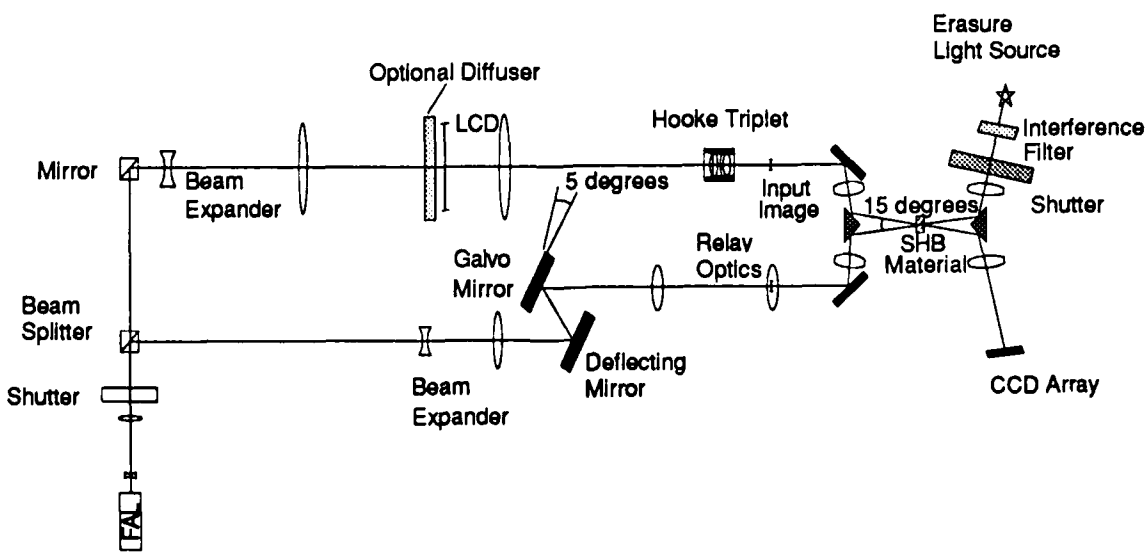


Figure 34. General layout of the proposed optical system for the experimental 4D optical memory.

Image data is transferred directly into PC memory in parallel and the effective image capture rate can be as high as 15 to 20 frames per second.

11.2.2 SLM and Reduction Optics

The principal function of this segment of the system (see Figure 36) is to reduce the image size of the SLM. We have chosen to utilize a LCD (liquid crystal display) as the input plane for our experimental system due to cost and convenience considerations. The advantages of LCD displays are that they are readily available as personal computer displays or small portable TVs of significant resolution and already have the necessary hardware and software available to present any image to the memory system in a convenient and adequate contrast format.

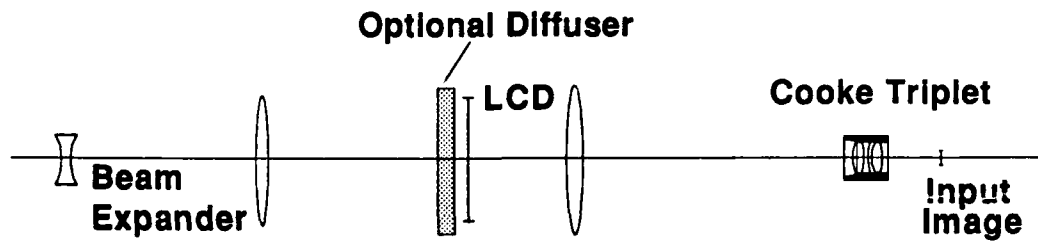


Figure 36. Details of the optical elements which permit illumination and reduction of the image provided by the LCD.

The penalty which must be paid for using an LCD display (instead of a more sophisticated and compact SLM) is that the illuminating beams must be broadened to about 3.6 cm diameter and the images must be significantly reduced. We have chosen to provide an intermediate image of the LCD plane before entering the cryostat and detector optics to permit inspection of the images for experimental purposes.

The reduction is carried out by use of a simple Cooke triplet having a focal length of 3 cm and an entrance pupil of 1.07 cm. The Cooke triplet is a high resolution component which will certainly not limit optical performance over a field of 1.06 cm (the required image field is only 0.7 cm). The use of a simple triplet to carry out the reduction requires that the illumination optics focus the light at the pupil of the triplet. The illumination optics will be discussed in the following section.

array. The second output leg will serve a dual purpose as a beam dump for the reference beam (or reading beam) and as the source of radiation for the photoinduced erasure. Since the erasure light need not be monochromatic, a simple lamp with an interference filter will provide adequate performance.

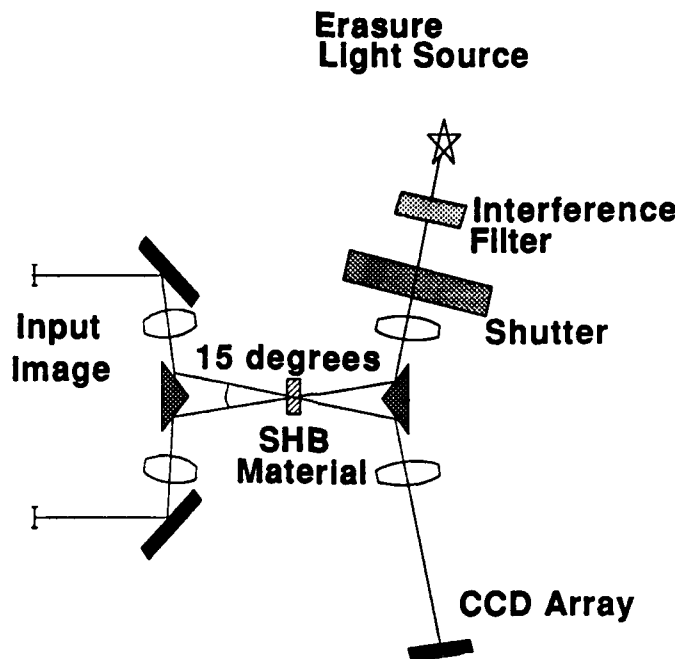


Figure 35. Details of the optical elements surrounding the SHB material (located in the cryostat) and the elements leading from the immediate input to the output plane.

Each of the four lenses has a focal length of 6 cm. The folding mirrors shown are flat to $\lambda/10$ over 25 mm. The entrance pupil diameter is set by the area of the SHB material which will be used for storage, which is 0.5 cm diameter. This makes this section of the system have an F number of 12, which leads to a resolution of 8.4 μm at 700 nm. This well exceeds the image resolution required which is 0.5 cm/128 pixels, or 39 μm between pixels.

Component	Melles Griot Part Number	Number Required
Lens	06-LAL-007	4
Mirrors	02-MFG-001	2
Mirror-Coated Prism	01-PRS-013	2
Interference Filter	03-FIM-008	1

The CCD detector array selected will be an 8 bit CCD array from Electrim Corporation. This array is thermoelectrically cooled to 35 degrees C below ambient for low light level operation and permits software control of the frame storage time from 30 milliseconds up to 200 seconds.

Component	Melles Griot Part Number	Number Required
Cooke Triplet	01-LAS-001	1
Concave Lens	01-LDK-007	1
Convex Lens	01-LAO-159	2
Diffuser	*	1

* This is a non-standard item since only a modest diffusion is required. This can be easily achieved with a simple ground glass plate, and a smooth glass plate having index matching fluid between them to tailor the degree of angular dispersion.

The selection of a personal computer is not necessarily critical since they all have comparable pixel resolution and generally acceptable screen size. The PC selected will be an IBM PC or compatible which will readily permit interfacing with the output plane CCD camera and utilization of simple software compatible with other PC's at SPARTA to permit writing of software off-line. The use of a PC may even permit direct use of graphics packages for construction of specific bit-plane patterns.

In actual use, the display must be partially disassembled to permit transmission of the laser beam through it. Optical flats can be optically coupled to the front and back surfaces of the LCD should it be determined that the wavefront distortion of the display must be improved upon. We may also choose to remove the glare prevention coverglasses to enhance transmission for some experiments.

11.2.3 Beam Steering and Relay Optics

This segment of the optical system is quite simple and is shown in Figure 37. The angular change in the reference beam light path is induced by the mechanical motion of a galvanometer mirror. To prevent the beam from wandering across the recording medium as the galvo is turned, the surface of the galvo is reimaged on the recording medium by the relay optics. To create the proper beam size at the galvo mirror, the beam must be expanded to approximately 0.5 cm. In order to match beam path lengths on the two legs of the system, the length of the "Z" created by the folding mirror can be adjusted to permit them to match.

The range of angular deflection required for the recording and readout of multiple holograms at the same frequency is determined by the resolution and field of view of the optics as well as the thickness of the recording medium. In this system, a 5 degree range of angular deflection will provide adequate motion to record as many as 100 superimposed holograms.

Component	Melles Griot Part Number	Number Required
Lens	06-LAL-007	2
Mirror	02-MFG-001	1
Concave Lens	01-LDK-007	1
Convex Lens	01-LAO-037	1

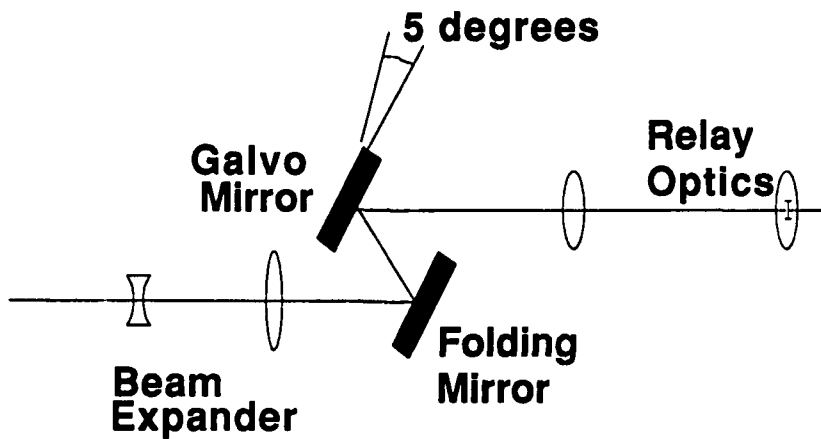


Figure 37. Details of the optical elements which expand the illuminating laser beams and also direct the beam as a function of laser wavelength.

11.2.4 Laser and Beamsplitting Optics

This section of the optical system merely has the function of providing a coherent source of light which is collimated, shaped, and split into two beams to enter the two separate legs of the optical system as seen in Figure 38. The collimated beam passes through an electronic shutter and a 50 percent beamsplitter which sends half of the light into leg B and the other half of the beam into leg A.

The requirements on the laser itself are much more significant. The minimal requirements are that the laser be tunable over a range of 10 nm in the vicinity of 600 to 670 nm. For minimal experimental needs, rapid tuning and digital control are not required. For suitably rapid experimentation however, it will be worth having a frequency agile system which can be computer controlled with reasonably rapid tuning capability. In this wavelength region, a tunable dye laser would be a convenient choice. The pump source would be an Argon-ion laser. Digital control would be provided by a PC which can be directly linked to the computer which controls the LCD as well as the CCD arrays and the electronic shutter.

Because of the high sensitivity of the SHB materials of interest, the power requirements on the FAL will be minor (10 mW or less). To provide interesting storage capability and frequency selectivity, these experiments would be adequately carried out with frequency selectivity of the order of 1 GHz, which is readily obtainable from the SPARTA FAL.

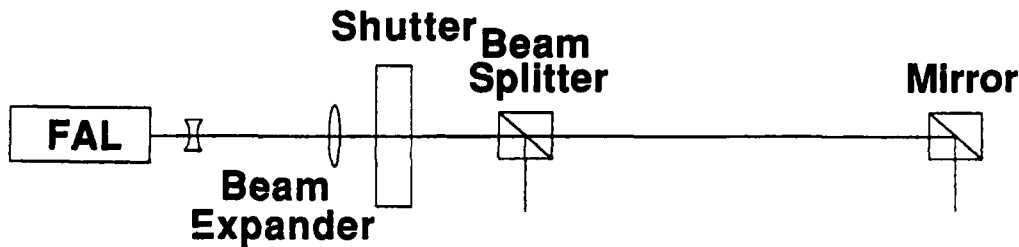


Figure 38. Details of the optical elements which expand and split the illuminating laser beams. After shaping, the beam is then split to permit simultaneous illumination of the two legs of the system.

Component	Melles Griot Part Number	Number Required
Concave Lens	01-LLD-001	1
Convex Lens	01-LAO-059	1
Beamsplitter	06-LAI-007	1
Mirror	02-MFG-001	1

11.2.5 Incrementally Assembling the Complete Design

The initial experiments which will provide important information on material performance and optical details will not require much of the optics in the complete design shown above. Writing simple gratings will only require the modest beam expansion and splitting seen in the Laser and Beam Shaping section, coupled with the few mirrors and the CCD camera seen in the Cryostat and Detector optics section (see Figure 39). This configuration will permit storage of gratings at several independent frequencies. With a modest capability to alter the beam angle on leg B, the experiments which demonstrate storage of multiple holograms at the same frequency can be carried out. By introducing computer controlled scanning of the FAL, one or more "frequency channels" can be bleached in the SHB material.

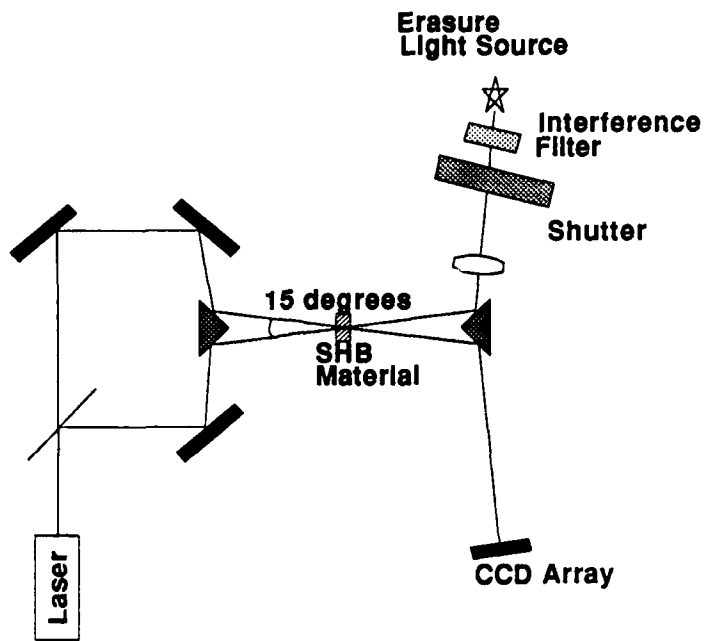


Figure 39. Details of the optical elements required for the initial recording of simple gratings. By incrementally expanding on this simple layout, the complete system can be built up.

11.2.6 Summary of the Experimental Design

An experimental optical design is presented which meets the needs of the final complete 4D optical memory system. This design can be built up in segments and introduced as the program proceeds though the necessary experiments. All the components are either commercially available, or can be readily obtained by minor mechanical modification of existing components. The approach of building up the system in pieces will permit section by section implementation and set-up of the system, with a minimum of cost and rework.

It is also worthy of note that the system outlined above is significantly "over-designed" at present, (even with off-the-shelf components) having greater resolution than really needed for these experiments. Without altering any other components, the pixel density of the SLM could be increased by a factor of 4 in each dimension. This expandability would effectively permit the storage capacity of this system to reach 256 kilobits per frame.

11.3 Electronic Interface and Memory System Control

Complete system operation requires laser illumination control, digitization of the readout images, frame composing of the images for the input SLM, control of erasure functions, and general system management. These functions can all be controlled from a central PC-based processor. All the system components are available as off-the-shelf items and are compatible with standard C language software available for PCs.

It will be our objective to make the demonstration optical memory system appear to the user

as being the equivalent of a conventional magnetic disk drive.

11.3.1 System Description

A schematic overview of the system is seen in Figure 40. The key property of the system is that the flow of data into and out of the SHB medium is managed by a single PC which carries out all the functions relate to data management. In the high end system envisioned for the future all these functions would be carried out by special purpose electronic circuits, but for the demonstration planned here, it will be convenient to carry out these functions using a general purpose PC.

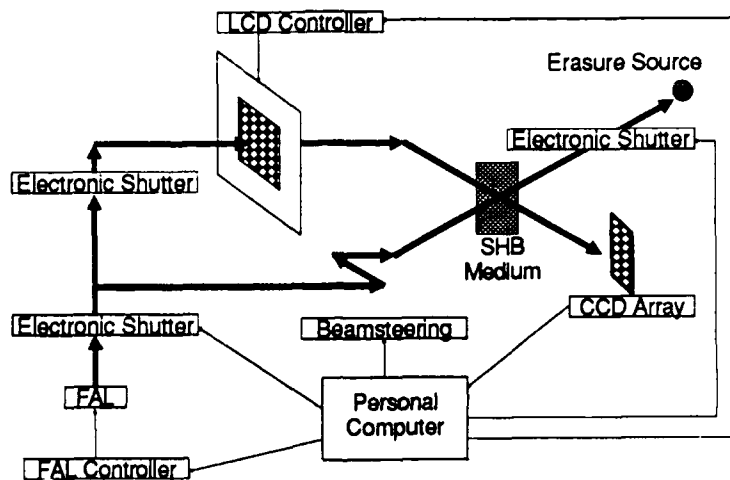


Figure 40. Schematic of the complete 4D memory system highlighting aspects of the electronic control system.

The major components of the experimental control system are:

1. A CCD array which will feed the digitized image directly into PC memory,
2. LCD display and controller,
3. FAL and controller,
4. Electronic Shutters,
5. Personal Computer.

11.3.1.1 CCD Arrays

The detector array will be a commercially available CCD array which can be operated cooled. The above attribute permit very low noise operation and efficient light collection. Reading the digitized image directly into PC memory permits rapid and efficient data handling.

11.3.1.2 LCD Display and Controller

The developments in the PC industry have made this particular component easy to obtain and use as it can be simply a laptop PC which has an LCD display. The LCD display must be partially disassembled to permit transmission of the laser beam. The laptop PC can be used as the controller itself with fully programmable capabilities including grey scale and reliable interface to the master PC or directly from the CCD camera frame storage units. Being a fully operational PC one can also make use of readily available graphics software to permit display of detailed images on the LCDs for generation of demonstration bit planes.

11.3.1.3 FAL and Controller

This component of the system will be a dye-based frequency agile laser (FAL) pumped by an Argon-ion laser. The FAL system is manufactured by SPARTA and will be available for use during the later stages of the program. The FAL is controlled by a PC system of its own, with easy interface capabilities to the master PC system.

11.3.1.4 Electronic Shutter

These components will simply be electronic shutters which can be directly controlled by the master PC.

11.3.1.5 Personal Computer

This component is the central control point for system control and feedback of information from the CCD array. While the controllers from the FAL or the LCD systems could have provided the capability demanded by the overall system to meet the functions of central control and data manipulation, such operation would have been clumsy at best, for experimental purposes. Therefore, having a PC dedicated to being the central control unit of the system will permit complete experimental flexibility with maximum data acquisition analysis and control being possible in a minimum amount of time. Being fitted with IEEE 488 and other standard interface cards, this unit will be able to communicate directly with all major system components in a timely manner.

11.3.2 Summary of the Electronic Interface

It is readily seen that the electronic interface system can be directly implemented with a minimum of effort and with little software development. From the earliest stages of introduction, the system can be extremely helpful in the experiments to provide easy and detailed examination of the results. The electronic system proposed will not only permit full electronic interface capability but will enhance the efficiency of the entire experimental effort allowing us to concentrate our efforts on the more fundamental issues surrounding the recording of holograms in SHB materials.

12 Summary

All the tasks in our Phase I Statement of Work have been completed successfully. The results of this analysis point a clear direction for achieving success during the proposed Phase II effort. Moreover, our analysis has shown that a significant need exists within the user community for mass storage devices having the characteristics which our proposed approach can provide.

Analytical models have examined the potential operating characteristics of high performance systems based on frequency channels in SHB materials. The systematics of erasure have been examined in detail and determined to be compatible with our proposed memory system architecture via several approaches. All the necessary system components required for the assembly of high performance systems are presently under development or already exist. A projection of final system costs based upon estimated component costs has shown that the proposed system will have a highly competitive cost/Mbyte as well as performance in a compact form.

Finally, a detailed plan has been presented to permit a laboratory demonstration of an early version of the 4D memory system which comprises all the key operational characteristics of an optical memory system. This demonstration will make use of available off-the-shelf components to provide a first test of this memory system at a modest cost.

References

1. U. P. Wild, S. E. Bucher, and F. A. Burkhalter, "Hole burning, Stark effect, and data storage," *Appl. Opt.* **24** 1526 (1985).
2. J. McHugo, Boston Technologies, private communication.
3. K. Wallgren, "Supercomputing and Storage," *SPIE Proc.* **695** (1986) 334.
4. J. Neff, E. I. DuPont, private communication.
5. J. Goodhue and T. Downey, Bolt, Beranek, and Newman, private communication.
6. S. Brand, *The Media Lab*, Viking Press, New York (1987).
7. G. Davenport, MIT Media Lab, private communication.
8. D. Simpson, "RAIDs vs. SLEDs," *System Integration*, (1989) 70-82.
9. C. Stanfill, Thinking Machines, Inc., private communication.
10. Heliplex HS-4 System, APD Cryogenics, Inc., 1919 Vultee Street, Allentown, PA 18103.
11. 1988 Disk Trend Report, Rigid Disk Drives, DISK/TREND, Inc., 1925 Landings Drive, Mountain View, CA 94043, RSPEC-47.
12. M. L. Levene, "Applications for a high capacity, high data rate optical disk buffer," *SPIE O-E LASE '88*, January 15, 1988, Los Angeles, CA.
13. G. J. Ammon, "Archival optical disc data storage," *Opt. Engineer.* **20** (1981) 394.
14. Storage Technology Corp. 2270 South 88th St. Louisville CO., 80028, Specification ED009-4, July 1987.
15. Albert Rose and Paul K. Weimer, *Physics Today*, **42** (9) 24-32 (1989) and the references noted therein.
16. D.Haarer, "Photochemical Hole-Burning in Electronic Transitions", **Topics in Current Physics - Persistent Spectral Hole-Burning: Science and Applications**, W.E. Moerner ed., Springer-Verlag, (1988) 107.
17. R.M. Macfarlane and R.M. Shelby, "Persistent Spectral Hole-Burning in Inorganic Materials", **Persistent Spectral Hole-Burning: Science and Applications**, W.E. Moerner ed., Springer-Verlag, (1988) 127-150.
18. Robert C. Weast, *Handbook of Chemistry and Physics*, 50th edition, The Chemical Rubber Company, 1969, page D-129.
19. S. Burgess and D. Greig, Proceedings of the Fourteenth International Conference on Thermal Conductivity, Storrs Conn., June 2-4, 1975, **Thermal Conductivity 14** , Ed. by P.G. Klemens and T.K. Chu, Plenum Press, (1976) p 45-48.
20. H.S. Carslaw and J.C. Jaeger, *Conduction of Heat in Solids*, 2nd Edition, Clarendon Press, (1986) 130.
21. Charles Kittel, *Introduction to Solid State Physics* 4th Edition, John Wiley and Sons Inc., (1971) 230.
22. A. Renn, A.J. Meixner, U.P. Wild and F.A. Burkhalter, *Chemical Physics* **93** (1985) 157-162.
23. J.P. Huignard, J.P. Herriau and F. Micheron, *Applied Optics* **26** (5) 256-258 (1975).
24. W. E. Moerner and M. D. Levenson, *J. Opt. Soc. Am. B* **2** (1985) 915-924.
25. H. Kogelnik, *Bell Syst. Tech. J.*, Vol 47, 2909 (1969).

26. R. M. MacFarlane and R. M. Shelby, J. of Luminescence **36** (1987) 179-207.
27. H. P. H. Thijssen and S. Volker, J. Chem. Phys. **85** (1986) 785-793.
28. W. Lenth, R. M. Macfarlane, W. E. Moerner, F. M. Schellenberg, R. M. Shelby, G. C. Bjorklund, SPIE Vol. 695, Optical Mass Data Storage II, (1986) 216-223.
29. A. R. Gutierrez, J. Friedrich, D. Haares, H. Wolfrum, IBM J. Res. Dev. **26** (March 1982) 198-207.
30. M. Romagnoli, W. E. Moerner, E. M. Schellenberg, M. D. Levensen, G. C. Bjorklund, J. Opt. Soc. Am. **B1** (1984) 341-348.
31. A. Renn, A. J. Meixner, U. P. Wild and F. A. Burkhalter, Chem. Phys. **93** (1985) 157.
32. U. Itoh and T. Tani, Appl. Opt. **27** (1988) 739-742.
33. A. Yariv, *Introduction to Optical Electronics*, (1971) Holt, Rinehart and Winston, Inc, 85.
34. K.K. Rebane and L.A. Rebane, "Basic principles and Methods of Persistent Spectral Hole-Burning", *Persistent Spectral Hole-Burning: Science and Applications*, W.E. Moerner; ed. (1988) Springer-Verlag, 17-78.
35. Max Born and Emil Wolf, *Principles of Optics (Electromagnetic Theory of Propagation, Interference and Diffraction of Light)*, 3rd Edition, Pergamon Press, (1965) 468.
36. A. Renn, A.J. Meixner, U.P. Wild and F.A. Burkhalter, Chemical Physics, Vol 93 (1985) 157-162.
37. N. Kishi, S. Tamura, N. Asai, K. Kawasumi and J. Seto, "Photochemical Hole Burning of Tetraphenylporphine Derivatives", Presented at SPIE Conference, LA'89, Optical Data Storage Symposium.
38. Kazuaki Sakoda, Kazuhiko Kominami and Masao Iwamoto, Japanese Journal of Applied Physics **27** (7) L1304-L1306 (1988).
39. Brimrose Corporation of America, 5020 Campbell Blvd., Baltimore, MD 21236, Product Catalog, October, 1990.
40. I. C. Chang, "Acoustooptic Devices and Applications," IEEE Trans. on Sonics and Ultrason. **SU-23** (1976) 2.
41. Cambridge Technologies, 23 Elm St., Watertown, MA 02172.
42. General Scanning, Inc., 500 Arsenal St., Watertown, MA 02272, Optical Scanners.
43. A. Sanchez, P. D. Henshaw, and R. B. McSheehy, "Fabry-Perot optical switch driven by a fast PZT transducer," Appl. Opt. **18** (1979) 2359.
44. Thomson Military and Space Components, Totowa, NJ, private communication (3 January, 1991).
45. L. Stuart, Displaytech, 2200 Central Avenue, Boulder, CO 80301, private communication.
46. L. K. Cotter, T. J. Drabik, R. J. Dillon, and M. A. Handschy, "Ferroelectric-liquid-crystal/silicon integrated-circuit spatial light modulator," Opt. Letters **15** (1990) 291.
47. T. J. Drabik and M. A. Handschy, "Silicon VLSI/Ferroelectric Liquid Crystal Technology for Micropower Optoelectronic Computing Devices, Appl. Opt. **29** (1990) 5220.
48. R. Wolfe and R. M. Duboc, Jr., "Small Wonders: Microminiature Refrigerators for Cooling Detectors," Photonics Spectra (July, 1983) 52.
49. F. Quelle, Office of Naval Research, private communication.

50. J. McHarg, MMR, private communication.
51. Janis Research Co., Inc., 2 Jewel Dr., Wilmington, MA 01887, Cryogenics in Progress.
52. W. L. Wolfe and G. J. Zissis, eds., *The Infrared Handbook* (ERIM, IRIA Center) 1978, p.15-19.
53. N. Baran, "The Bus Stops Here," Byte (February, 1990) 340.
54. P. L. Borrill, "High-speed 32-bit buses for forward-looking computers," IEEE Spectrum (July, 1989) 34.
55. L. Brett Glass, "The SCSI Bus: Part 1," Byte (February, 1990) 267.
56. L. Brett Glass, "The SCSI Bus: Part 1," Byte (March, 1990) 291.
57. B. Van Dyke, "SCSI: The I/O Standard Evolves," Byte IBM Special Issue (Fall, 1990) 187.
58. J. A. Gallant, "Futurebus+," Electronic Data News (1 October, 1990) 87.
59. P. B. Scott, "Frequency-Agile Laser Systems," U. S. Patent 4,897,843, 30 January, 1990.
60. J. M. Telle and C. L. Tang, "Direct Absorption Spectroscopy Using a Rapidly Tunable CW Dye Laser," Opt. Commun. **11** (1974) 251.
61. H. W. Messenger, "Lasers move into the spotlight at CLEO," (May, 1990) 115.
62. D. Mehuys, L. Eng, M. Mittelstein, T. R. Chen, and A. Yariv, "Ultra-Broadband Tunable External Cavity Quantum Well Lasers," SPIE Proc. **1219** (1990) 363.
63. A. Schremer and C. L. Tang, "Single-Frequency Tunable External-Cavity Semiconductor Laser Using an Electro-optic Birefringent Modulator," Appl. Phys. Lett. **55** (1989) 19.
64. M. J. Mahoney, "Semiconductor Laser Optical Amplifiers for Use in Future Fiber Systems," J. Lightwave Tech. **6** (1988) 531.
65. W. F. Sharfin, J. Seppala, A. Mooradian, B. A. Soltz, R. G. Waters, B. J. Vollmer, and K. J. Bystrom, "High-power, diffraction-limited, narrow-band, external-cavity diode laser," Appl. Phys. Lett. **54** (1989) 1731.
66. A. Mooradian, "Laser linewidth," Phys. Today (May, 1985) 43.
67. Micracor, Inc., Two Comtech Park, 696 Virginia Road, Concord, MA 01742.
68. K. Kobayashi and I. Mito, J. Lightwave Technol. **LT-6** (1988) 1623.
69. V. Chan, MIT/Lincoln Laboratory, private communication, 28 November, 1990.
70. H. P. Thijssen and S. Volker, Chemical Physics Letters **120** (1985) 496.
71. T. Nishi, K. Arishima, H. Tabei and H. Hiratuka, Japanese Journal of Applied Physics **27** (1988) 225.
72. H. P. Thijssen and S. Volker, J. Chem. Phys. **85** (1986) 785.
73. Uichi Itoh and Toshiro Tani, Applied Optics **27** (4) 739-742 (1988).
74. N. Kishi, S. Tamura, N. Asai, K. Kawasumi and J. Seto, "Photochemical Hole Burning of Tetraphenylporphine Derivatives", Presented at SPIE Conference, LA'89, Optical Data Storage Symposium.
75. Kazuaki Sakoda, Kazuhiko Kominami and Masao Iwamoto, Japanese Journal of Applied Physics **27** (7) L1304-L1306 (1988).
76. N. Kishii, S. Tamura, N. Asai, K. Kawasumi and J. Seto, presented at SPIE LA 1989, Optical Data Storage Symposium, paper PDP-1.

APPENDIX A A Bibliography of Papers on Spectral Hole Burning Materials

- Burland, D. M., F. Carmona, G. Castro, D. Haarer, and R. M. Macfarlane, "Write and Read Scheme for Photochemical Hole Burning Storage Systems," IBM Tech. Disc. Bull. **21** (1979) 3770.
- Cadogen, K. D., and A. C. Albrecht, "Detailed Studies of a One-Electron, Two-Photon Ionization in a Rigid Organic Solution at 77 K," J. Phys. Chem. **72** (1968) 929.
- Chraplyvy, A. R., W. E. Moerner, A. J. Sievers, and R. H. Silsbee, "Persistent Nonphotochemical Hole-Burning of a Molecular Vibrational Mode in Alkali Halide Lattices," Appl. Phys. B **28** (1982) 264.
- de Vries, H., and D. A. Wiersma, "Homogeneous Broadening of Optical Transitions in Organic Mixed Crystals," Phys. Rev. Lett. **36** (1976) 91.
- Friedrich, J., and D. Haarer, "Photochemical Hole Burning: A Spectroscopic Study of Relaxation Processes in Polymers and Glasses," Angew. Chem. Int. Ed. Engl. **23** (1984) 113.
- Friedrich, J., and D. Haarer, "Tunneling and Relaxation Processes in Organic Glasses as Studied by Photochemical Hole Burning," Appl. Phys. B **28** (1982) 262.
- Friedrich, J., D. Haarer, and R. Silbey, "Reversible and Irreversible Line Broadening of Photochemical Holes in Amorphous Solids," Chem. Phys. Lett. **95** (1983) 119.
- Gutiérrez, A. R., J. Friedrich, D. Haarer, and H. Wolfrum, "Multiple Photochemical Hole Burning in Organic Glasses and Polymers: Spectroscopy and Storage Aspects," IBM J. Res. Develop. **26** (1982) 198.
- Huston, A. L., and W. E. Moerner, "Detection of persistent spectral holes using ultrasonic modulation," J. Opt. Soc. Am. B **1** (1984) 349.
- Itoh, U., and T. Tani, "Research activities on materials for wavelength-multiplexed optical recording in Japan," Appl. Opt. **27** (1988) 739.
- Janowiak, R., and H. Bässler, "Non-Photochemical Hole Burning in Tetracene-Doped Amorphous Anthracene," Chem. Phys. Lett. **95** (1983) 124.
- Kishii, N., S. Tamura, N. Asai, K. Kawasumi, and J. Seto, "Photochemical hole burning of tetraphenylporphine derivatives," SPIE Proceedings (1989).
- Kohler, W., J. Zollfrank, and J. Friedrich, "Stability of frequency domain information bits in amorphous organic materials," American Institute of Physics (1989) 3232.
- Lee, H. W. H., M. Gehrtz, E. E. Marinero, and W. E. Moerner, "Two-color, photon-gated spectral hole-burning in an organic material," Chem. Phys. Lett. **118** (1985) 611.
- Lee, H. W. H., and W. E. Moerner, "IBM Scientists Develop Novel High-Density Optical Storage Mechanism," Laser Focus/Electro Optics (1986) 24.
- Lenth, W., R. M. Macfarlane, W. E. Moerner, F. M. Schellenberg, R. M. Shelby, and G. C. Bjorklund, "High-density frequency-domain optical recording," SPIE **695** (1986) 216.
- Lenth, W., C. Ortiz, and G. C. Bjorklund, "Pulsed frequency-modulation spectroscopy as a means for fast absorption measurements," Opt. Lett. **6** (1981) 351.
- Macfarlane, R. M., and R. M. Shelby, "Homogeneous line broadening of optical transitions of ions and molecules in glasses," J. Luminescence **36** (1987) 179.
- Moerner, W. E., ed., *Persistent Spectral Hole-Burning: Science and Applications*, Springer-Verlag, New York (1988).

- Moerner, W. E., M. Gehrtz, and A. L. Huston, "Measurement of Quantum Efficiencies for Persistent Spectral Hole Burning," American Chemical Society (1984) 6459.
- Moerner, W. E., and M. D. Levenson, "Can single-photon processes provide useful materials for frequency-domain optical storage?" *J. Opt. Soc. Am. B* **2** (1985) 915.
- Moerner, W. E., F. M. Schellenberg, and G. C. Bjorklund, "Photochemical Hole-Burning at GaAlAs Laser Wavelengths," *Appl. Phys. B* **28** (1982) 263.
- Mossberg, T. W. "Time-domain frequency-selective optical data storage," *Opt. Lett.* **7** (1982) 77.
- Mossberg, T. W., "Single shot stores bits," *Technology Report* **25** (1986) 36.
- Mossberg, T. W., "Time-Domain Frequency-Selective Optical Memories," Proceedings 1989 LEOS Annual Meeting (Orlando, FL) 435.
- Nishi, T., K. Arishima, H. Tabei, and H. Hiratuka, "Temperature Dependence of PHB Hole Profiles in Polymer Matrices," *Jap. J. Appl. Phys.* **27** (1988) 225.
- Ortiz, C., R. M. Macfarlane, R. M. Shelby, W. Lenth, and G. C. Bjorklund, "Thin-Film Aggregate Color Centers as Media for Frequency Domain Optical Storage," *Appl. Opt.* **25** (1981) 87.
- Pokrowsky, P., W. E. Moerner, F. Chu, and G. C. Bjorklund, "Reading and writing of photochemical holes using GaAlAs-diode lasers," *Opt. Lett.* **8** (1983) 260.
- Rebane, A., "Associative space-and-time domain recall of picosecond light signals via photochemical hole burning holography," Elsevier Science Publishers B. V. **65** (1988) 175.
- Rebane, A., and J. Aaviksoo, "Holographic interferometry of ultrafast transients by photochemical hole burning," *Opt. Lett.* **13** (1988) 993.
- Rebane, K. K., R. K. Kaarli, P. M. Saari, and A. K. Rebane, "Time-and-space domain holography and optical information processing based on photoburning of spectral holes," SPIE Proceedings **963** (1988) 182.
- Rebane, L. A., A. A. Gorokhovskii, and J. V. Kikas, "Low-Temperature Spectroscopy of Organic Molecules in Solids by Photochemical Hole Burning," *Appl. Phys. B* **29** (1982) 235.
- Renn, A., S. E. Bucher, A. J. Meixner, E. C. Meister, and U. P. Wild, "Spectral hole burning: Electric field effect on resorufin, oxazine-4 and cresylviolet in polyvinylbutyral," *J. Luminescence* **39** (1988) 181.
- Renn, A., A. J. Meixner, U. P. Wild, and F. A. Burkhalter, "Holographic Detection of Photochemical Holes," *Chemical Physics* **93** (1985) 157.
- Renn, A., and U. P. Wild, "Spectral hole burning and hologram storage," *Appl. Opt.* **26** (1987) 4040.
- Romagnoli, M., W. E. Moerner, F. M. Schellenberg, M. D. Levenson, and G. C. Bjorkland, "Beyond the bottleneck: submicrosecond hole burning in phthalocyanine," *J. Opt. Soc. Am. B* **1** (1984) 341.
- Saari, P., R. Kaarli, and A. Rebane, "Picosecond time- and space-domain holography by photochemical hole burning," *J. Opt. Soc. Am. B* **3** (1986) 527.
- Sakoda, K., K. Kominami and M. Iwamoto, "High Temperature Photochemical Hole Burning of Tetrasodium 5,10,15,20-tetra(4-sulfonatophenyl)porphin in Polyvinylalcohol," *Japanese Journal of Applied Physics* **27** (1988) L304.

- Schmitt, U., and D. M. Burland, "Use of Holography to Investigate Photochemical Reactions from Higher Excited States. Action Spectrum of the Second-Photon Step in the Two-Photon Dissociation Reaction of Carbazole," *J. Phys. Chem.* **87** (1983) 720.
- Shelby, R. M., R. M. Macfarlane, and D. P. Burum, "Optical Hole Burning and Coherent *rf* Double Resonance Spectroscopy of Rare Earth Ions in Solids," *Appl. Phys. B* **28** (1982) 262.
- Tani, T., H. Namikawa, and K. Arai, "Photochemical hole-burning study of 1,4-dihydroxyanthraquinone doped in amorphous silica prepared by alcoholate method," *J. Appl. Phys.* **58** (1985) 355.
- Thijssen, H. P. H., R. van den Berg and S. Völker, "Optical relaxation in organic disordered systems submitted to photochemical and non-photochemical hole-burning," *Chem. Phys. Lett.* **120** (1985) 503.
- Thijssen, H. P. H., and S. Völker, "Pitfalls in the determination of optical homogeneous linewidths in amorphous systems by hole-burning influence of the structure of the host," *Chem. Phys. Lett.* **120** (1985) 496.
- Thijssen, H. P. H., and S. Völker, "Spectral hole burning in semicrystalline polymers between 0.3 and 4.2 K," *J. Chem. Phys.* **85** (1986) 785.
- Tomlinson, W. J., E. A. Chandross, R. L. Fork, C. A. Pryde, and A. A. Lamola, "Reversible Photodimerization: a New Type of Photochromism," *Appl. Opt.* **11** (1972) 533.
- Trommsdorff, H. P., J. M. Zeigler, and R. M. Hochstrasser, "Spectral hole burning in polysilanes," *J. Chem. Phys.* **89** (1988) 4440.
- van den Berg, R., and S. Völker, "Does non-photochemical hole-burning reflect optical dephasing processes in amorphous materials? Pentacene in polymethylmethacrylate as an affirmative example," *Chem. Phys. Lett.* **127** (1986) 525.
- Wild, U., *Laser Focus/Electro-Optics* (1987) 33.
- Wild, U. P., S. E. Bucher, and F. A. Burkhalter, "Hole burning, Stark effect, and data storage," *Appl. Opt.* **24** (1985) 1526.
- Winnaker, A., R. M. Shelby, and R. M. Macfarlane, "Photon-gated hole burning: a new mechanism using two-step photoionization," *Opt. Lett.* **10** (1985) 350.
- Wu, W-Y, J. N. Schulman, T. Y. Hsu, and U. Efron, "Effect of size nonuniformity on the absorption spectrum of a semiconductor quantum dot system," *Appl. Phys. Lett.* **51** (1987) 710.
- Yoshino, K., S. Nakajima, D. Park, and R. Sugimoto, "Spectral Change of Polymer Film Containing Poly(3-Alkylthiophene) with Temperature and Its Application as Optical Recording Media," *Japanese Journal of Applied Physics* **27** (1988) L454.